Transsolar
KlimaEngineering

Energy optimization of a geothermal heat-pump system through dynamic system simulation

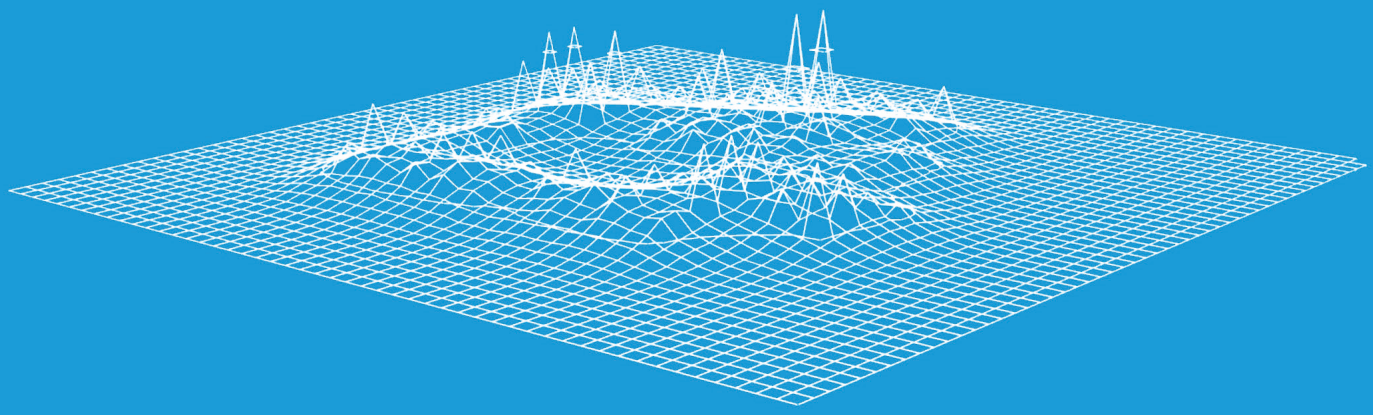

Master Thesis - Christian Hepf

Christian Hepf, B.Sc.

Energy optimization of a geothermal heat-pump
system through dynamic system simulation
A case study for the International Airport Calgary
Master Thesis, Technische Universität München
Munich, March, 29th 2018.

This thesis was typeset with Microsoft Word using Arial. The figures were prepared using Adobe Illustrator, Adobe InDesign and Microsoft Excel.

Master Thesis

Energy optimization of a geothermal heat-pump system through dynamic system simulation

A case study for the International Airport Calgary

Christian Hepf
Munich, Germany

Supervisors: Prof. Dipl.-Ing. Thomas Auer
Dipl.-Ing. Tobias Wagner
Chair of Building Technology
And Climate Responsive Design

Advisors: Dipl.-Ing. Stefan Holst
Dipl.-Phys. Björn Röhle
Transsolar Energietechnik GmbH

Abstract

The sustainable principle of the “three-pillar-model” containing ecologic, economic and social targets, pursues three strategies to realize sustainability in the long term. Those strategies are made up of the principle of efficiency, consistency and sufficiency. A great number of the burgeoning sustainability movements focus on promising potential in the consistency and sufficiency strategies. In general, the potential of efficiency in industrialized countries, like Germany, is classified as well-developed while the phenomenon of a performance gap is rising. The performance gap describes the discrepancy between the intended, desired building performance and the actual, observed performance. [1]

The building sector in Germany, responsible for 40 % of total end energy use, holds a great potential for energy savings [2]. At the level of the building services of an edifice the code DIN 18599 indicates the thermal energy demand. [3] Studying the extension of the International Airport in Calgary, this master thesis investigates the effects of an energy optimization of the airport’s geothermal heat-pump system.

Its subsystems are divided into two categories. The first category is defined by fixed parameters that must be set at the beginning of the design process of a building system, as they cannot be changed throughout the life of the building. Conversely, the adjustable category is determined by components of the building system that can be adjusted by the control strategy of the subsystem or even through a replacement of single components on a reasonable effort basis. The two categories will be investigated by changing individual characteristic values of the components in the subsystem for each optimization variant. Through the evaluation of the two classifications, the influence of the categories on the aspect of energy efficiency and the service life of a geothermal heat-pump system are going to be clarified. Furthermore, this master thesis endeavors to emphasize which of the two categories of optimization variants has a bigger energy savings and longevity potential.

This energy analysis is performed through a dynamic system simulation with the software TNRSYS. The parametric values of the geothermal field are the undisturbed ground temperature, the architecture of the geothermal borehole pipes, the thermal conductivity of the ground, the medium in the geothermal loop and the balance of the building load of the system. The category for variable components includes the control strategy of the hydraulic separators, the power of the heat-pump/chiller component, the mass flow in the loops, as well as the heat transfer effectiveness of the plate heat exchangers. The variants are evaluated according to the non-renewable primary energy demand and the number of system changes of the building services.

The category of the fixed parameters of the geothermal field mainly influences the demand of non-renewable primary energy, especially depending on the implemented borehole pipes and the thermal ground conductivity. The adjustable components of the building system influence both factors, above all depending on the performance of the heat-pump and the hydraulic separators. All in all, the adjustable components have a wider array of effects on the system.

Kurzfassung

Das Drei-Säulen-Modell der Nachhaltigkeit beinhaltet, basierend auf der Ökologie, Ökonomie und dem sozialen Verhalten, wiederum drei Strategien, um das Konzept der Nachhaltigkeit langfristig umzusetzen. Die drei Strategien verfolgen die Prinzipien der Effizienz, Konsistenz und Suffizienz. Viele der aufstrebenden Nachhaltigkeitsbewegungen sehen besonderes Potential in den Strategien der Suffizienz und Konsistenz. Im Allgemeinen wird in einem Industriestaat wie Deutschland die Effizienzstrategie als gut entwickelt eingestuft. Doch genau diese Tatsache stellt das Prinzip der „performance gap“, die Lücke zwischen dem geplanten und dem realen Zustand eines Systems, in Frage. [1]

Besonders im Gebäudebereich ist, mit einem Anteil von 40 % am gesamten Verbrauch an Endenergie in Deutschland, ein sehr großes Energieeinsparpotential vorhanden. [2] Auf der Ebene der Gebäudetechnik stellt die DIN 18599 die Rahmenbedingung für die Analyse der thermischen Lasten dar. [3] In Anlehnung an die Erweiterung des Flughafens Calgary in Kanada analysiert diese Masterarbeit die Auswirkungen einer energetischen Optimierung der geothermischen Wärmepumpenanlage.

Insbesondere wird der Fokus daraufgelegt, die Optimierung in zwei unterschiedliche Kategorien aufzuteilen. Differenziert wird zum einen zwischen Parametern, die über die Lebensdauer des Gebäudes nicht mehr verändert werden können. Zum anderen werden Faktoren betrachtet, welche durch eine Veränderung der Kontrollstrategie oder zumindest durch einen Austausch einzelner Komponenten, mit einem vertretbaren Aufwand, in der Praxis umgesetzt werden können. Durch die Analyse der Optimierungsvarianten soll geklärt werden, welchen Einfluss die beiden Kategorien auf die Energieeffizienz und die Lebensdauer eines geothermischen Wärmepumpensystems haben. Weiter soll herausgearbeitet werden, welche der beiden Kategorien größere Einsparungen erzeugt.

Die Fragestellung wird durch eine dynamische Simulation mit der Software TRNSYS geprüft. Bei den charakteristischen Werten des geothermischen Feldes werden die ungestörte Erdreichtemperatur, der Aufbau der Bohrpfähle, die thermische Leitfähigkeit des Bodens, das Medium des geothermischen Kreislaufes sowie unterschiedliche Balancen der thermischen Gebäudelasten evaluiert. Die Kategorie der veränderbaren Faktoren wird anhand der Kontrollstrategie der hydraulischen Weichen, der Leistungsfähigkeit der Wärmepumpe, des Massenstroms und der Übertragungsfähigkeit der Wärmetauscher analysiert.

Die Kategorie der nicht veränderbaren Parameter des geothermischen Feldes beeinflusst vor allem den Bedarf an nicht erneuerbarer Primärenergie, speziell durch die verwendeten Geothermiepfähle und die Leitfähigkeit des Bodens. Die Kategorie der veränderbaren Faktoren hingegen hat Einfluss auf beide Analysefaktoren, besonders durch die Leistungsfähigkeit der Wärmepumpe und die Kontrollstrategie der hydraulischen Weichen. Prinzipiell haben die veränderbaren Komponenten des Gebäudesystems einen größeren Einfluss, als die unveränderbaren Parameter des geothermischen Feldes.

Contents

Abstract i
Kurzfassung iii
Contents iv
Acronyms vi
List of symbols vii

1. Introduction 1

1.1 Prospects of the construction industry 2
1.2 Performance gap 2
1.3 Hypothesis 3
1.4 Methodology 4

2. Principles of the simulation 8

2.1 Thermal comfort 8
2.2 Building energy simulation 9
2.3 Coupled and uncoupled system simulation 11
2.4 TRNSYS 12
2.5 Geothermal heat-pump 13

3. Fundamental analyses of the initial status 18

3.1 Comparison of the measured & simulated data 18
3.2 Analysis of the heat exchangers 19

3.2.1 Performance of the heat exchangers in the CHW loop 21
3.2.2 Performance of the heat exchangers in the LTHW loop 22
3.2.3 Conclusion 22

3.3 Weather data analysis 23

3.3.1 Global radiation 24
3.3.2 Ambient temperature 25
3.3.3 Humidity 26
3.3.4 Wind direction and velocity 26
3.3.5 Conclusion of the weather data analysis 27

3.4 Internal energy balance of MR01 28

4. Project specific data 32

4.1 Thermal simulation 32
4.2 Thermal load of the MR01 of the International Airport Calgary 34
4.3 Geothermal system 35
4.4 System states 38

5. Optimization of a geothermal heat-pump system 42

5.1 Structure of the plant simulation 42
5.2 Base case model 43
5.3 Reduction of the geothermal borehole system 46
5.4 Principles of the variant analyses 49
5.5 Evaluation of the fixed parameters of the geothermal field 51

5.5.1 Thermal conductivity of the ground 51
5.5.2 Undisturbed ground temperature 53
5.5.3 Architecture of the geothermal borehole pile 54
5.5.4 Fluid of the geothermal loop 56
5.5.5 Variation of the building load 57

5.6 Evaluation of the adjustable factors of the building system 59

5.6.1 Variation of the performance of the heat-pump/chiller 59
5.6.2 Variation of the control strategy of the hydraulic separators 62
5.6.3 Variation of the performance of the heat exchanger 64
5.6.4 Variation of mass flow 66

6. Comparison of the optimization variants 70
7. Discussion 73
8. Outlook 77
Appendix A – Project specific information 82
Appendix B – Subsystems of the plant simulation 89
Appendix C – System states of the plant simulation 99
Bibliography 102
List of Figures 106
List of Tables 107
Declaration of Autonomy 109

Acronyms

AHU	Air handling unit
BES	Building energy simulation
BMS	Building management system
CHW	Chilled hot water
COP	Coefficient of performance
CO_2-equivalent	Carbon monoxide equivalent
dT	Temperature difference
EH	Excess heat
HP	Heat-pump
HVAC	Heating ventilation and air conditioning
HW	Hydraulic separator
HWS	Hot water supply
HX	Heat exchanger
IT	Information technology
LTHW	Low temperature hot water
MF	Mass flow
MRXY	Mechanical room nr. XY
PG	Performance gap
PLR	Part load ratio
TRNSYS	Transient system simulation

List of symbols

$\mathbf{A}$	Cross-sectional area	[m^2]
$\mathbf{a_{th}}$	Thermal diffusivity	[m^2]
$\mathbf{c_p}$	Specific heat capacity	[J/K]
$\mathbf{d}$	Pipe diameter	[m]
$\boldsymbol{\varepsilon_{HX}}$	Efficiency plate heat exchanger	[-]
$\mathbf{L}$	Length of the geothermal pipes	[m]
$\boldsymbol{\lambda_{th}}$	Thermal conductivity	[W/(m K)]
$\boldsymbol{\lambda}$	Friction coefficient	[-]
$\dot{\mathbf{m}}$	Mass flow of the geothermal loop	[kg/h]
$\mathbf{n}$	Mechanical efficiency factor	[-]
$\mathbf{P_{el}}$	Electrical energy demand	[KW]
$\Delta\mathbf{p}$	Pressure drop	[Pa]
$\mathbf{Q_{th}}$	Thermal energy	[kW]
$\mathbf{RE}$	Reynolds number	[-]
$\boldsymbol{\rho_{medium}}$	Density of the medium	[kg/m^3]
$\mathbf{T_{in/out}}$	Inlet/outlet temperature	[°C]
$\mathbf{T_{set}}$	Set temperature	[°C]
$\mathbf{u}$	Wetted girth	[m]
$\dot{\mathbf{V}}$	Volume flow	[km^3/s]
$\boldsymbol{\nu}$	Velocity of the medium	[m/s]
$\boldsymbol{\upsilon_{medium}}$	Kinematic viscosity of the medium	[m^2/s]
$\boldsymbol{\omega}$	Flow velocity	[m/s]
$\mathbf{Y_{on/off}}$	On/off-Controller of mode	[-]

1. Introduction

1.1 Prospects of the construction industry

1.2 Performance gap

1.3 Hypothesis

1.3 Methodology

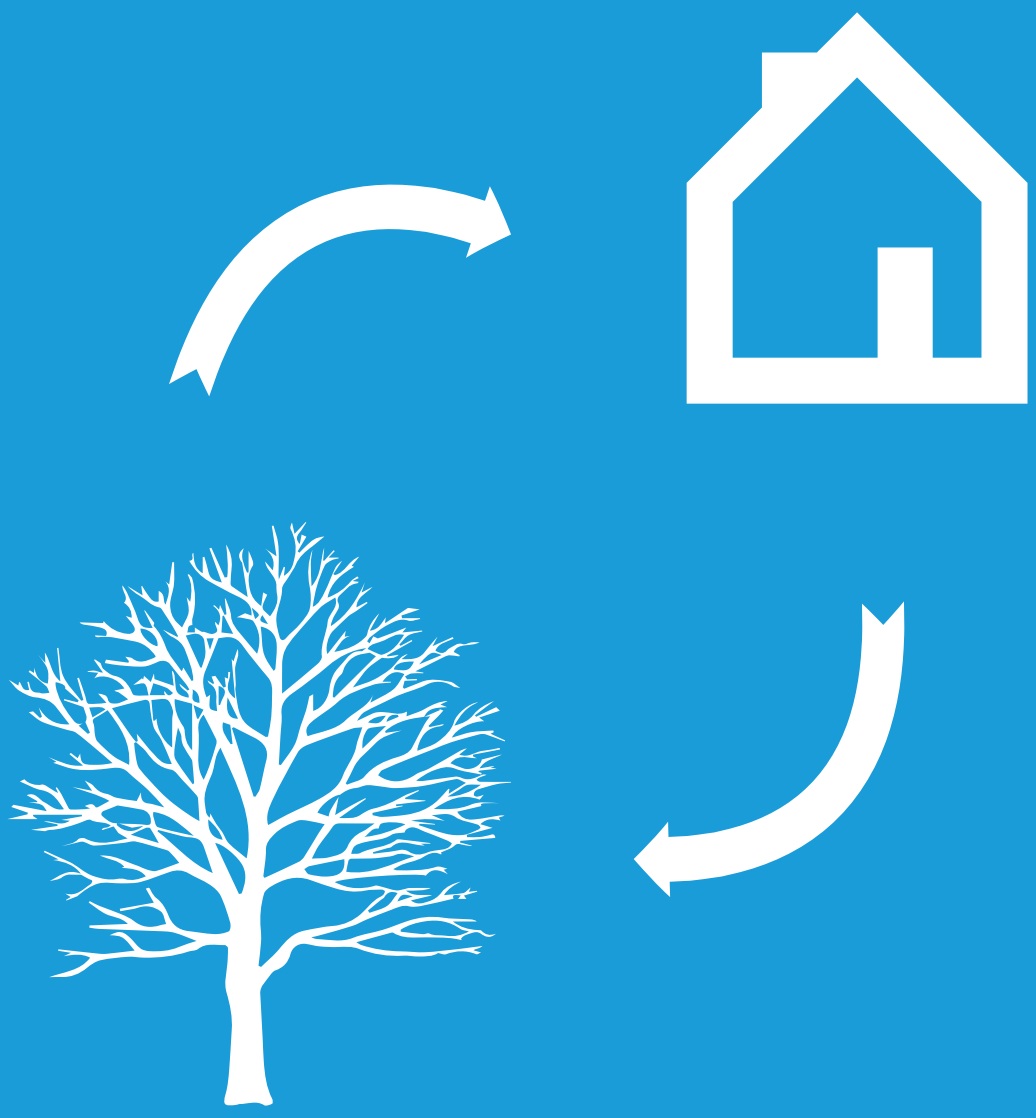

1. Introduction

„A society that allows itself to admit and articulate its nonmaterial human needs, and to find nonmaterial ways to satisfy them, would require much lower material and energy throughputs and would provide much higher levels of human fulfillment. “ [4]

This statement describes a core message of the 2004 update of the world-renowned report *“The Limits of Growth*”, one of the most influential works on sustainability. Besides the fact that a sufficient use of the resources of the world is necessary, the two other parts of the triad of the sustainable strategies should be fulfilled. The principle of sustainability and its strategies are displayed in figure 1.

The principle of consistency means coherence within a system, in this case either the technical or biological life cycle. Ideally, every life cycle of a product is circular, which means, that all matter is used again after its service life. The third part of the triad is efficiency. Every process needs to produce the maximum output while using the minimum input. This principle is the most integrated one in modern society. [5]

Particularly in the process of planning buildings and cities, there are not many concepts for integrating sufficiency into operation. One of the core tasks of the recent planning generation is based on an intelligent connection of efficiency and sufficiency to generate *“compass of an enlightened policy of sustainability”.* [6]

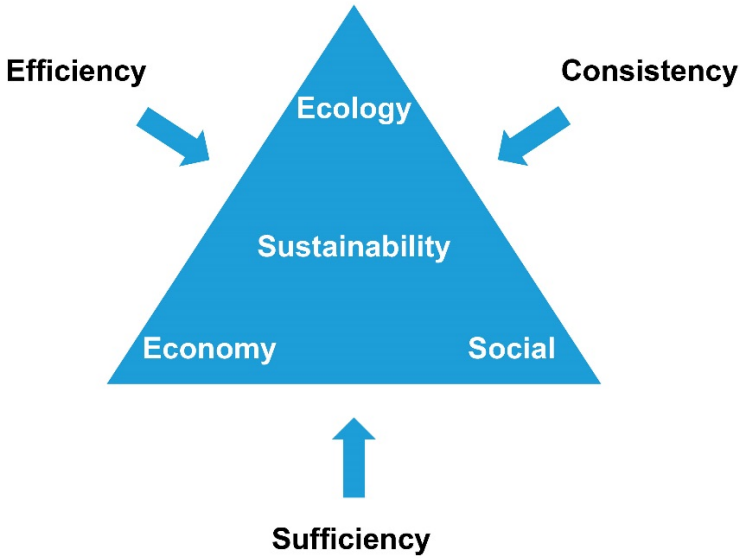

Figure 1 Dimensions of sustainability (own representation based on [5])

1.1 Prospects of the construction industry

As the report of the *Intergovernmental Panel on Climate Change* (IPCC) of 2013 shows, human activities' effect on the energy system of the world, as well as on the local and worldwide climate on earth, trigger in short-, mid- and long-term consequences. The complexity of these implications can hardly be summarized or distinguished, because single consequences strengthen and weaken each other and even lead to new repercussions in the environment. To mention just a few: sea levels are rising, desertification is spreading throughout large parts of the planet, the ecological diversity is decreasing and besides the constant rise in the worlds ambient temperature, the occurrence of weather extreme events is more frequent. Unprecedented population growth of the last decades combined with the escalating globalization and urbanization leads to a huge demand for transportation and a higher standard of living and consequently to a heavy burden on the earth. Dividing the whole processes into pieces, the heating energy in Germany generates more than 17 % of the overall CO_2-equivalent emissions. CO_2-equivalent emissions are the summed-up greenhouse gases according to their individual greenhouse gas potential. [7] This shows that on the one side, planning engineers and architects are burdened with a high responsibility in their work. On the other side, one must realize that the potential of optimization in the construction industry is tremendous. This leads to the point that the building industry needs to find solutions for optimizations. [8]

1.2 Performance gap

"The Carbon compliance limit should apply to 'built' performance." [9]

As digitalization becomes more and more common in the modern building industry a comparison of the measured and simulated data is state of the art. Thus, the principle of a performance gap is to be discussed very controversial nowadays. In general, it is the difference between the intended and the actual situation of a system and is therefore an indicator of the real efficiency of an edifice in comparison to its intended design. [1] The appearance of a performance gap makes it difficult to accurately predict the performance of a building. A calculation of a performance gap is based on detailed information about every process in all phases of the building's life cycle. In the course of digitalization more and more measurement data can be monitored. Based on this trend, an accurate and detailed performance gap can be evaluated.

In numerical terms, the performance gap is the ratio between measured and calculated energy use of a building, as illustrated in the following equation. As per the calculation, a PG-value of 0 % means that the operation matches perfectly the intended design performance. Further, the PG-value can be positive or negative. A negative PG-value corresponds with a building that is operating better than the design's intent. A positive PG-value points out the underperformance of a building. [10]

$$PG = \left(\frac{measured\ energy\ demand}{intended\ energy\ demand} - 1 \right) \times 100 \quad [\%] \quad \text{Equ. 1} \qquad [10]$$

With the rise of digitalization, especially in the United States of America, data monitoring becomes an ever more important factor of a building. The UK Green Building Council published a report during their campaign for a sustainable built environment called:" Building Zero Carbon – the case for action". This report presents recommendations to the government on how to generate zero carbon dioxide emissions from commercial buildings. Based on measurement data provided by AECOM, who also managed the International Airport Calgary as a main agent, one of the main conclusion and recommendation is to implement the calculation of the performance gap into the process of monitoring a building. [11]

Technically, the performance gap is created among other things by a wrong assumption of the energy demand of a building in the planning process, an absence of energy usage during the modelling of a building, assumptions of the planners resulting from missing information and communication and many other negative effects associated with the planning process of a building. [12]

While technical solutions may be feasible and appropriate for individual challenges, the deeply rooted problem of the performance gap has its base in the principle of the whole planning process. Based on the fact, that a group of many different agents are involved in the planning process of a building, imperfect communication cannot be prevented. Hence this scrutinizes the comprehensive process of building but is not the topic of this thesis and would overplay the hand of this master thesis. As one example, out of many in North America, this thesis undertakes a generic approach to the achievement of energy efficiency in practice by outlining energy optimization variants at the International Airport Calgary

1.3 Hypothesis

A very common and popular source of renewable energy, especially for non-residential buildings, is a geothermal heat-pump system. Under suitable circumstances, the stored thermal energy of the ground is used to feed a heat-pump/chiller device which then supplies a heating and cooling system of a building. As mentioned in the previous chapter, the performance of a building system is not always living up to its intended function. The performance of a geothermal heat-pump mainly depends on the dimensioning of the geothermal field, as well as on the control strategy and the performance of the key system components. The geothermal system is defined by the undisturbed ground temperature, the thermal conductivity of the ground, the number, length and characteristics of the implemented borehole pipes and the medium used in the geothermal loop. In fact, the performance of the building services is conditional on the power of the heat-pump/chiller device, the heat transfer ability of the heat exchangers between the geothermal and the building loop, as well as on the mass flow and the sizing of the hydraulic separators.

Looking closer into the specific factors of the performance of such a system, one can separate them between fixed, in the design process set parameters that cannot be changed after the construction of the building, and variable, interchangeable factors of the system. In accordance to the fact that over 40 % of the costs of geothermal wells are related to the drilling of the borehole pipes and the fact that the thermal condition of the ground cannot be changed, all

parameters of the geothermal field are generally fixed parameters. [13] In contrast to this, the other components of the building system normally are set according to the design process of the building but can be replaced and even more the control strategies of the single devices can be adapted easily. These aspects influence the energy efficiency and the performance in terms of a system longevity.

This thesis claims that an optimization of the operating components' control strategies of the building services has a bigger potential in terms of energy saving and longevity compared to the influence of the parametric planning of the geothermal wells at the beginning of the design process. By comparing and evaluating the characteristic values of the geothermal field, as well as the control strategies and the performance of the devices of a geothermal heat-pump system, this master aims to answer the following research questions:

- How does the variation of the design parameters of the geothermal field effect the energy efficiency and the service life of a geothermal heat-pump system?

- What effect does the performance and the control strategy of the key devices of a geothermal heat-pump system have on the energy efficiency and the service life?

1.4 Methodology

To validate the hypothesis and answer the research questions, a thermal system simulation is implemented. Using the project specific information of the extension of the International Airport in Calgary, this thesis analyses the variation of the components and the geothermal field according to the initial situation in Calgary. By implementing the project data in a system simulation, this master thesis uses the dynamic simulation tool TRNSYS to create a detailed and accurate model of the building system. The components of the building system are integrated in such a way that each characteristic factor can be varied.

In the following chapter, the thermodynamic principles of a building simulation, as well as the principles of a geothermal heat-pump system are detailed. Hence, chapter 3 evaluates the actual building situation of the International Airport in Calgary by analyzing the weather data, the current energy situation using data from the building measurement system and the internal energy balance of the building system. In addition, in chapter 4, the project specific information, the implied building load, as well as the structure of the geothermal field of the airport are described. Chapter 5 forms the main part of the analysis. In this section, the base case model as well as the structure of the plant simulation are pointed out. Furthermore, the evaluation of the two categories are analyzed. In chapter 6, the individual optimization results are compared and the ongoing hypothesis, as well as the scientific questions are answered. In the end an outlook is presented, and a brief assessment of the current situation of the building industry is given.

2. Principles of the simulation

2.1 Thermal comfort

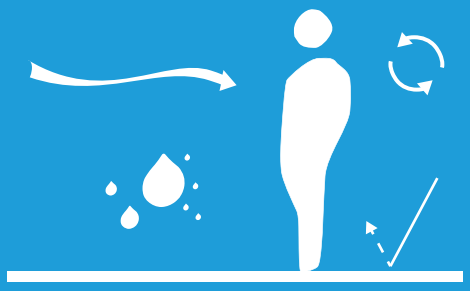

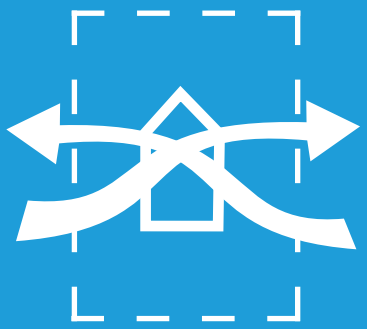

2.2 Building energy simulation

2.3 Coupled and uncoupled simulation

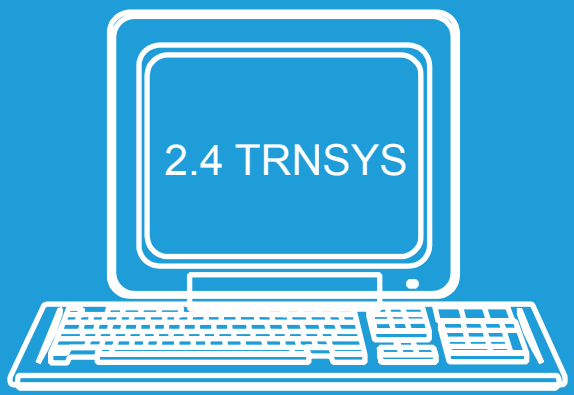

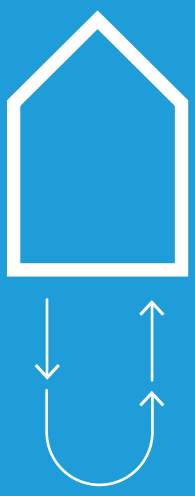

2.5 Geothermal heat-pump

2. Principles of the simulation

In this chapter, the focus is on the general principles of a simulation. The overall objective of a simulation can be to achieve thermal comfort in all rooms of a building. The key factors, the calculation principles and the conditions for a pleasant thermal comfort are described in section 2.1. To generate thermal comfort in buildings, nowadays a simulation is used to analyze the building comfort. The principle and the functionality of such an analysis are touched upon in the following section. Furthermore, the principles of a coupled and uncoupled simulation are pointed out. One very common and accurate simulation software is TRNSYS. The functionality and setup of this tool is described in section 2.4. Finally, the specific situation of the International Airport Calgary with a geothermal heat-pump system will be showcased. In the following section, the general structure and the functionality of a geothermal heat-pump system will be depicted.

2.1 Thermal comfort

The complex principle of the Danish scientist and professor Ole Fanger from 1970 still defines thermal comfort and made it possible to calculate thermal comfort with a mathematical equation. In his dissertation, he pointed out that thermal comfort for human beings in interior spaces depends on six variables. [14]

- Ambient temperature
- Radiant temperature
- Humidity
- Air velocity
- Clothing insulation
- Activity level

As Fanger emphasized, thermal comfort heavily depends on user activity and clothing levels. The building industry incorporated this information into their codes and nowadays the different functional usages of buildings and the year's seasonal components influence the norms and codes. In figure 2, key factors for thermal comfort are listed. Today, the thermal comfort is the base for nearly every planning process of a building. As mentioned, thermal comfort can be calculated. This calculation was also the base for the initial analysis of the International Airport in Calgary. The heating and cooling demands are used to analyze the optimization of a geothermal heat-pump system. As the aim of this master thesis is to optimize the HVAC system of the airport, the building model of the airport is fixed. In the following section, this thesis delineates, how building energy simulation connects these components of thermal comfort within buildings and how it is possible to simulate building energy use and performance.

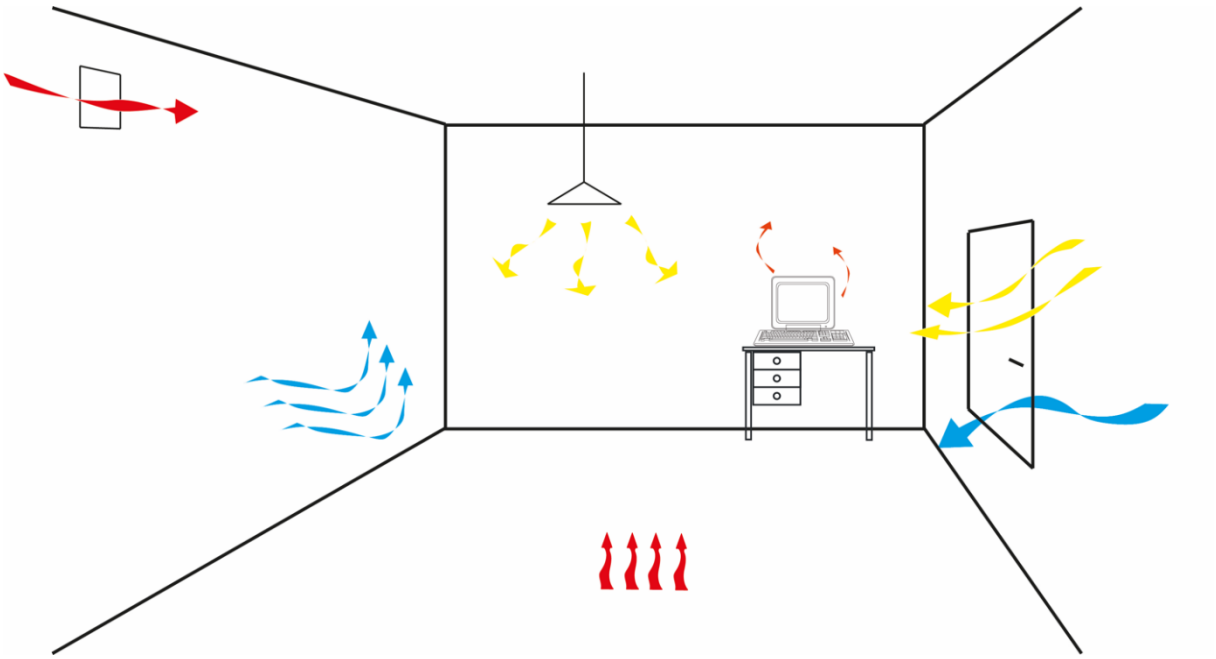

Figure 2 Thermal comfort (own representation based on [15])

2.2 Building energy simulation

As mentioned in the previous section, the aim of a building energy simulation can be the generation of thermal comfort in a building. Building energy simulation is the response to generate a virtual replica of an edifice. A building energy simulation is based on physical calculations representing the energy flows in a building. Besides the construction of the building, a building energy simulation takes the heating and cooling system, the lighting system, internal gains from devices and humans, the ventilation system, the hot water system and the local weather conditions of the location of the building into account (Figure 3 Components of a building energy simulation). The individual components can be controlled via schedules for the occupancy with the goal being to achieve a more accurate calculation. As an output, the total energy demand, heating and cooling loads or the electrical energy consumption can be provided. [16]

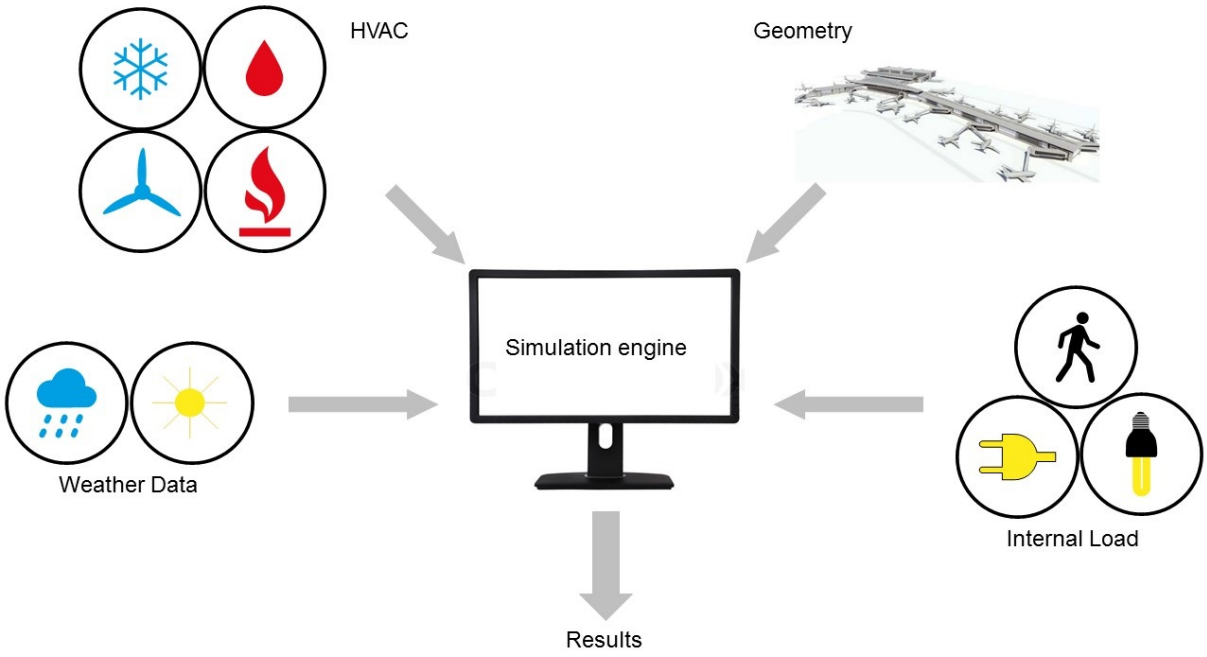

Figure 3 Components of a building energy simulation

As a starting point, it must be noted that the results of a simulation can only be as accurate as the input data of the simulation. Usually a building simulation is implemented in the design phase of a building. In this master thesis, the building energy simulation is done to analyze optimization variants of the building system.

In general, the tools consist of a *graphical user interface* and a *simulation engine*, which performs the actual simulations. This user interface collects the required data and hands it over to the simulation engine, where the actual calculation is performed and the desired output is generated. A thermal energy simulation can use the local weather data, the thermal envelope, the HVAC system and the internal loads, consisting of devices and humans, to predict the energy use and thermal comfort conditions in a building. Finally, one must mention, that a thermal energy simulation is based on many assumptions, starting with the weather data and the internal loads. During the whole simulation process many other assumptions must be included which plays a large role in the scrutiny of the reliability of the simulation results. [17]

A building energy simulation can be done with different goals. Architects use this tool to analyze the interaction between the construction and the other components of the building to generate an energy-efficient design. HVAC orientated simulations are implemented to reduce the energy demand of the building. This energy demand can be reduced in the form of heating, cooling or electrical loads. It also helps to test the control strategies of a building. Another reason to do a building energy simulation is to figure out the performance of a building during operation. This, in many cases correlates with certification and financial incentives. Furthermore, building energy simulation is used to provide information for standards and codes

through analyzing prototype models. Overall, the aim of a building energy simulation is to evaluate potential decisions and help to achieve long term goals. One of this simulation tools is TRNSYS that is used for the calculations of this master thesis and examined in section 2.4. [16]

2.3 Coupled and uncoupled system simulation

In general, an optimization of energy system is as good as the accuracy of its calculations. To increase the effectiveness of the interaction of two systems which affect each other, these systems can be connected via so called coupled simulations. A building system simulation also has two possibilities to implement the loads of a building with the system simulation. One distinguishes between a coupled and uncoupled simulation. A coupled simulation in this case connects to the thermal simulation of the building and calculates the thermal load in every time step. Through interaction with the building system the thermal comfort in the single rooms can be generated. This calculation process requires a lot of computing power and follows very complex structures in connecting the building with its mechanical system.

Another possibility to perform a building simulation with a connected building is an uncoupled simulation. In this case, one uses a time-step based data reader to implement the building loads. Moreover, the planner must know the thermal loads of the building in advance. For this process, the user needs to know the supply and return temperatures as well as the mass flows of the total building. This has the advantage that the implementation is simpler, and the calculation time is decreased in comparison with a coupled simulation. Since the focus of this thesis is to optimize the performance of the building services and not the building itself, an uncoupled system simulation is the more reasonable approach. By keeping the calculation time short, the number of optimization calculations can be increased.

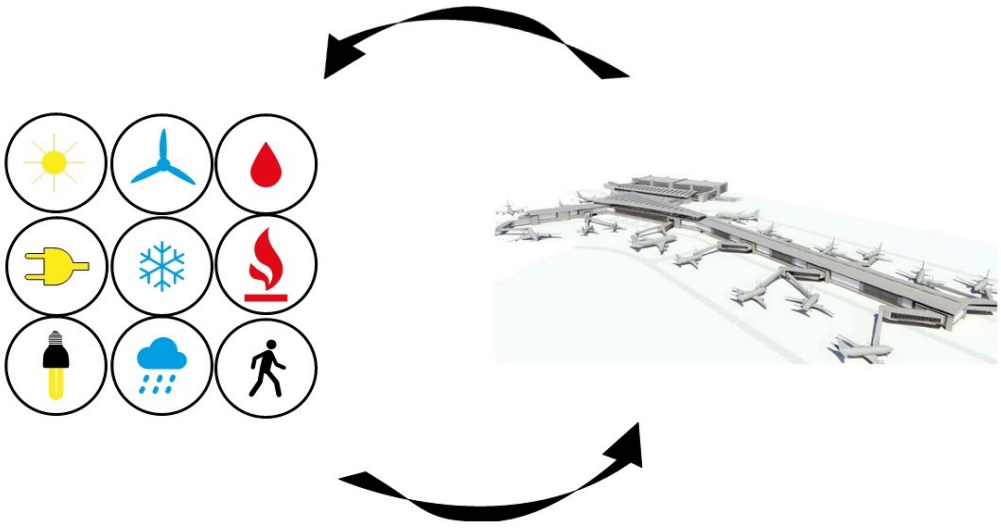

Figure 4 Interaction between thermal and building system simulation

2.4 TRNSYS

The Software used for the building energy simulation in this master thesis is called TRaNsient SYstems Simulation (TRNSYS). It was developed by the University of Wisconsin and was first released in 1981. TRNSYS is a simulation software to calculate energy concepts for multizone buildings. It is used for energy simulations on a small and large scale, from domestic water systems up to complex multizone building simulations. TRNSYS can simulate solar systems, HVAC systems, renewable energy systems, cogeneration plants or geothermal heat-pump systems. [18]

The modular software works with a variety of more than 150 components. These components are called *types*. The software to manage the wide ranges of types is called *Simulation Studio.* In the *Simulation Studio* the different *types* of the model can graphically be linked to each other and the connection settings can be defined. In the building type *TRNbuild* a multizone building with its mechanical system can be defined. The building component models a thermal envelope for the building based on the structure, the materials and the orientation of the constructions. The *TRNSYS simulation engine* also refers to the kernel type *Simulation Studio* and performs the transient simulation. It is based on a mathematical solver for differential equations. Reading all data, it runs a detailed simulation. [19]

TRNSYS makes a distinction between an input that changes with time and an input that is set for the whole simulation. Therefore, TRNSYS separates between *inputs* (time dependent) and *parameters* (time independent). In every defined time step TRNSYS generates a time dependent *Output*. With the so-called *plotter type* a result file of the simulations, which can be visualized, is produced. Based on the modular structure of the software the linking of TRNSYS with further simulation or calculation software is possible. [19]

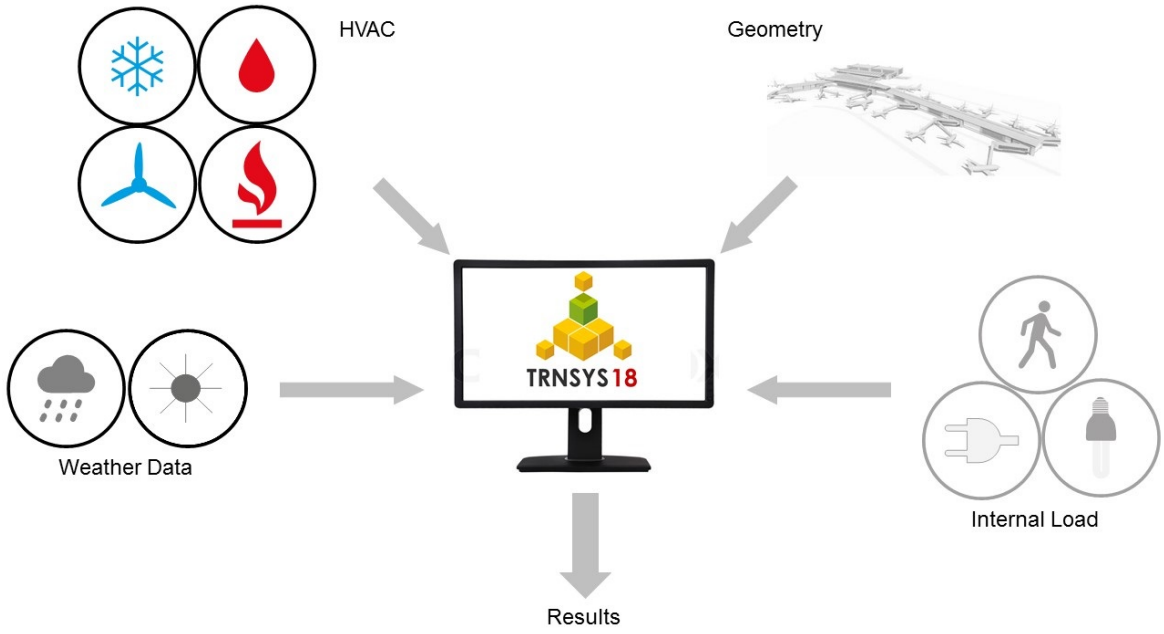

Figure 5 Simulation situation for the International Airport Calgary

In this master thesis, some of the input files are fixed in relation to the simulation base, as illustrated in figure 5. As the extension of the airport has been in operation since 2016, the components of the geometry are set and it is not the goal of this thesis to evaluate changes in the geometry. Furthermore, the location of the airport in Calgary is defined. A last assumption is, that the occupancy and the internal loads schedules are fixed. Since the occupancy schedules and the control management of the building were implemented in the simulation in a very detailed way in earlier phases of the project, this thesis does not deal with the adaption of these components. As it is the aim of this thesis to analyze different optimization model variants of the HVAC system, the next section details the specific situation of a geothermal heat-pump system.

2.5 Geothermal heat-pump

A very common configuration for a building system is the combination of a geothermal field with a heat-pump/chiller device. Geothermal energy is usually located very close to the boundaries of the tectonic plates of the earth. By using near-surface geothermal energy, it is possible to utilize the energy for the heating and cooling system of a building. In the summer period, it is possible to inject the heat from the building into the ground. For the utilization of near surface geothermal systems an elevation of the energy level is needed. This is usually provided through a heat-pump, which can increase the temperature of a liquid by applying pressure. This principle was developed by the German engineer, winner of the Nobel Prize and former professor of the nowadays called Technical University of Munich, Carl von Linde. During his studies dating back to 1868 he invented the principle of the heat-pump system and made it possible to produce heating or cooling energy in a very simple manner. This principle is also applied in a geothermal heat-pump system. [20]

In general, one can differentiate between an open or closed loop geothermal system. The International Airport Calgary uses a closed loop geothermal system with ethanol as a refrigerant agent in 588 vertical boreholes. The share of ethanol in the mixture with water is 20 %. The refrigerant agent is used to ensure a liquid state of the medium at temperatures below 0°C. A geothermal heat-pump consists of two heat exchangers, a compressor and an expansion valve, as pictured in figure 6. The geothermal heat-pump uses the earth or ground water or both as an energy source. Heat is removed by using liquid. This liquid is heated up by heat exchangers and transferred to the interior of the building in the heating mode. During the summer months, the process is reversed. The thermal energy inside of the building is transferred to the geothermal field and the heat is injected into the ground. In this case, the heat-pump component is called a chiller. [21]

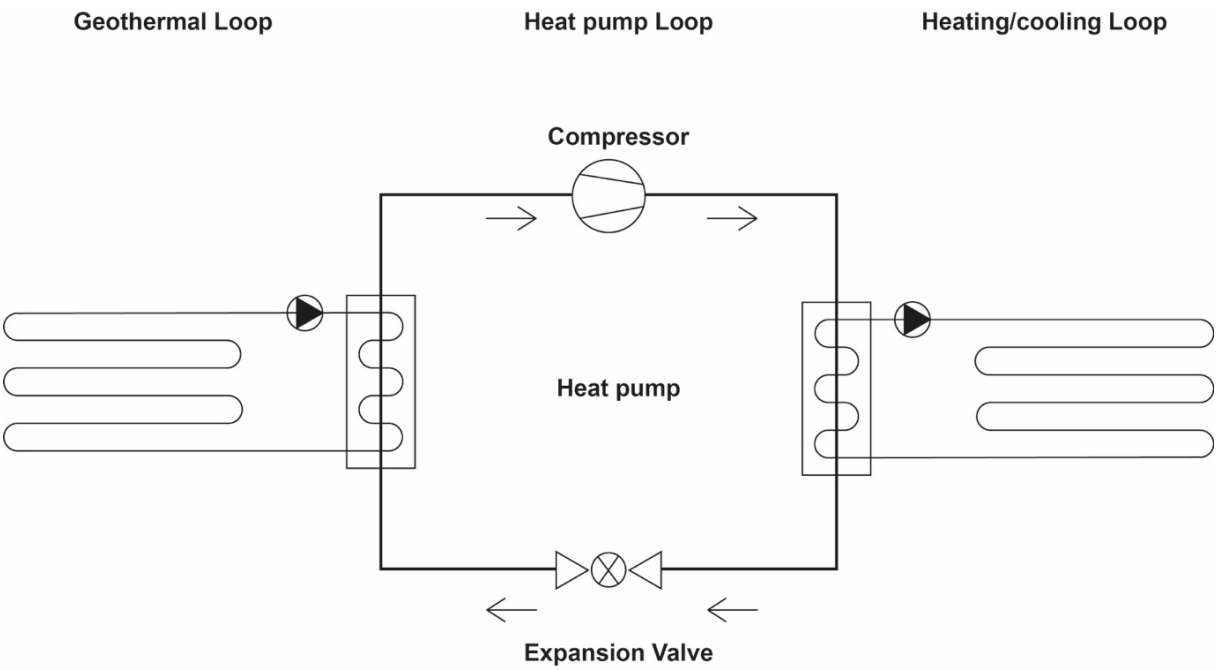

Figure 6 Geothermal heat-pump schematic (own representation based on [21])

In figure 7, the two states of a geothermal heat-pump are shown. During the winter period, the geothermal heat-pump can provide heat from the ground. In the geothermal loop a heat exchanger conducts the heating energy from one medium to another. The compressor condenses the medium by increasing its pressure. During this compression, the temperature of the medium rises. In the second heat exchanger on the heating/cooling loop side, the heat is transferred to the building. The return flow of the second heat exchanger passes the expansion valve and cools down during this process. The refrigerant is pumped back to the underground piping system to be heated up again. For a cooling device, this process acts in reverse. The medium collects the heat from the building, cools it down and transfers the heat into the ground. In the underground piping, the heat is rejected to the ground and the refrigerant is transported back to collect heat from the building interior. [21]

In addition to being used as a heating and cooling system for building, a geothermal heat-pump can also be the base for a domestic hot water loop, profiting from the excess heat. Excess heat usually is available throughout the summer period and as well in the winter period, when the building system is not working at its full capacity or the weather conditions are mild. Preheating of domestic hot water is therefore possible even during the winter period. The process of preheating uses a coil through which the refrigerant of the geothermal system can transfer the heat to the water. [22]

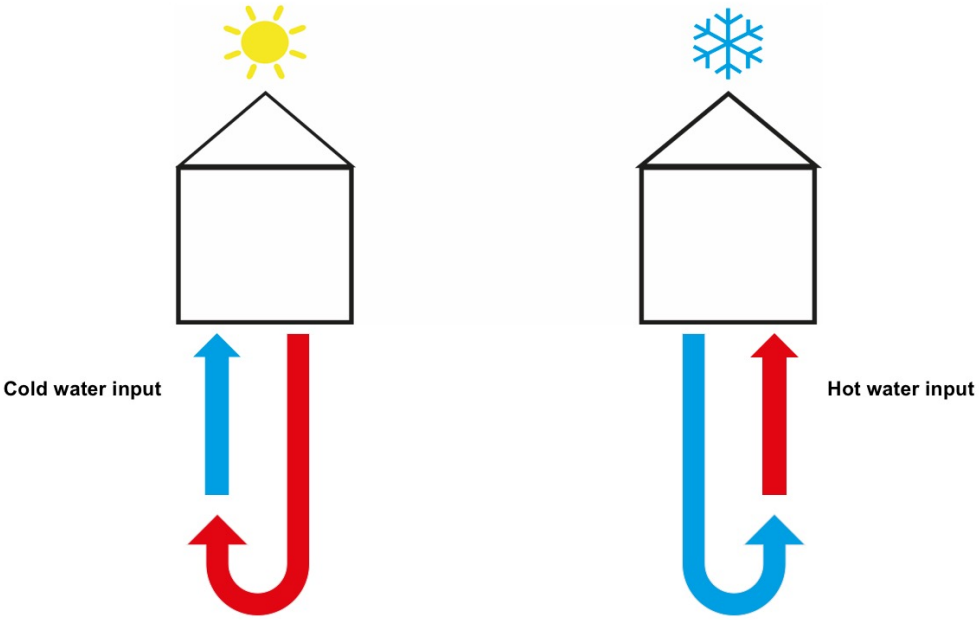

Figure 7 Geothermal utilization in summer & winter

The temperature of the ground below ten meters converges towards the annual mean outside air temperature of the location. In Canada, where the temperatures can go below -25°C, the ground temperature is between -2°C and 8°C. With such constant temperatures, the energy system can reach a coefficient of performance (COP) between 2.5 to 4. This proves that a geothermal heat-pump can be a suitable and efficient system for the location of the airport in Calgary.

If a geothermal field is imbalanced it can lead to negative effects for the upper 10-30 meters of the ground, where animalistic life can still be found. If the imbalance of the building load is too high, an operation of the building services related to a too small temperature difference between the supply and ground temperatures, is not possible anymore. Nowadays, the refrigerant agent must be composed of non-ozone-damaging materials. Based on the fact that near surface systems typically are closed loop systems, there is no direct connection between the system and the ground. Subsequently only the energy demand for the operation must be considered. This energy demand is commonly situated in the range of 20-25 % of the total energy heating demand of the building. [23]

Furthermore, a key factor for near surface geothermal systems is the temperature difference with the ground water. The consequences of temperature variations depend on the respective substance in the ground itself. Small temperature differences ($\Delta T \leq 5°C$) do not have a major effect on the ground water system. Constant heating of the ground water system, based on an imbalanced building system, significantly increases the likelihood of the occurrence of germs and bacteria. [24]

3. Fundamental analyses of the initial status

3.1 Comparison of measured & simulated data

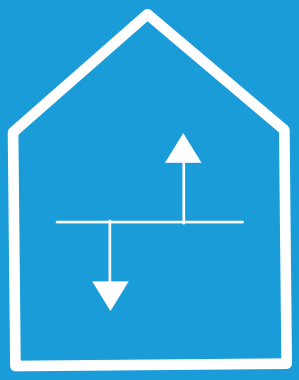

3.2 Analysis of the heat exchangers

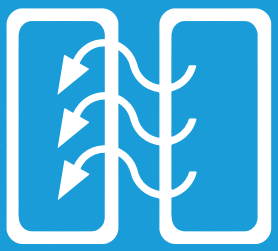

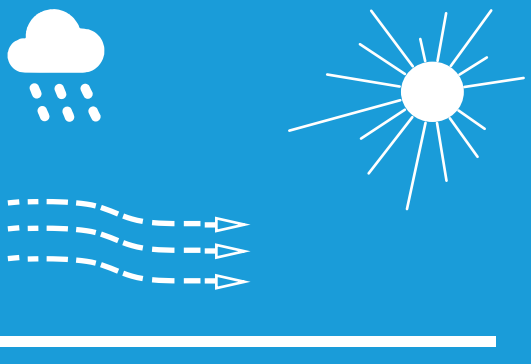

3.3 Weather data analysis

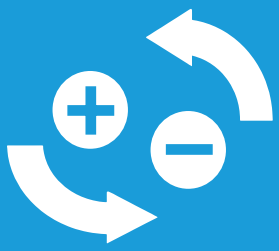

3.4 Internal energy balance of MR01

3. Fundamental analyses of the initial status

In the following chapter, analyses are made to examine the prevailing, current situation at the International Airport Calgary. Beforehand, a comparison between the measured and simulated data is undertaken. The thermal simulation of the building was conducted in February 2017 and is now used to evaluate optimization variants of the building system. The measured data for the cooling demand of the building management system (BMS) is available for the period from May until September in 2017.

As a further analysis, the performance of the heat exchangers in the airport are examined. According to the temperatures on both sides of the heat-exchangers in combination with the mass flows of the fluids, the performances of the heat exchangers in the heating and cooling loop can be calculated.

Furthermore, two sets of weather data are evaluated against each other. The first set of weather data is based on statistical weather data of the last three decades for the city of Calgary. The other weather data set represents the current weather data for 2017. The goal of this analysis is to prove that the statistical weather data is representative of the current weather in Canada.

Subsequently, an analysis of the energy balance of the mechanical room one (MR01) of the airport is performed. Using data from the BMS, an energy balance of MR01 is calculated. The resulting energy balance, applied to mechanical room one, stands representative for the whole building. The determined energy balance should prove that the internal energy flows are fulfilled related to the 1st law of thermodynamics. In this analysis, all in- and output energy flows are measured quantitatively and evaluated according to the system boundary.

3.1 Comparison of the measured & simulated data

As a first analysis of the current status of the airport, a comparison between the real, measured data and the simulation data has been established. The comparison has been done for the cooling demand for the period from May until September. Because the measured data is available from May 2017 and this represents the time of the year, when the cooling demand is much higher than the heating demand, cooling data is used as the basis for the comparison.

With the comparison of the data sets, this section attempts to shed light on the performance gap of the airport. In the course of this master thesis, the gained data will be used to represent the thermal loads of the building and analyze variants of the building system. As shown in the following figure 8, the simulated cooling demand represents at least 60 % of measured demand for every single month. In total, the simulated demand for the four-month period only represents 68 % of the measured demand. This leads to the fact that the predicted energy demand is more than 30 % lower than the real energy demand of the building. In comparison with the other mechanical rooms, the simulation of mechanical room one covers the actual energy demand the most. The simulation of MR01 is coincides better with the actual energy demand than the other mechanical rooms.

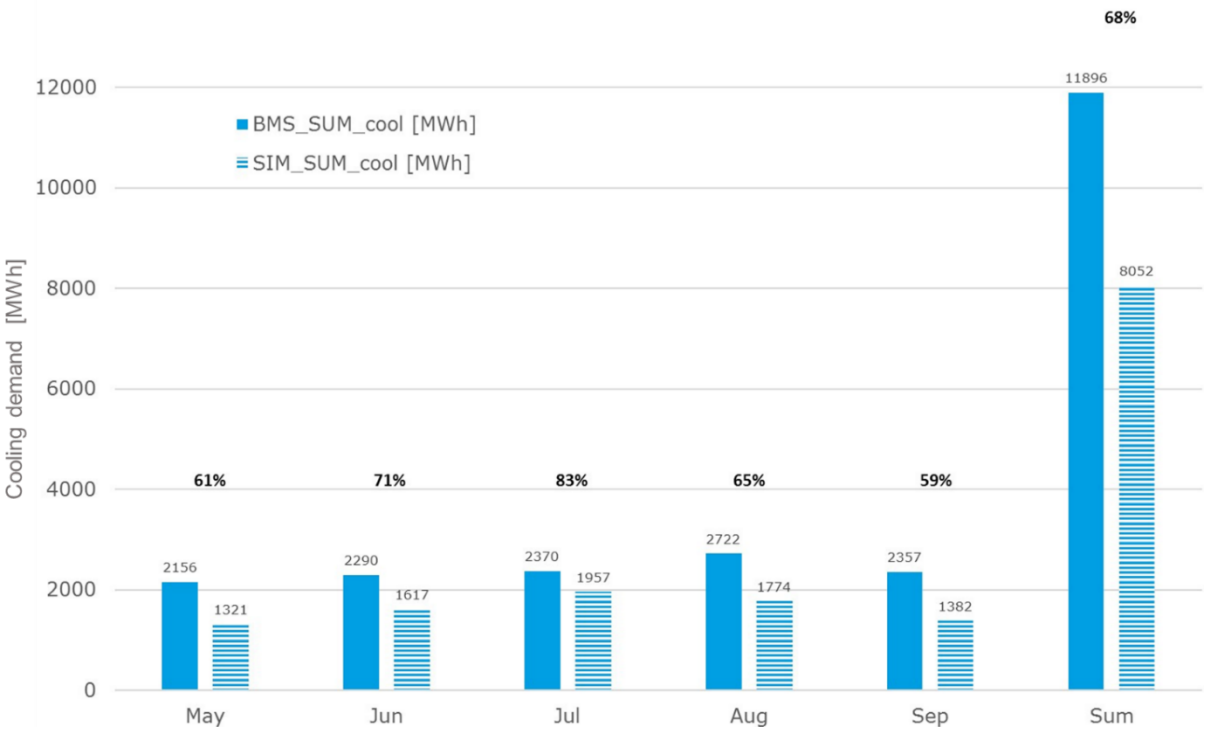

Figure 8 Comparison of the measured & simulated cooling demand

3.2 Analysis of the heat exchangers

One of the main components in the building system of the International Airport Calgary are the heat exchangers. An analysis of the heat exchangers in the heating and cooling system helps to draw conclusions about the quality of a building system. An established method to generate the coefficient of performance of the heat exchangers is an energy balance based on the 1st law of thermodynamics, as illustrated in the equation below.

Energy balance heat exchanger - 1st law thermodynamics [25]

$$\rho_1 \times c_{P,1} \times (T_1' - T_1'') = \rho_2 \times c_{P,2} \times (T_2' - T_2'') \qquad \text{Equ. 2}$$

ρ	Density of a medium	[kg/m^3]
c_P	Specific heat capacity of a medium	[J/(kg K)]
T	Temperature of a medium	[°C]

In general, a heat exchanger is a device which transfers thermal energy from one loop to another while keeping both loops separated from each other. The working media can be represented by fluids or gases. As illustrated in figure 9, a heat exchanger has a cold and a hot side. In case of a plate heat exchanger the thermal energy from the hot side is transferred to the cold side via the plates, according to the 2nd law of thermodynamics. In general, the heat rejection medium has the index 1 and the heat absorbing media the index 2. The incoming flow is marked with the index ‘ and the leaving flow is marked with the index ’’. The heat transfer coefficient depends on the size of the total plate area, the temperature difference and the attributes (viscosity, flow velocity, heat transfer rate) of the medium constituting the two loops. [26]

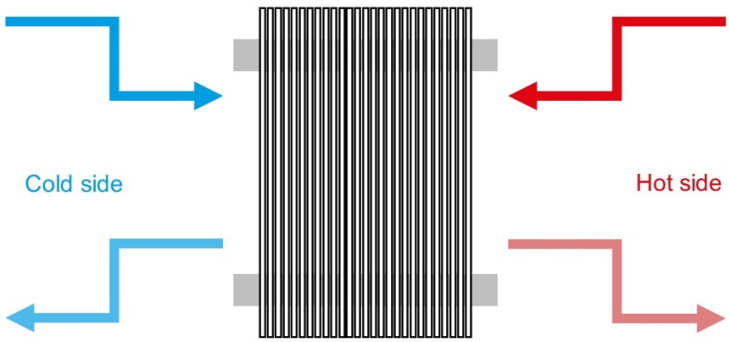

Figure 9 Schematic drawing of a heat exchanger (own representation based on [26])

The International Airport Calgary uses the geothermal field and a heat-pump/chiller system to supply the heating and cooling loop of the building. Since the geothermal loop is operated with a mixture of water and 20 % ethanol and the heating and cooling system is operated with water only, a direct connection between the systems is not possible. This principle is applied to all four mechanical rooms. The heat exchangers with the number HX01, HX05, HX10 and HX14 supply the chilled hot water loop. The heat exchangers HX02, HX06, HX11 and HX 15 use the waste heat of the chillers to supply the low temperature hot water system. A schematic drawing including the HX01 and HX02 which influence the performance of MR01 is included in Appendix A. In the following two sections, the performance of the heat exchangers in the chilled hot water loop (CHW) and low temperature hot water (LTHW) system are studied.

3.2.1 Performance of the heat exchangers in the CHW loop

In figure 10, the heat transfer rates for the five heat exchangers for the chilled hot water loop are shown. The solid bars show the planned design intent for the analyzed heat exchangers, while the dashed bars represent the current power status based on measured data provided by the BMS of the airport. As the data base of this master thesis analyzes the MR01, representing the performance of the entire extension of the airport in Calgary, the heat exchanger of MR01 is colored for clarity. The total calculation is based on the summer period between May and September, when the building has the peak cooling demand. (See external Appendix: calculation HX_CHW)

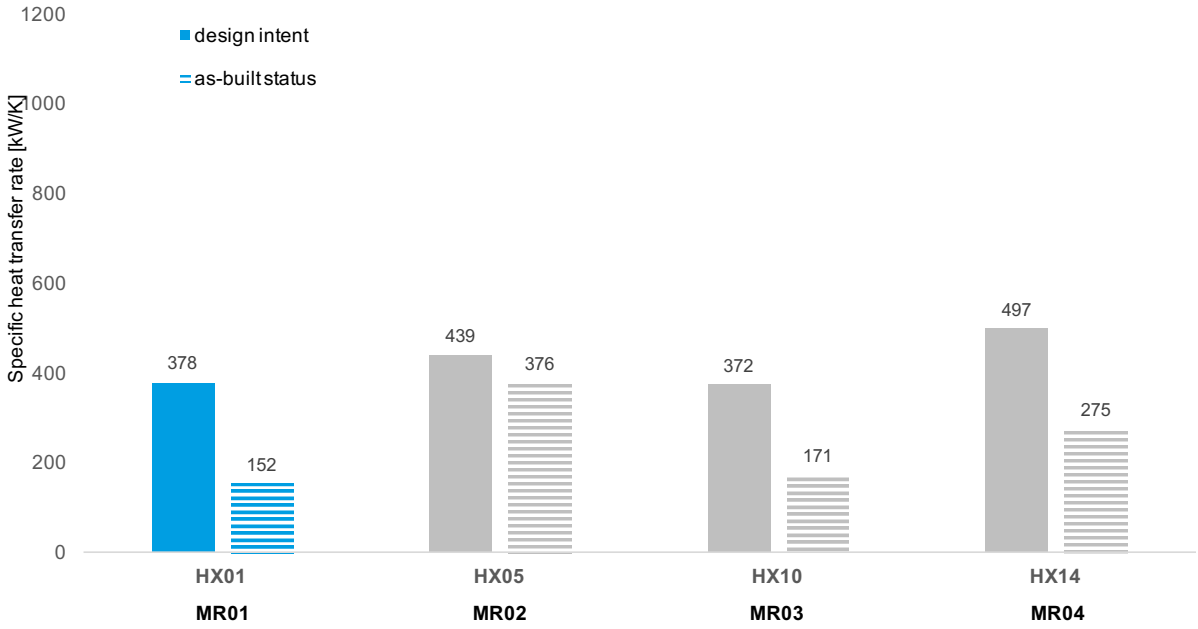

Figure 10 Performance of the heat exchangers in the CHW loop

The specific performances of all heat exchangers in the chilled hot water loop do not live up to the intended design. HX01, HX10 and HX14 only show a cooling performance between 40 % to 60 % of the design intent. This results in the cooling energy demand of the building being much higher than intended. Prior calculations show that the reasons for the low performance of the heat exchangers are, on the one hand, the low specific heat transfer rates of 20-50 % of the initial design. On the other hand, the flow rates of the two separated loops stay below the target value. Furthermore, the volume flow rates on the hot side of the heat exchangers are mainly above the design intent. For a full performance of the heat exchanger these volume flow rates should be switched with regards to the design intent.

3.2.2 Performance of the heat exchangers in the LTHW loop

The analysis of the low temperature hot water system is completed in the heating period of the airport. Figure 11, depicting the performance of the heat exchangers, is structured in the same way as the CHW loop, represented in figure 10. Remarkably, both figures show similar results. As with the exchangers in the CHW loop, all four mechanical rooms do not perform as intended. HX02 and HX06 operate especially badly, with capacities of 20 to 40% of the intended design. In this case, a detailed calculation shows that the volume flow rates on both sides are not consistent with initial design. Furthermore, the heat transfer rate is mainly below the design value. All in all, the heat exchangers in the low temperature hot water system are underperforming. (See external Appendix: calculation HX_LTHW)

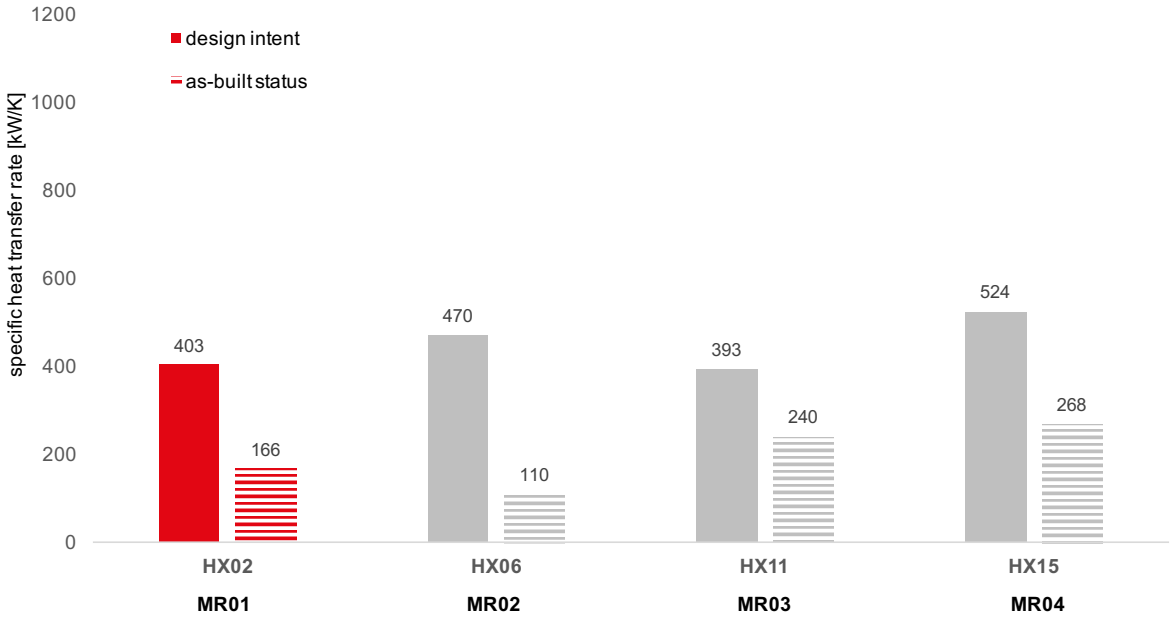

Figure 11 Performance of the heat exchangers in the LTHW loop

3.2.3 Conclusion

As results from the analysis of the heat exchangers on the two temperature levels show, both systems are failing to perform to the level of the set design. Further investigations by the facility operators of the International Airport in Calgary revealed that the heat exchangers of the system are covered with sludge and mud. Fouling can be one possible explanation for the underperformance of the heat exchangers. An optimization of the heat exchangers could be achieved by cleaning the whole heating and cooling loop in order to get rid of the contamination in the system. This is the reason, why in the following analysis the heat-transfer rate of the heat exchangers is set to 0.57. In general, heat-exchangers can reach better performances when they are no contaminated.

3.3 Weather data analysis

One of the main critical aspects of a thermal simulation, as mentioned in section 2.2, is the weather data that influences the thermal performance of a building significantly. This section outlines the local weather conditions in Calgary and describes a comparison of two weather data sets. Based on the fact, that the extension of the airport has been in operation since 2016, it is possible to compare the measured weather data of 2017 with the weather data which was used for the energy simulation in the design process of the edifice. In the following figures the measured weather characteristics are shown. The blue values represent the measured weather data of the airport while the statistical CEWC values are pictured in red.

The measured weather data represents the mean meteorological values of different climate stations in the whole urban area of Calgary. The climate stations are run individually and the data is collected and processed by the Canadian government. In comparison to the opposing dataset, this data shows actual weather data from the year 2017. This service is part of the Climate change program of the government of Canada. [27]

The weather data, used for the simulation, is based on the Canadian Weather Year for Energy Calculation (CWEC). This information is provided by the Government of Canada. The data set contains twelve, typical metrological months, drawn from a selection of 30 years of measurement. The information includes mean, minimum and maximum dry bulb and dew point temperature, global radiation and information about the direction and velocity of the wind system. [28]

In the following sections, the individual climate categories are described and the similarity of the datasets is analyzed. The goal of this analysis is to prove that the statistical data used in the original simulation is accurate and realistic in terms of representing the actual weather situation at the International Airport of Calgary.

3.3.1 Global radiation

The global radiation for the city of Calgary, located in the northern hemisphere, is typically higher in the summer months from April to August. The highest amount of radiation is 210 kWh/ (m^2 a) and occurs in July. Furthermore, a similar amount of insolation can be observed in Calgary in the other summer months. These values cause a constant cooling demand during summer period. Even in the winter period, a small amount of radiation still reaches Calgary and the heating demand can be slightly reduced through solar radiation. [29]

As highlighted in figure 12, the actual data sows very similar results compared to the per monthly totals extracted from the building simulation database. In total, the statistical values are 30 % higher, though the measured data do not provide values for the month of December. The smaller amount of deviation per month, shows that both datasets are alike regarding to global insolation.

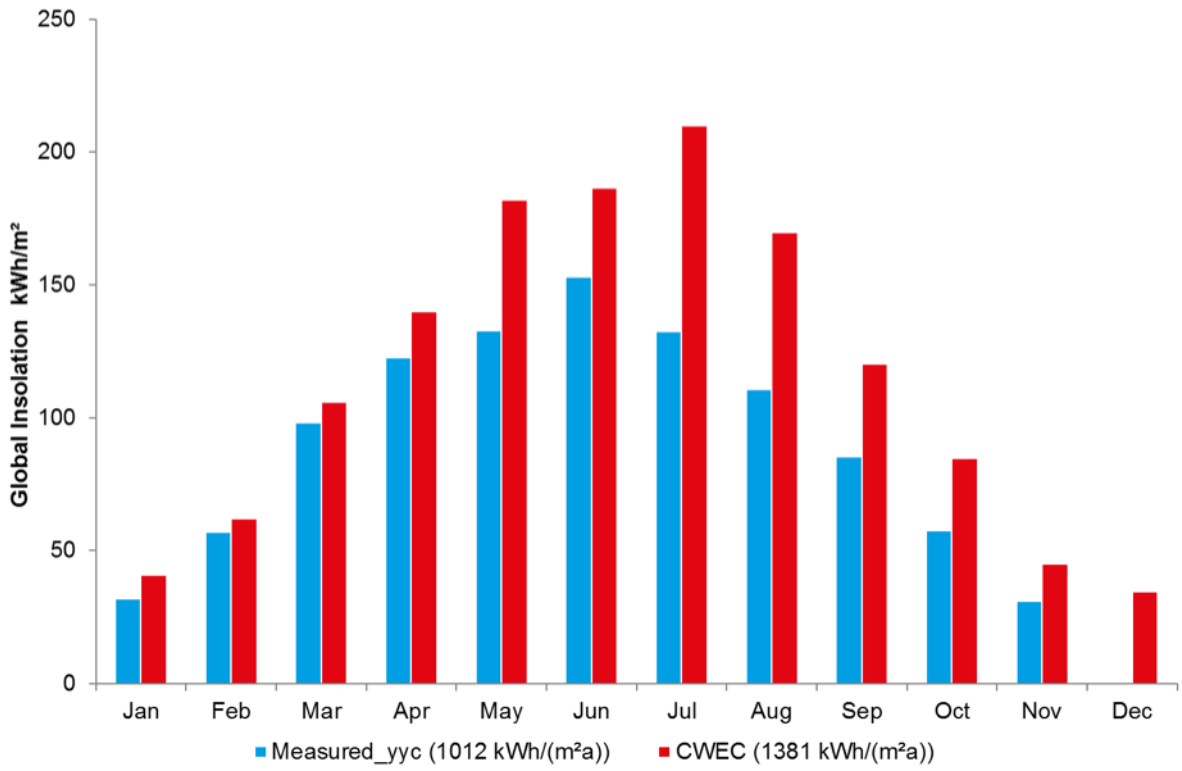

Figure 12 Global radiation Calgary (own representation based on [27] & [28])

3.3.2 Ambient temperature

The continental location of Calgary is represented in the temperature distribution. The mean ambient temperature is around 5°C. The location of Calgary, situated close to the Rocky Mountains is also reflected in the temperature distribution. During the summer period from May to September, the temperatures fluctuate daily by around 20°C. The hottest month is July, with a peak mean temperature of 24°C. In the winter period from October to April, the mean ambient temperature is around the freezing point and the minimum peak temperature of - 20°C is reached from December to February. [29]

The temperature values of the two datasets are, similar to the values of the solar radiation, very congruent. The value distribution of the two datasets display almost parallel outcomes. The values of the CEWC datasets are a little bit more extreme at the peaks of the summer and winter period, but the overall comparison of the ambient temperature shows that the two datasets are similar.

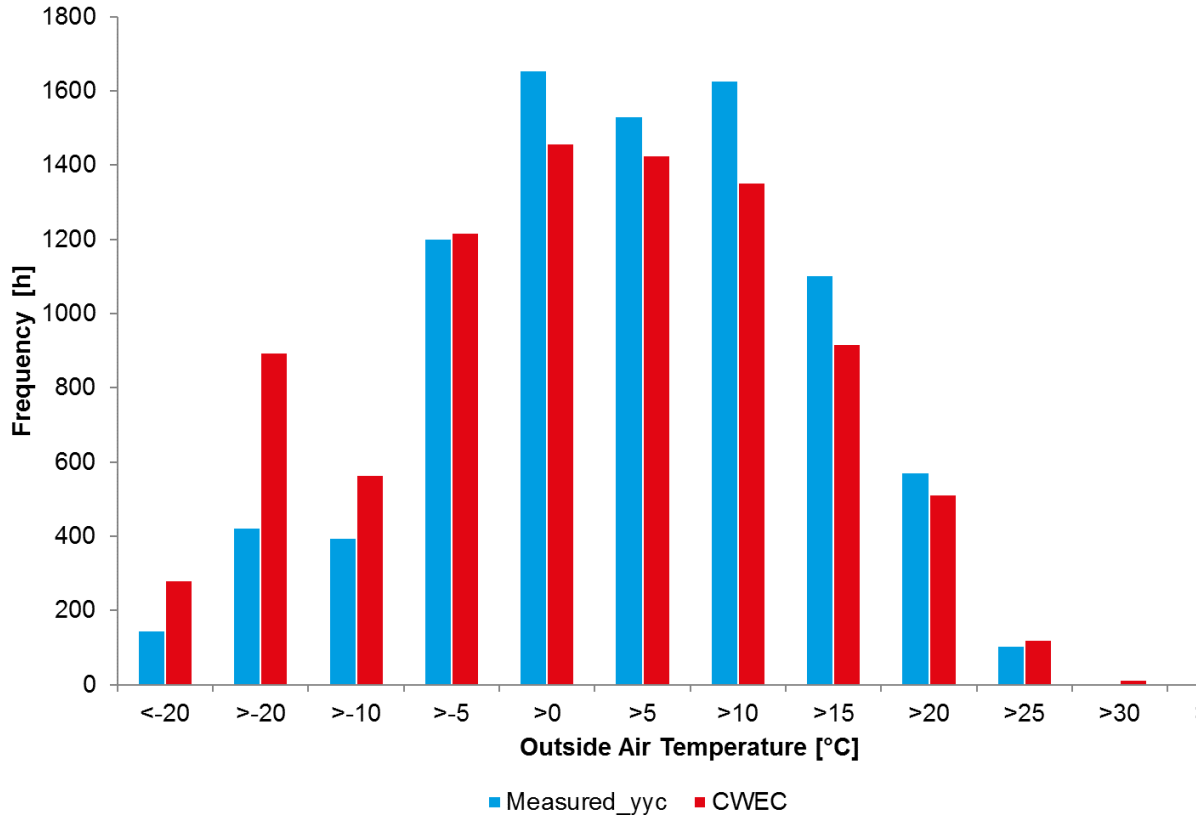

Figure 13 Ambient temperature Calgary (own representation based on [27] & [28])

3.3.3 Humidity

The summer period in Calgary is usually dry and cold, because of its location east of the Rocky Mountains, which prevent the moist air flow from the Pacific Ocean. Compared to an oceanic climate, the cumulative annual precipitation of 220 mm is significantly lower. This leads to low humidity throughout the year. For the planning process of a building, this means that a dehumidifier is usually not required. Short periods of high humidity, such as those occurring during periods of rainfall, are generally not a problem [29]

The ongoing trend of the similarity of the datasets is also seen when looking at humidity. The values of the humidity ratio exhibit close to equal values in both data sets. The difference between the values, pictured in figure 14, is less than 10 % at every step. This leads to the conclusion that the datasets are equivalent in terms of humidity.

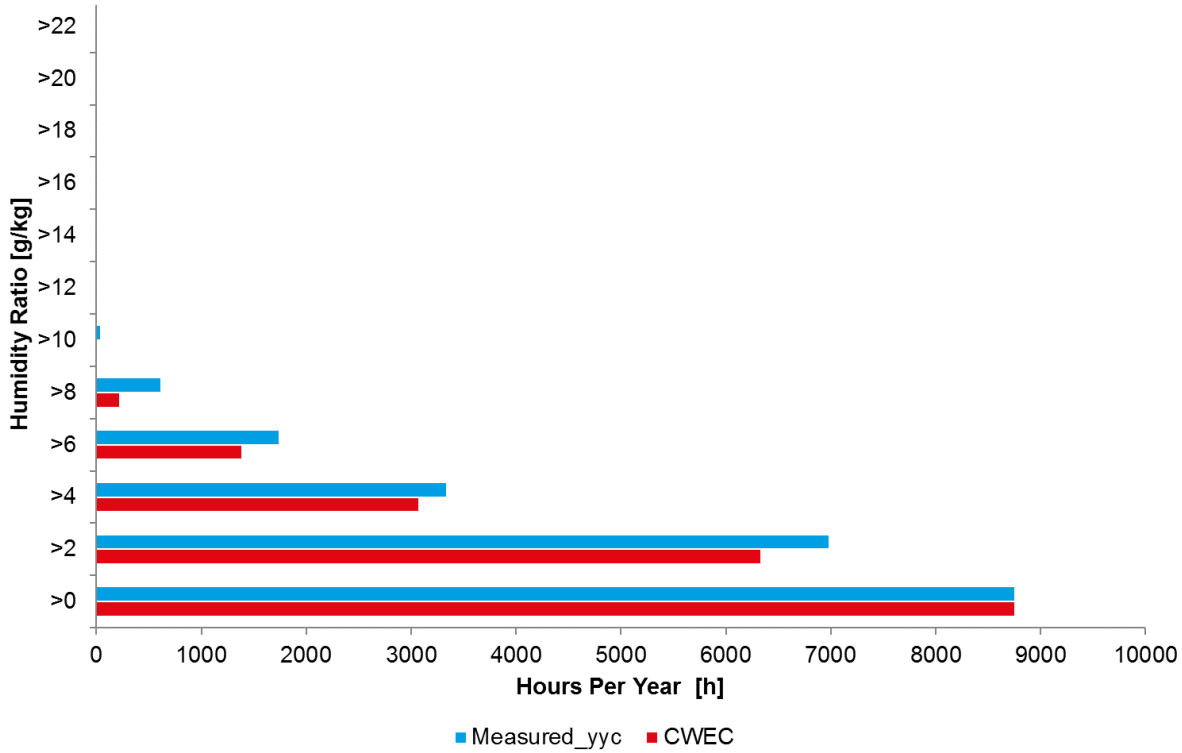

Figure 14 Humidity conditions Calgary (own representation based on [27] & [28])

3.3.4 Wind direction and velocity

The main wind direction in Calgary is north. These winds carry the cold from the arctic region to the prairies. A special phenomenon within the region is the so called “Chinook” that is fairly comparable to the Bavarian “Föhn”. These air streams create very high temperature differences in a very short period of time and carry warm air into the city of Calgary. As an effect, on the one hand the temperature rises and according to that, the thermal comfort in the winter period increases. On the other hand, the sky becomes very clear. The Chinook can free the city of Calgary from ice and snow quickly. The annual average wind speed is 14.2 km/h, which

is one of the highest for Canadian cities. Thunderstorms in the summer period have also become a more frequent sight during the last decades. [29]

The distribution of the wind direction only varies to a small extent. There is just a variation in the occurrence of different wind velocities. The statistical weather data of CEWC shows a wider range and a higher wind velocity than does the measured data from 2017.

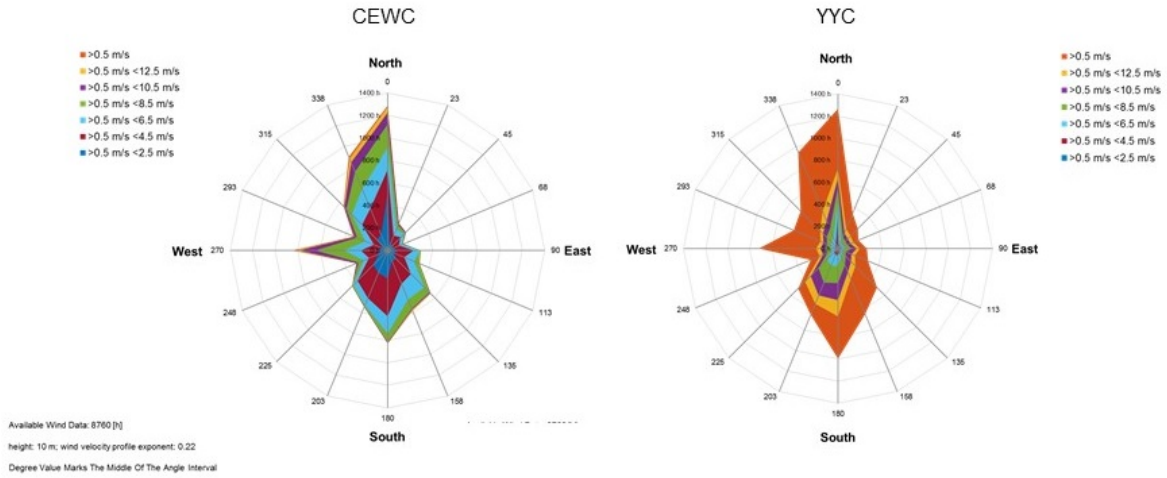

Figure 15 Wind direction/velocity Calgary (own representation based on [27] & [28])

3.3.5 Conclusion of the weather data analysis

All in all, the two weather data sets exhibit very similar values. The assumption presented at the beginning of the chapter, that the statistical weather data from CEWC represent the current weather conditions at the International Airport of Calgary very well, can be seen as validated.

The weather data analysis also shows that the mean temperature in Calgary compared to Munich is lower, but still a summer period exists. The wind transports the cold air streams from the north and sometimes the Chinook relieves the city from the cold by bringing warm air streams into the urban area of Calgary. Further, neither the precipitation nor the humidity affect the planning process of a building. The global radiation is much lower compared to the radiation empirically observable at Munich. For a short summer period, solar radiation is provided. This shows that weather conditions in Calgary are dry and cold, but especially at the International Airport Calgary, with many interior rooms with no connection to the outside of the building, there is a perceptible amount of cooling demand. In TRNSYS, weather data is implemented through a weather type. These weather types contain information about the solar radiation, the wind direction and velocity, the relative humidity, the cloud cover factor and the ambient temperature. With this information, TRNSYS can calculate effects of the weather on the considered building.

3.4 Internal energy balance of MR01

As a further step of the analyses of the initial status in the building system of the International Airport in Calgary, an energy balance of MR01 has been done. This analysis has been performed for every mechanical room. To keep the focus on the results rather than on the mass of analyzed data, this master thesis chooses the MR01 to represent the performance of the whole airport.

In this calculation, every energy flow into and out of the building has been considered. Based on the system boundary, illustrated in figure 16, every energy flow coming into the system is considered positive and every energy flow leaving the system boundary is stipulated as negative. If the total sum of all energy flows is zero, the energy balance is fulfilled due to the energy conversation law under the assumption that no energy storage is integrated in the system. In MR01 the low temperature chilled water system, the high temperature chilled water system and the three boilers are considered as inputs. The high temperature hot water system, the low temperature hot water system and the geothermal energy are classified as energy outputs.

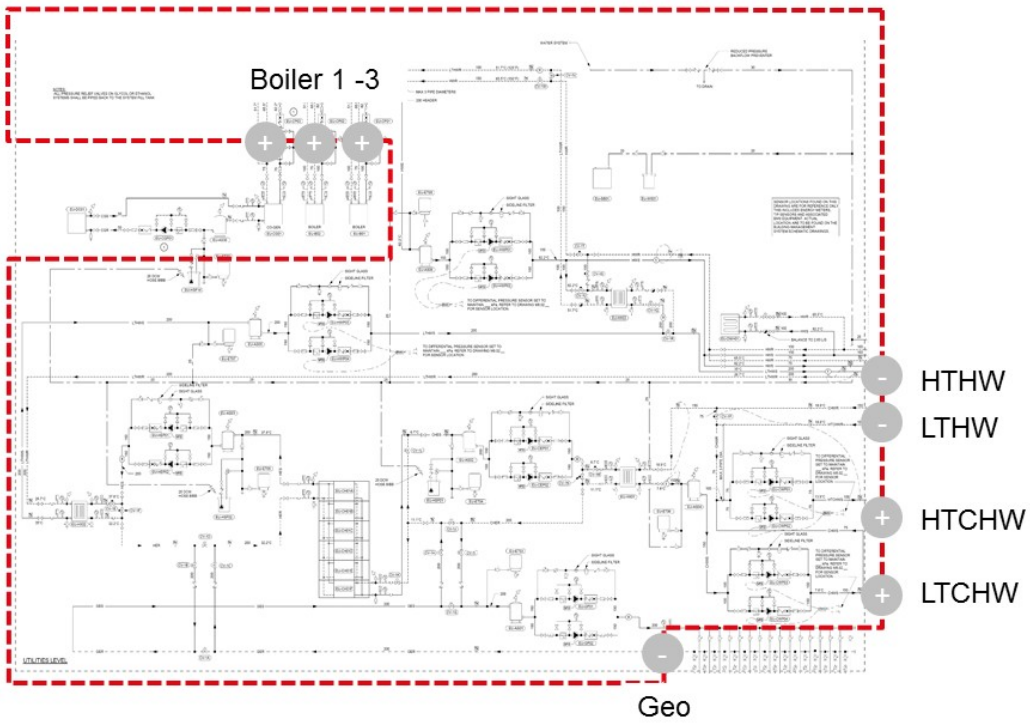

Figure 16 System boundary energy balance for MR01

The results of the evaluation of the trend log data from the BMS are shown in the following figure 17. The calculation error of the energy balance for each of the single time steps (15 min) is smaller than 3 %. (See external Appendix: Calculation energy balance MR). This leads to the conclusion that the individual energy flow is highly reliable. The total energy balance error is at 11.5 %. Overall, the cooling load is much higher than the heating load, which results in an imbalance. Based on this disparity an overwhelming amount of rejected heat must be dumped into the geothermal field. This state appears also in the other tree mechanical rooms. The total energy balance shows that the geothermal field is heating up over the course of the year because more heat is dumped into the geothermal field than is taken out. As mentioned in section 2.5, an imbalanced geothermal field can have negative impacts on the condition of the affected soil and on the ability to operate the building services to their full extent.

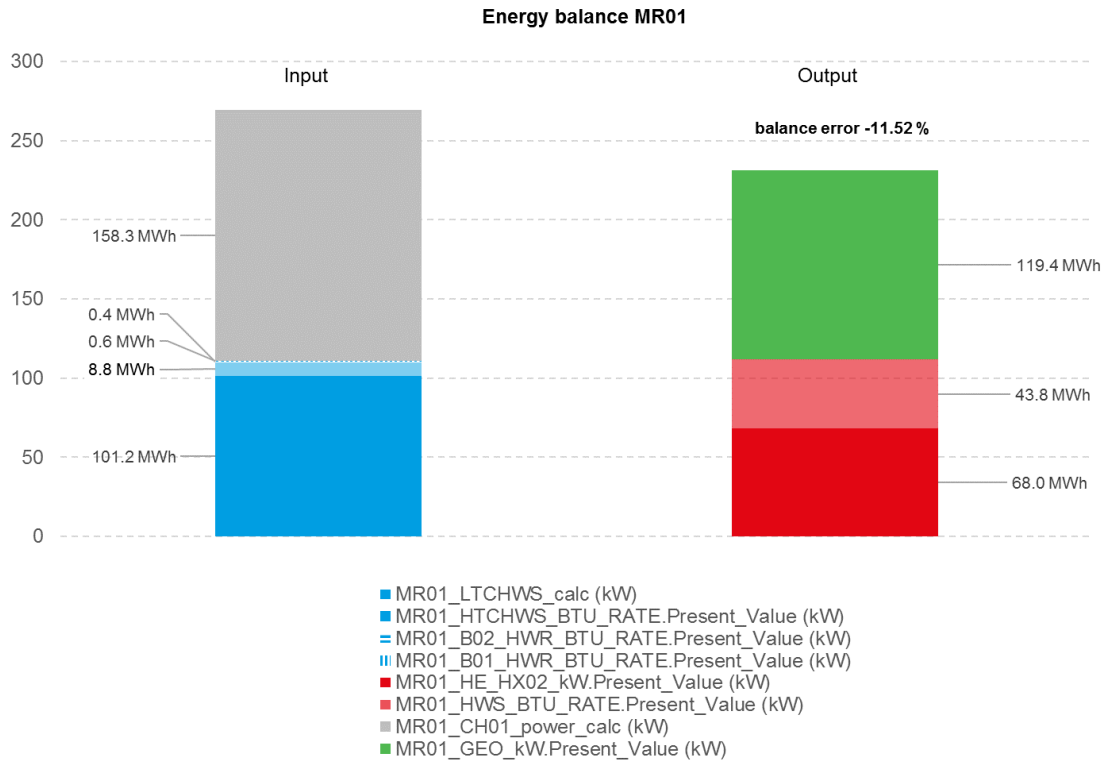

Figure 17 Total energy balance for MR01

4.Project specific data

4.1 Thermal simulation

4.2 Thermal load

4.3 Geothermal system

4.4 System states

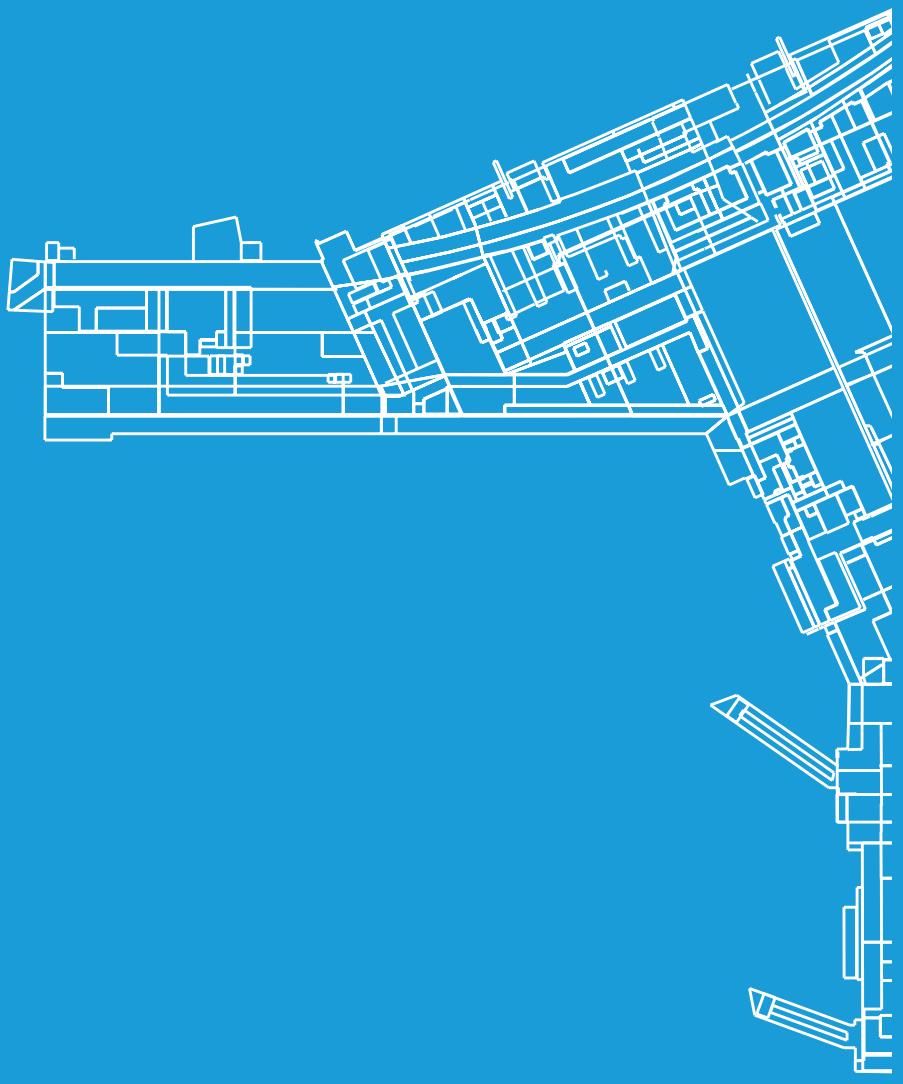

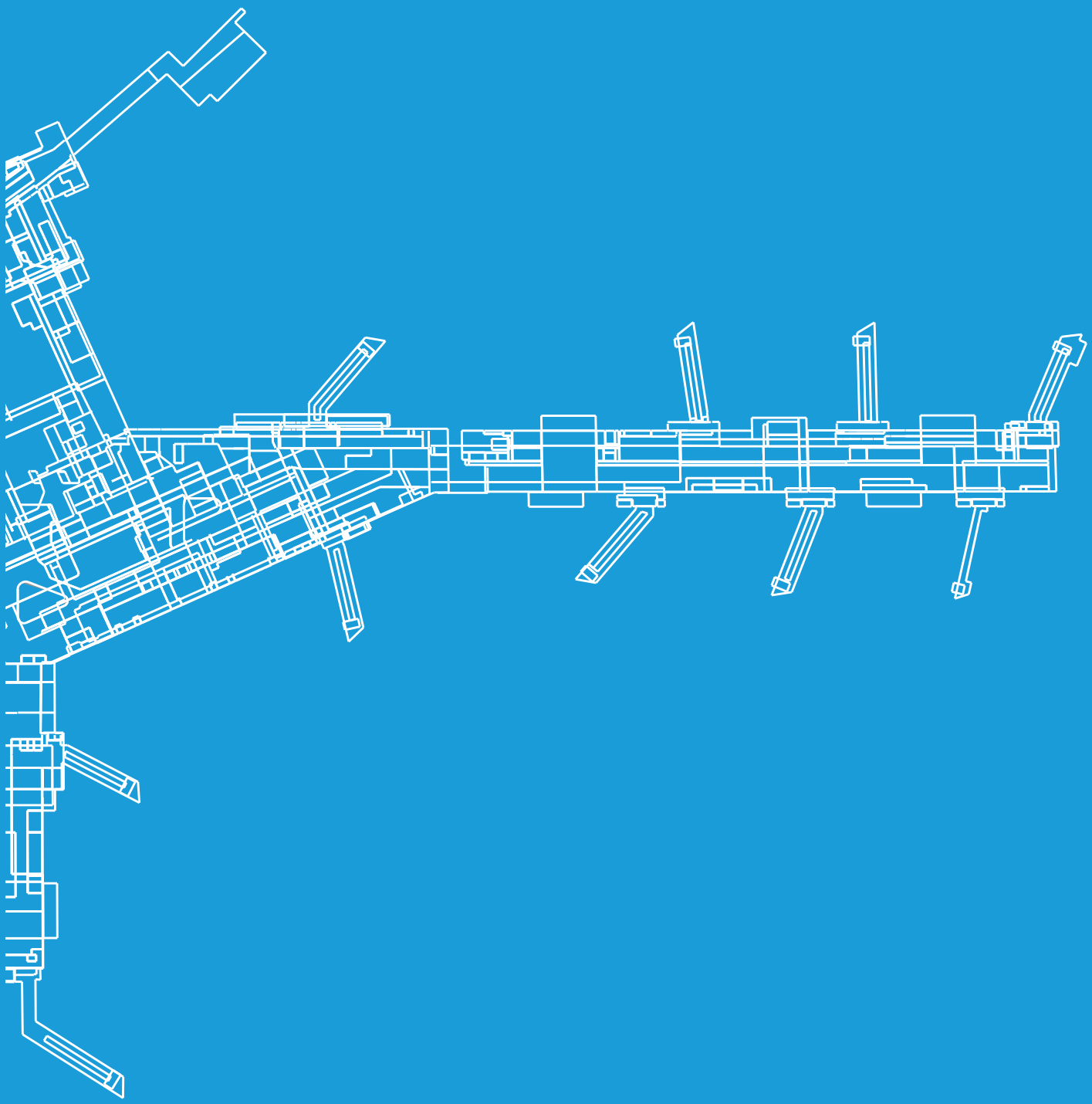

4. Project specific data

This chapter describes the data of the simulation which is related to the project specific data of the International Airport Calgary. The general project information, two internal load categories, the construction, and the operating of the building are scrutinized and illustrated. Firstly, the general structure of the thermal simulation, which correlates with the building loads of the airport, is described. In addition, the thermal load, in the form of an annual frequency as well as the load duration curve, is outlined. A further, important part of the project specific data is generated by taking a closer look at the geothermal field. In chapter 4.3 the characteristic values of the geothermal field of the system in Calgary are explained and the structure of the whole geothermal field is analyzed. Finally, the system states of the building system are addressed. These system states define the six combinations of the components involved with supplying the building with thermal energy.

4.1 Thermal simulation

The International Airport Calgary forms the backbone of the simulation of this master thesis. By extending the international terminal of the airport, a complete new section of the building has been added. This tract was completed in 2016. After further investigation, the operator of the building realized that the building system did not match the intended design and therefore commissioned the *Transsolar Energietechnik GmbH,* in the role of an energy consultant, to investigate the optimization of the building system. Based on the fact, that *Transsolar Energietechnik GmbH* was included in the design process of the extension of the airport itself, a very accurate and detailed thermal simulation model of the building already existed. The loads of this simulation are used to investigate the optimization variants of the mechanical system. This chapter describes the principles and the structure of the airport before scrutinizing the thermal simulation of the building.

In general, the whole extension of the new international terminal in Calgary comprises 167.000 m^2 with a building volume of more than 545.000 m^3. In full operation mode, more than 10.000 passengers per hour should pass through the newly formed terminal. To perform an accurate and detailed simulation, the airport was divided into 17 zones. The 17 zones are distinguished with regards to their usage, construction and occupancy. In Appendix A, a list of all included zones is provided to give an impression of the distribution of the building. Another key factor in the thermal simulation is the construction of the building. In combination with the implemented materials, the orientation and the glazing ratio of the windows, the construction of a building has a huge impact on the thermal conditions in a building. As described in previous chapters, some parts of the input data can be considered as fixed values. Since the airport is already operating, the construction is considered a fixed parameter. With the focus on the simulation being on the HVAC system, a detailed investigation of the airport building's thermal performance is not focus of this master thesis

One can separate the internal loads of the airport into two main categories. The first internal loads are produced by the passengers of the airport. This internal heat source is implemented

in the thermal simulations via individual occupancy rates for each simulation zone. The single occupancy rates are predicted and provided by *Airbiz e.K.*, which is a planning consultancy with that focuses on statistics all around the operation of an airport. Based on the density of people in the airport and individual occupancy rate, the zone-specific loads are calculated and implemented in the thermal simulation. The individual assumptions of the density of people in a zone and the occupancy rates are shown in the accompanying graph with the specific occupancy rates in Appendix A.

The second internal source of heat gains can be traced back to the electrical and mechanical devices. In contrast to residential buildings, an airport has numerous special devices which are additional heat sources. Beyond the standard space uses, like restaurants and retail areas, and devices like a high-performance lighting system and a high number of elevators and screens, there are additional airport specific devices. These special devices, like a baggage handling system with over 12.000 m^3, moving walkways and computer tomography x-ray machines for the security check, are very energy intense and create a huge amount of additional heat. All internal device-based loads that have been integrated in the thermal simulations are also named in Appendix A for project specific information.

A last specific topic concerning the heat loads at the airport is the building mechanical system. The building is provided with heating and cooling energy through 4 main mechanical rooms. The structure of each mechanical room is identical and every single mechanical room supplies one part of the building. In total, the whole building is connected to a geothermal loop with 588 boreholes that, in combination with a heat-pump, supplies the building with water at a temperature level of 35° C. The cooling demand is regulated at a temperature level of 6°C. The single supply temperatures for mechanical ventilation, as well as for the active layer system, are reached through manifolds. For the sake of simplicity, the building system is reduced to one single mechanical room in this thesis. The considered part of the building is illustrated in figure 18.

Figure 18 Location of the rooms supplied by MR01

4.2 Thermal load of the MR01 of the International Airport Calgary

In order to keep the focus of this thesis on the building system, an uncoupled simulation was chosen to represent the thermal load at the International Airport in Calgary. The thermal load is integrated at two regulatory temperature levels. Both, the 6 °C temperature level for cooling and the 36°C temperature level for heating provide supply temperatures for a mechanical ventilation system as well as for an active layer network. The total implemented cooling demand is 971 MWh per year, while the heating load is nearly equal with 963 MWh. Consequently, the load can be described as balanced. As pictured in figure 19, the cooling demand is higher in summer, while the heating load is close to zero. The heating demand rises during the winter period. An ongoing issue of the International Airport in Calgary is the constant cooling demand required year-round. This is due to a high number of internal rooms that are fully enclosed and therefore independent from ambient conditions leading to a high internal load. These circumstances describe a very airport specific situation.

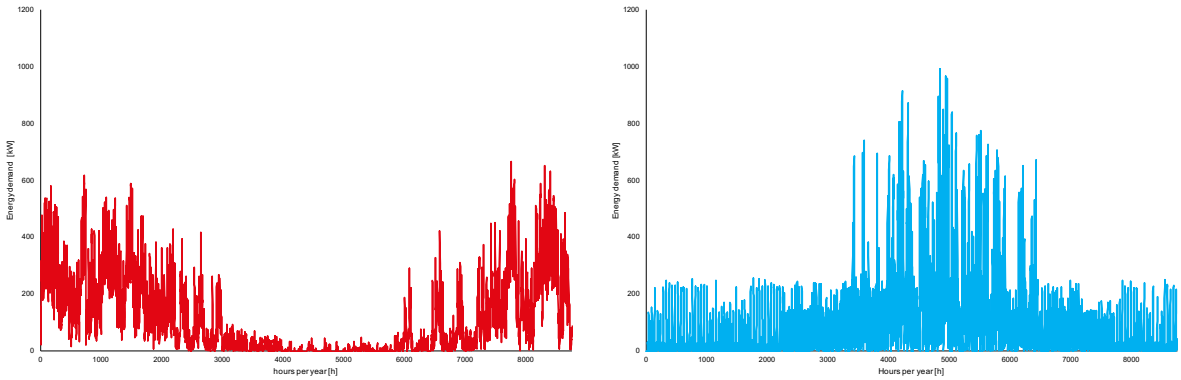

Figure 19 Annual heating & cooling demand

The dimensions of a heat-pump/chiller system strongly depend on the thermal loads of the considered building. Considering that the heat-pump determines the effectiveness of a geothermal loop, the sizing of the heat-pump is a key part of establishing a geothermal heat-pump system. With an implemented heat-pump with 244 kW of evaporator power, the cooling load can be covered with the geothermal heat-pump up to 90.2 % of the year. This is shown in the diagram of the load duration curves. The heating load can only be supplied 74.0 % of the time. With an evaporator power of 477 kW, the cooling load is covered up to 99.5 % and the heating load up to 92.6 %. Based on the fact that the heat-pump/chiller system runs the most efficiently at a part load ratio of 0.7-0.8, the heat-pump/chiller with the power of 244kW is sufficient. The specific details of the power numbers are taken from the correlated screw compressors built by the German company Bitzer. The boundary temperatures of the devices are set from 5°C to 50°C. The specific data sheets of the compact screw compressors by Bitzer are presented in Appendix A. [30]

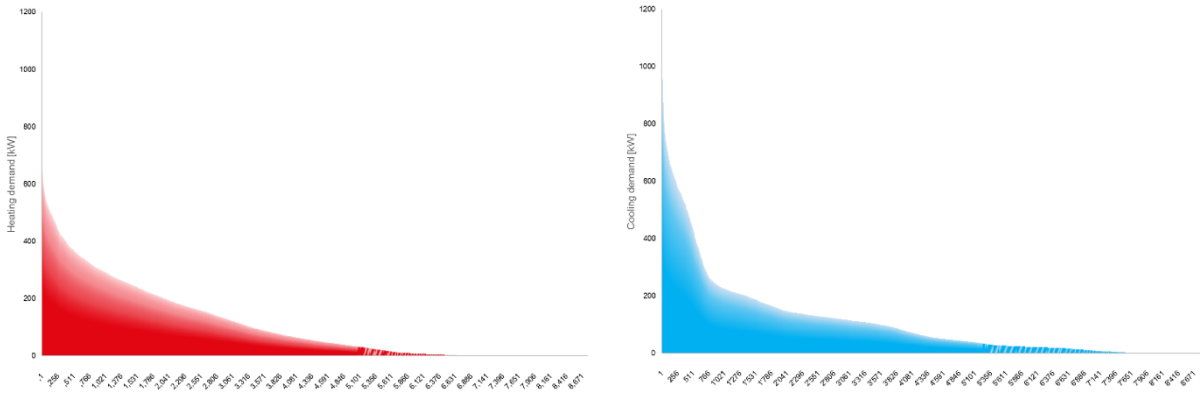

Figure 20 Load duration curve for the heating & cooling demand

As the load duration curves in figure 20 show, the graphs of the heating and cooling demand each form a very high slope at a certain point. This is an indicator for the wide-range of power requirements. In addition, the steepness of the slope and the slightness of the form is a hint at the fact that high power consumption occurs rarely. It can then be concluded that a stage-based heat-pump/chiller system is implemented which is capable of additionally activating another power supply, when the energy demand exceeds the power of a single stage of 244 kW.

4.3 Geothermal system

One of the main renewable energy sources in addition to the sun, wind and biomass, is the energy stored in the ground. This can be used for heat or energy production by implementing a geothermal system. A geothermal system is a typical part of a building system to provide thermal energy. A geothermal field uses the thermal energy stored in the ground and transfers this energy to the building via a network of borehole pipes. By feeding a fluid into the piping system, the energy of the ground layers can be transferred to the medium. In general, the performance of a piping system depends on the thermal conductivity of the pipes and the ground, the flow rate, velocity and the temperature difference between the pipes and the ground. In general, one distinguishes between coaxial, single-, double- and triple-u borehole pipes. In the project of the International Airport of Calgary a single-u pipe is used. The architecture and the dimensions of the borehole are pictured in the subsequent figure. The grout material bentonite has a thermal conductivity of 1.38 W/m K. [21]

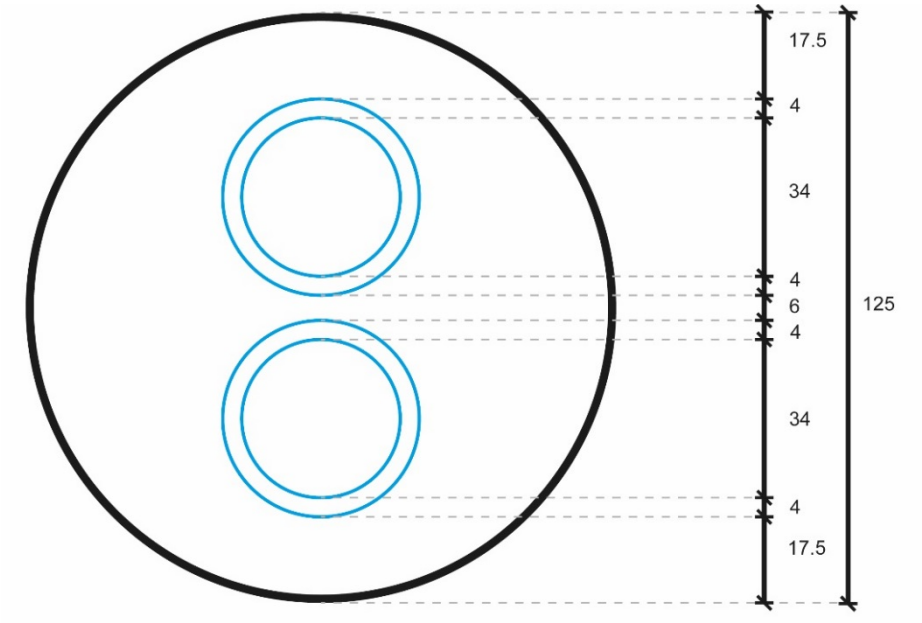

Figure 21 Dimensions of the implemented single-u-pipe [mm]

For the project at the International Airport Calgary the mean thermal conductivity of the mixture of clay and silicate layers in the ground is 2.85 W/(m K). The individual layers with their respective materials are listed in table 1. The ground underneath the airport mainly consists of clay, shale and sandstone. All these materials have a thermal conductivity close to 2.8 W/(m K). The medium in the geothermal loop is a brine of 20 % ethanol and 80 % water. The boreholes reach a length of 132 m.

Table 1 Geothermal layers of the ground in Calgary

Depth [m]	**Delta [m]**	**Material**
4.0	4.0	clay & sandstone
35.4	31.4	grey shale
36.6	1.2	hard sandstone
37.8	1.2	shattered shale
83.8	46.0	grey shale
84.7	0.9	shattered sandstone
132.5	47.6	mixed shale & sandstone
total	132.5	-

The MR01 represents nearly one fourth of the total geothermal loop. The whole building is subdivided into four mechanical loops that each supply individual parts of the airport. The whole geothermal system consists of 588 borehole pipes, while the loop in MR01 uses 128 boreholes which are located according to figure 22. For an analysis of the whole building, the reduction to one part of the building is suitable because the calculation time of the system simulation is highly dependent on the number of boreholes. Furthermore, the set-up of the boreholes in MR01 represent quite accurately the overall geothermal system of the airport because the two systems both have a wide spread and highly dense borehole distribution. As mentioned in the previous chapter, the geothermal loop must supply the energy demand in accordance with the project specific thermal loads of the building, which are supplied through MR01.

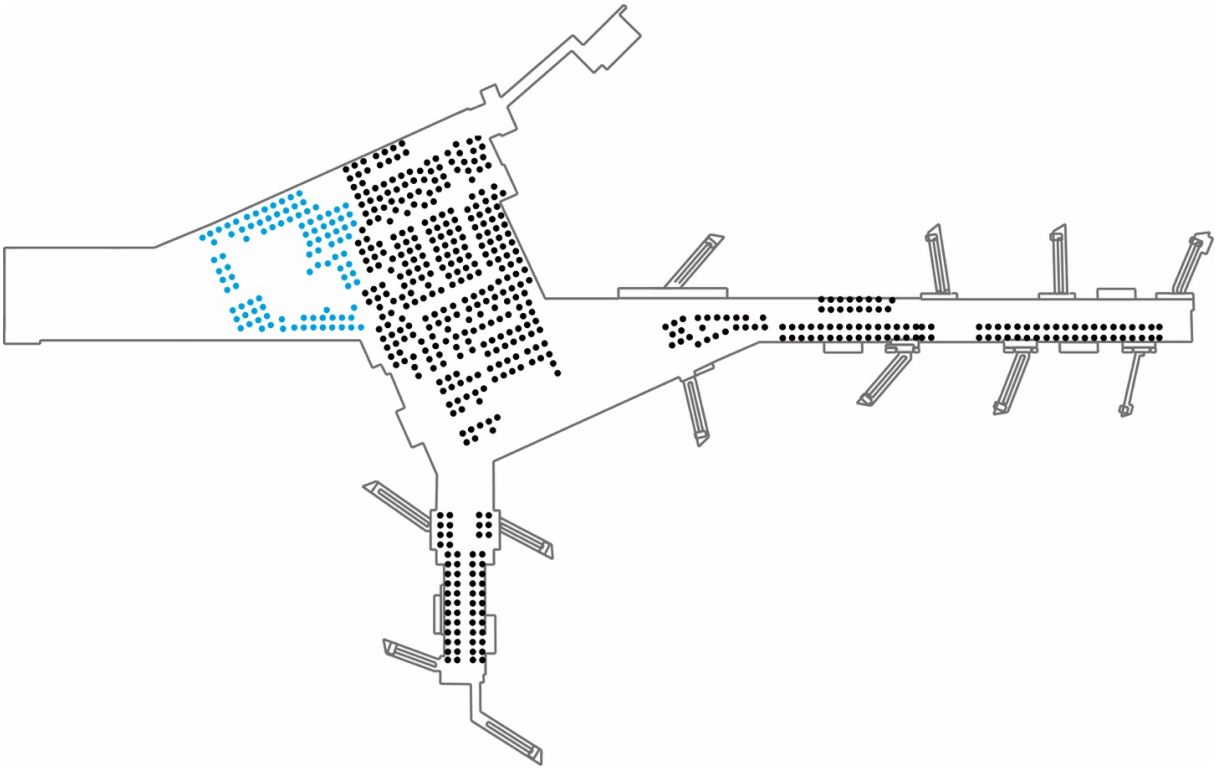

Figure 22 Location of the geothermal boreholes of MR01

4.4 System states

In combination with an energy balance of a building system, besides the mandatory criteria that the energy balance must be fulfilled, a further investigation can be executed. Critical information for the assessment of a system is the state the system is in. In every time step of the analysis, the system can only be in a single system state. The state of a system is characterized by the interaction of the internal components of the system. Every possible combination of the components forms a system state of its own. Once the maximum of theoretically possible combinations has been figured out, one can minimize the number of considered variants by specific boundary conditions.

In the building system implemented at the International Airport Calgary, the system states are defined by the thermally activated loops. The states are distinguished through the two different temperature levels set by the heating and cooling demand. These two temperature levels form four different possible states. In addition, one must differentiate between the thermal source of system states. Thus, the energy can be provided by a mechanical system in form of the heat-pump/chiller device, or it can be run in a so called “free cooling/heating mode”. When both hydraulic separators must be filled up, the heat-pump/chiller device alone provides the thermal cooling and heating energy without the additional help of the geothermal field. In this mode, the component acts as a chiller to produce cooling energy, while the waste heat is used to supply the heating side.

All in all, six system states exist. The schematics of each system state is pictured in Appendix C and is crucial to the understanding of the operation mechanisms integrated into the plant simulation. In the following table 2, the criteria for the six mentioned system states are displayed. If a temperature level is activated in a specific state, it has the value 1 otherwise the value 0 is attributed. The last column gives information about the thermal source of the system state.

Table 2 Overview system states

	Cooling 6°C	**Heating 35°C**	**Therm. Source**
State 1	0	0	-
State 2	1	0	HP
State 3	1	0	free
State 4	0	1	HP
State 5	0	1	free
State 6	1	1	HP

The information of the system state of a simulation is a very useful tool to analyze optimization variants. Based on this information a couple of conclusions can be solidified. Foremost, this analysis of the system states allows for a clarification of which system state is operating the most and which system state is occurring least often. This provides information about the system state, where the main energy flow is transformed. By means of this fact, the necessity of an individual system state can be evaluated. In terms of the concurrency of the individual system states, according to their amount of hours per year, one can work out the settings of the highly efficient states (In this case the free heating and cooling mode). This can be used in the evaluation and comparison of the single optimization variants. Finally, the principle of the system state gives you information about the number of changes of the system state. If the number of changes is low, the service life of the system components is longer, compared to a high number of system state changes. This provides feedback on a system's flexibility to adapt to changes in the circumstances, as well as an information about the longevity of a system. In the end this evaluates the quality of the sizing of the building system. The described analyzing factors are taken as the structural framework of the following outline of optimization variants.

5. Optimization of a geothermal heat-pump system

5.1 Structure of the plant simulation

5.2 Base case model

5.3 Reduction of the geothermal borehole system

5.4 Principles of the variant analyses

5.5 Evaluation of the fixed parameters of the geothermal field

5.6 Evaluation of the adjustable components of the building system

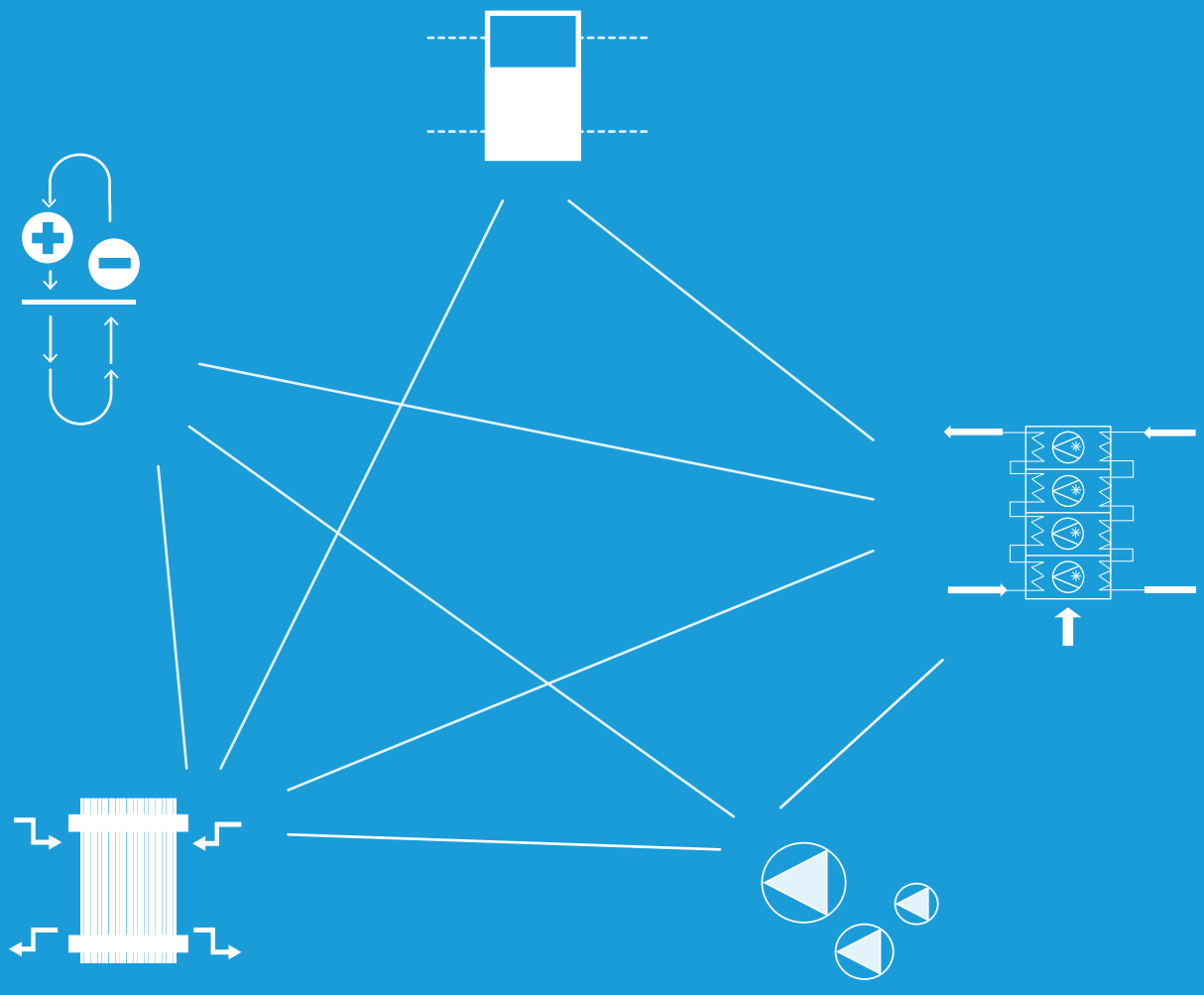

5. Optimization of a geothermal heat-pump system

The main part of this master thesis consists of the analysis of a geothermal heat-pump system through dynamic system simulation. In the first section, the general structure of the plant simulation of the building system is explained. Furthermore, a detailed catalogue of each component of the plant simulation is presented in Appendix B.

In the second section, the base case model of the simulation is conceptualized. In this section, the parameters of the geothermal field, as well as the control strategies and the performance of the components of the base case model are defined. To prove the functionality of the base case model, the overall energy balance, as well as the distribution of the system states are shown. In a next step, the process and the advantages of reducing the geothermal borehole system is explained. The base case model forms the foundation for the following two sections. To create a better understanding of the analyses, their fundamental principles are explained in a further section.

The analyses are carried out within two different categories. Category one deals with fixed parameters of the building system, mainly found in the geothermal field. This category examines the effects of the fluid of the geothermal field, the undisturbed ground temperature, the architecture of the borehole pipes, the thermal conductivity of the ground and the connected building load. Category two, however, looks at the adjustable components of the building services. This category is defined by components which can easily be changed or at least be replaced with reasonable effort. This analysis evaluates the effects of the mass flow, the performance of the plate heat exchangers, the control strategy of the hydraulic separators, as well as the power of the heat-pump. The hypothesis is scrutinized based on the two categories and examines the research questions. Those ask which factors influence a geothermal heat-pump system the most and which category has the bigger potential to create energy efficiency and longevity for a building system.

5.1 Structure of the plant simulation

By using the transient system simulation tool TRNSYS, it is feasible to generate a building system simulation. The fundamental equation solver, which is the core of TNRSYS, makes it possible to calculate the energy flows with an hourly time step. The general structure of the simulation is represented in the following figure 23. In general, the thermal heating and cooling demand is generated by a heat-pump/chiller system which feeds hydraulic separators. Based on the fact, that this master thesis utilizes an uncoupled system simulation, an auxiliary heater and cooler is implemented to match the supply temperatures of the building in every time step. [31]

The main components of the building system are represented by simulation types that can be divided in single subsystems. The whole system can be broken down into eight subsystems. In Appendix B, the functionality, as well as the single control strategies of the individual components can be found. Appendix B is a library for the single components and forms an important part of the thesis. To understand the whole process of the plant simulation it is essential to read the detailed description of the single components. The component catalogue has been included in an appendix to keep the focus of this master thesis on the analyses and the results of the building system simulation.

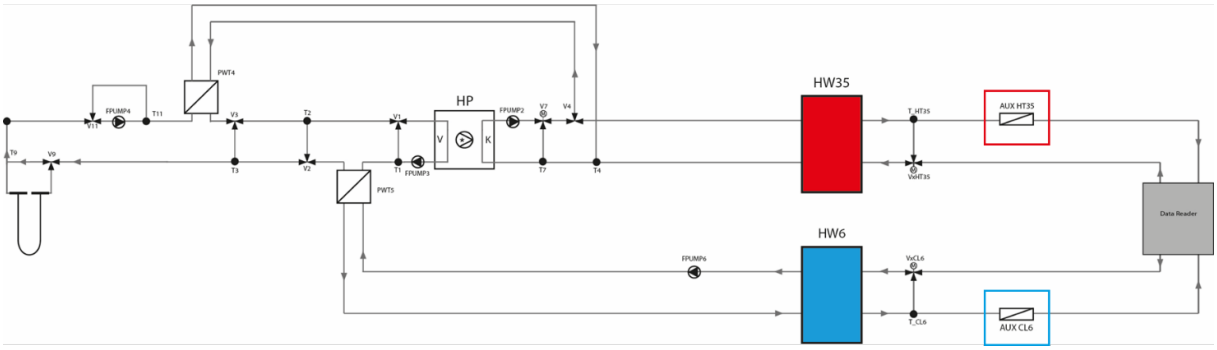

Figure 23 Structure plant simulation

5.2 Base case model

In this section, the variation of the single components of the building system, as well as the characteristic values of a geothermal field are defined according to the project specific values of MR01 of the International Airport in Calgary. In accordance with this, a geothermal energy balance is calculated. This specific combination of values forms the base case model of the analysis. In addition, one can analyze the distribution of the system states and compare these values over an investigation timeframe comprising 10 years.

First, the specific values for the single components are named. The heat-pump/chiller component runs at a stepwise 244 kW capacity. If the energy demand rises above this value, the heat-pump/chiller system has the possibility to activate a further stage with the same amount of power. The hydraulic separators operate with a temperature difference of 5°C related to the supply temperature of the building system. The storage units have a volume of 15 m^3. In the geothermal loop a brine of 20 % ethanol and 80 % water is used as the fluid. The thermal properties of the brine are represented in Appendix A. The heat exchangers perform with an effectiveness of 0.57 according to the designed flow rate of the international airport with the fouling phenomenon. The mass flow is sized according to the 128 borehole pipes of the geothermal system. Furthermore, those pipes have a grout conductivity of 1.38 W/(m K) and a borehole length of 132 m. The ground layers, which are described in the previous chapter, have a mean thermal ground conductivity of 2.85 W/(m K).

In addition, the boreholes have a diameter of 125 mm as represented in figure 21. On the supply side of the system, regular water is used. The whole building system is connected to the heating and cooling demand of the International Airport in Calgary as described in section 4.2.

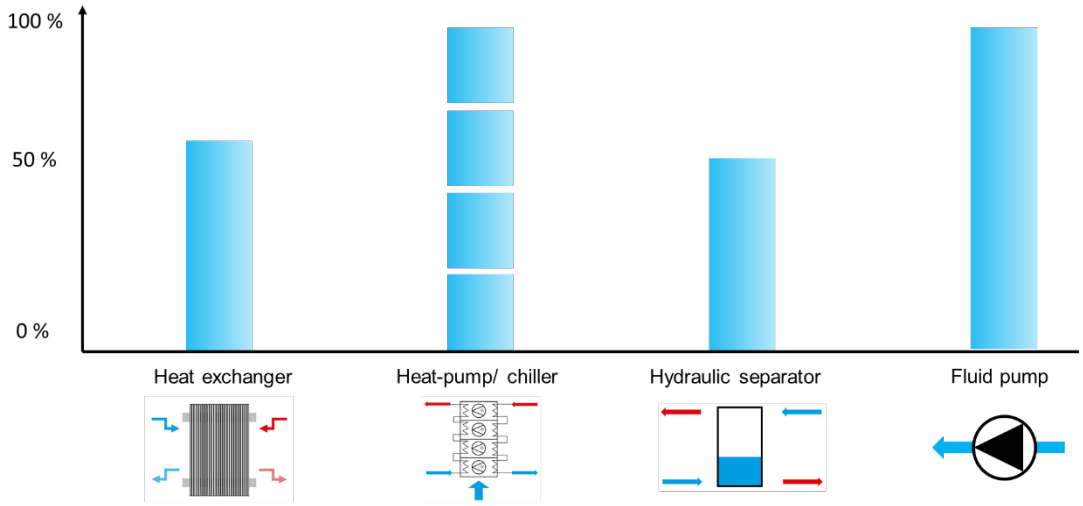

Figure 24 Performance of the components in the base case model

The previous figure displays the performance of the components of the building system. As mentioned before, the first part of the analysis evaluates the fixed parameters of the dimensioning of the geothermal field by varying its characteristic values. This represents the category of the fixed parameters, which must be defined at the beginning of the design process. In a second step, category two, with the adjustable components, is going to be analyzed. In figure 25, the occurrence of the system states in line with the base case model is illustrated.

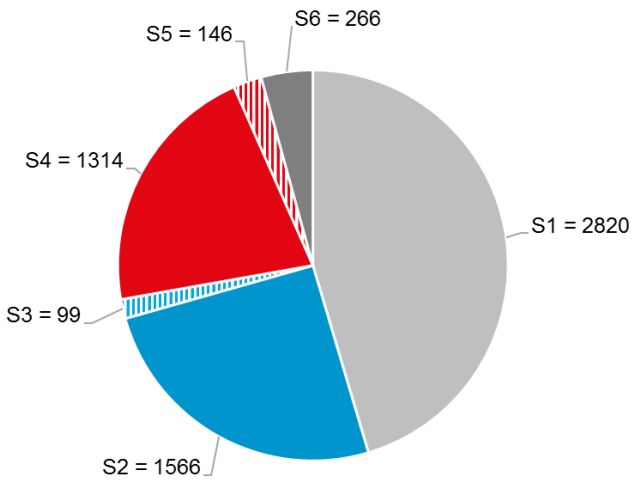

Figure 25 Occurrence of the system states of the base case model [hours/year]

Based on the tank capacity of the hydraulic separators, and in combination with the well performing heat-pump/chiller and the heat exchangers, the base case model operates nearly 50 % of the time in state 1. In this state, the building is supplied by using the energy stored in the hydraulic separators without reverting to the production of energy. State 2 and 4 represent the situations where one of the hydraulic separators must be filled up and the thermal energy is produced by the heat-pump/chiller system in combination with the geothermal field. A free heating and cooling mode, as represented by states 3 and 5, happens just for a short period of the year.

For a total number of 6339 hours a clear system state can be defined. During the remaining hours, the system is changing its state and therefore no defined system state can be observed. If the total number of hours in a clearly defined system state is lower, the system must change its state more often and is not performing as intended. The number of system state changes is an indicator of the performance of a building system.

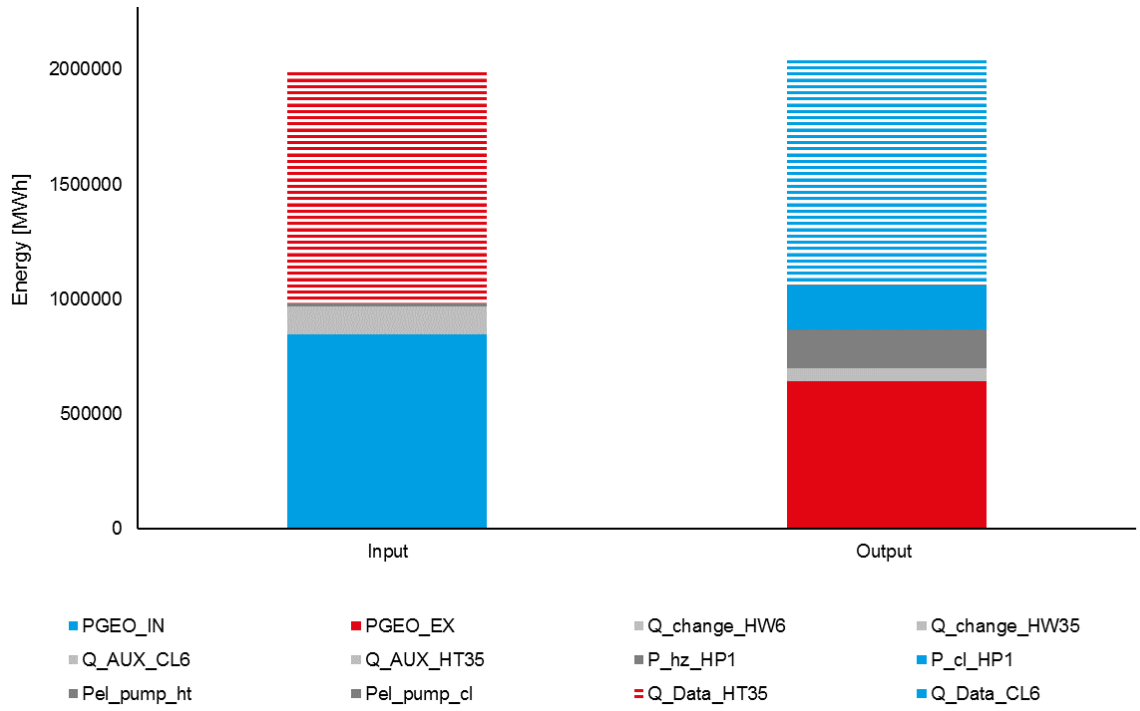

Figure 26 Energy balance of the base case model

The energy balance of the base case model is illustrated in figure 26. The overall balance error is lower than 1 %. In the base case model, most of the 6°C low temperature cooling demand is covered by using the geothermal field in combination with the chiller. Most of the heating demand at the 35°C temperature level is covered by the geothermal heat-pump system. The overall COP for the chiller is 5.9 and the COP of the heat-pump is 3.9. Furthermore, as described in Appendix B, the auxiliary heater/cooler is an indicator for the performance of the whole system simulation. The cooling and heating supply system is supported artificially by the auxiliary cooler/heater with a share of less than 1 % and 3 % of the total cooling and heating

demand respectively. This proves that the whole system simulation is running efficiently and the system can supply the building.

Despite this, the energy balance for every system state, as shown in the next figure 27, experiences small calculation errors. The calculation error for each of the system states never exceeds the value of 5 %. The cause for the single balance errors can be discerned by a time step based analysis. By changing the system state in a single time step, the system does not know what to calculate while the system state is changing. During this short period of time, the energy balance is not performed 100 % correctly and this thus leads to the small amount of balance errors for each system state. In addition, a thermal bridge for the piping system, as well as for the hydraulic separators is implemented and also results in small energy losses.

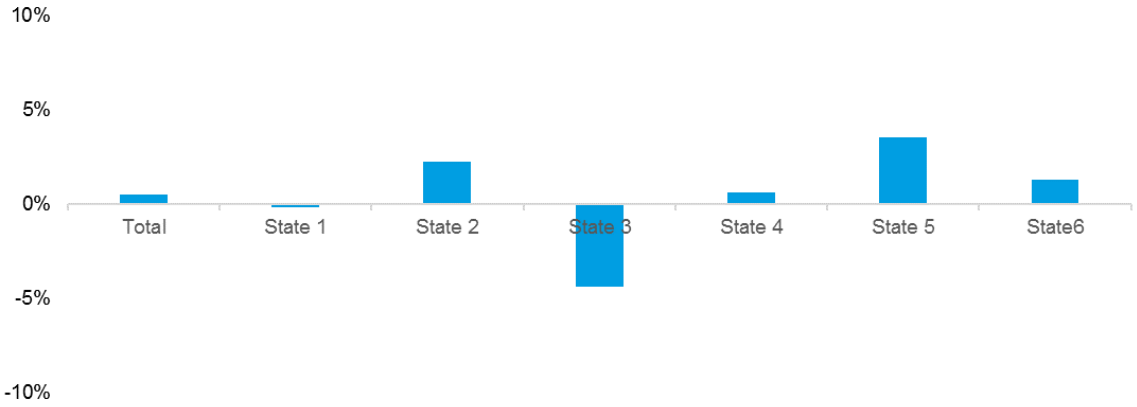

Figure 27 Energy balance errors per system state for the base case model

5.3 Reduction of the geothermal borehole system

By reducing the number of geothermal borehole pipes, the calculation time decreases dramatically. Since many variants must be calculated for this analysis, the reduction of the computation time is important. The most important issue about lowering the number of geothermal pipes is that the reduced pipe system must represent the original geothermal system. To verify that the reduced model represents the initial situation and leads to comparable results, it is evaluated according to the outlet temperature of the geothermal field, using both a balanced and imbalanced load.

When the number of borehole pipes is reduced, the heat transfer for the single borehole pipes is scaled up accordingly. The following development of the temperature shows that for an imbalanced load, where the cooling demand is 20 % higher than the heating demand, the area around the geothermal field heats up during the summer and winter period. This is especially true close to the geothermal borehole pipes, represented by the blue peaks (figure 28). Due to the fact that the building load is imbalanced, the temperatures in the summer increase significantly and even in the winter period the ground temperature rises.

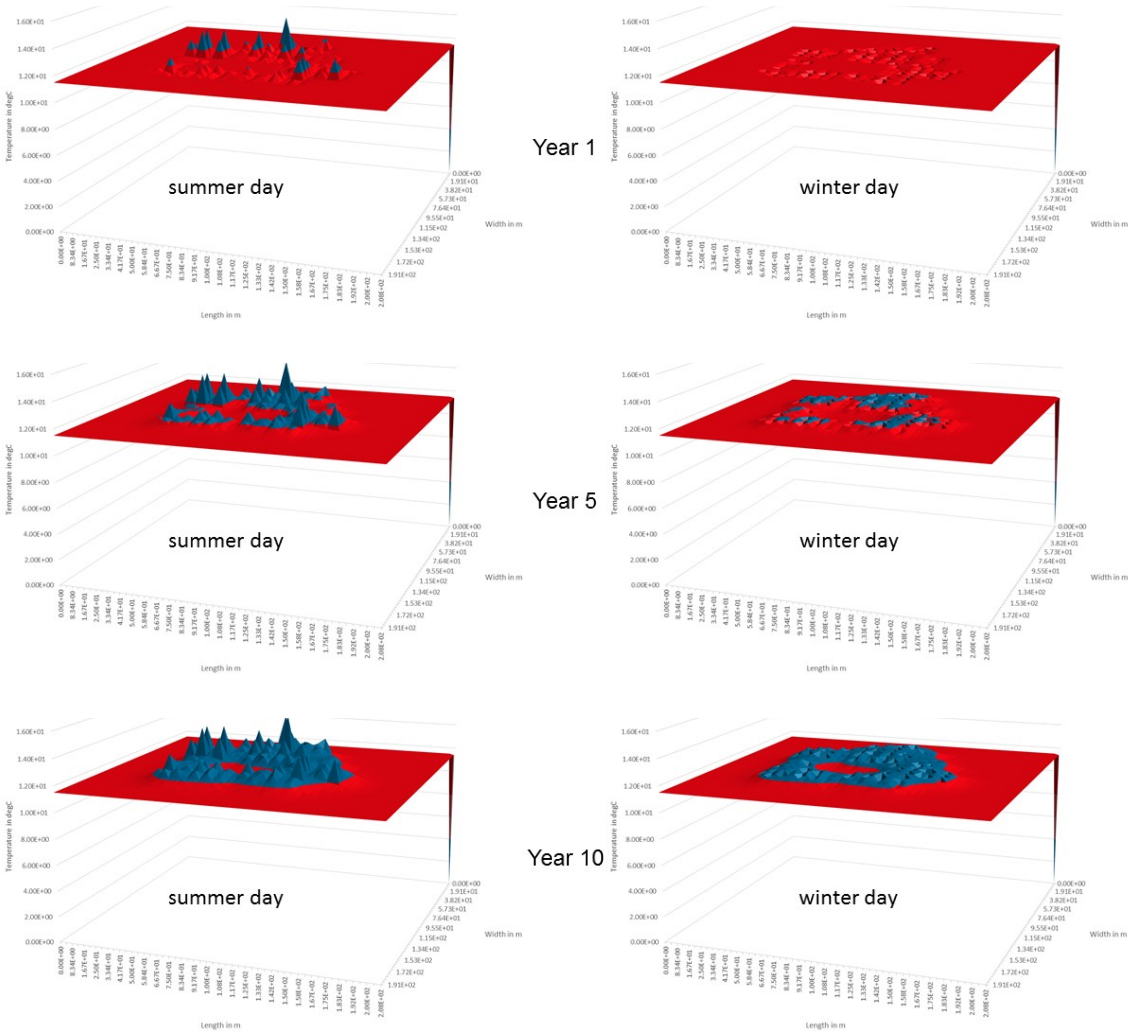

Figure 28 Development of the temperature level of the geothermal field over 10 years

In the following illustration (Figure 29), the different borehole pipe models are presented next to each other. The 128-pipe model represents the actual situation of MR01 of the International Airport Calgary. In contrast, the 9-pipe model is symmetrically designed with 3x3 borehole pipes. The 24-pipe model is also symmetrically arranged, but the inner borehole is left out to represent the current situation of Calgary. Based on the fact that the individual boreholes interact with each other in combination with the specific arrangement in Calgary, the 24-pipe system fits quite well to the real project situation.

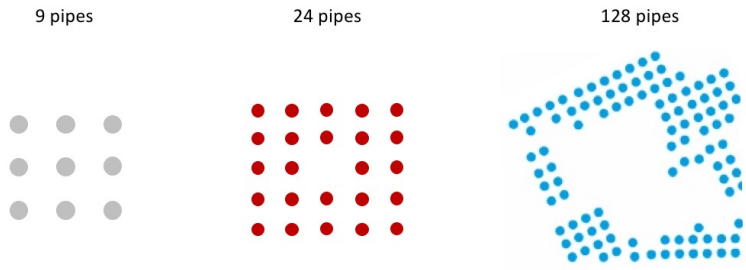

Figure 29 Overview of the pipe models

The comparison is accomplished by considering the outlet temperature of the geothermal field over a calculation time of 10 years. The analysis has been done on a typical summer and on a typical winter day when the system is operating in a single system state. The first comparison of the pipe models bases on a balanced load of heating and cooling demand. The illustrated comparison (Figure 30) shows that the real situation represented by the 128 boreholes is almost congruent with the other simulated pipe models. In winter, there is nearly no difference between the three models. In the summer time, the 24-pipe system reaches values around 1 K above the outlet temperature of the 128-borehole system. The 9-pipe system matches the values of the 128-pipe system with a temperature difference of 2-3 K. The preliminary analysis shows that both reduced pipe models correspond quite well to the 128-pipe system. The colors of the single variants in the following graphs (Figure 30 & 31) are correlated to the colors of overview of the pipe models (Figure 29).

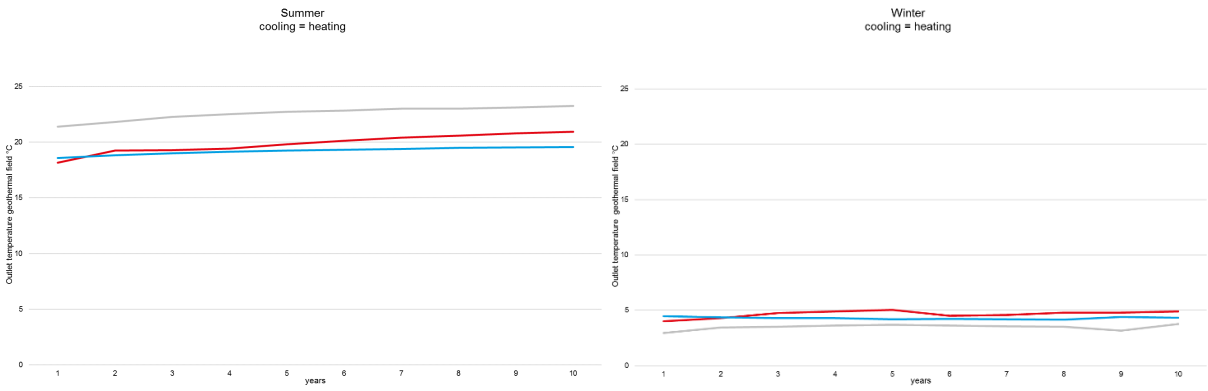

Figure 30 Comparison of the pipe models in summer & winter for a balanced load

To gain a deeper insight into the single pipe systems, the load of the system has been altered. Based on the fact that the performance of the total building system depends very much on the load, two imbalanced loads have been added. The upper two graphs of figure 31 show the outlet temperatures in winter and summer for an imbalanced load where the cooling demand is 20 % higher than the heating load. On the opposite side, the lower two graphs show the exact complementary situation. In these graphs, the heating load is 20 % bigger than the cooling load. The three different loads are described in detail in section 5.5.5, where the characteristic parameters of the geothermal heat-pump system are analyzed.

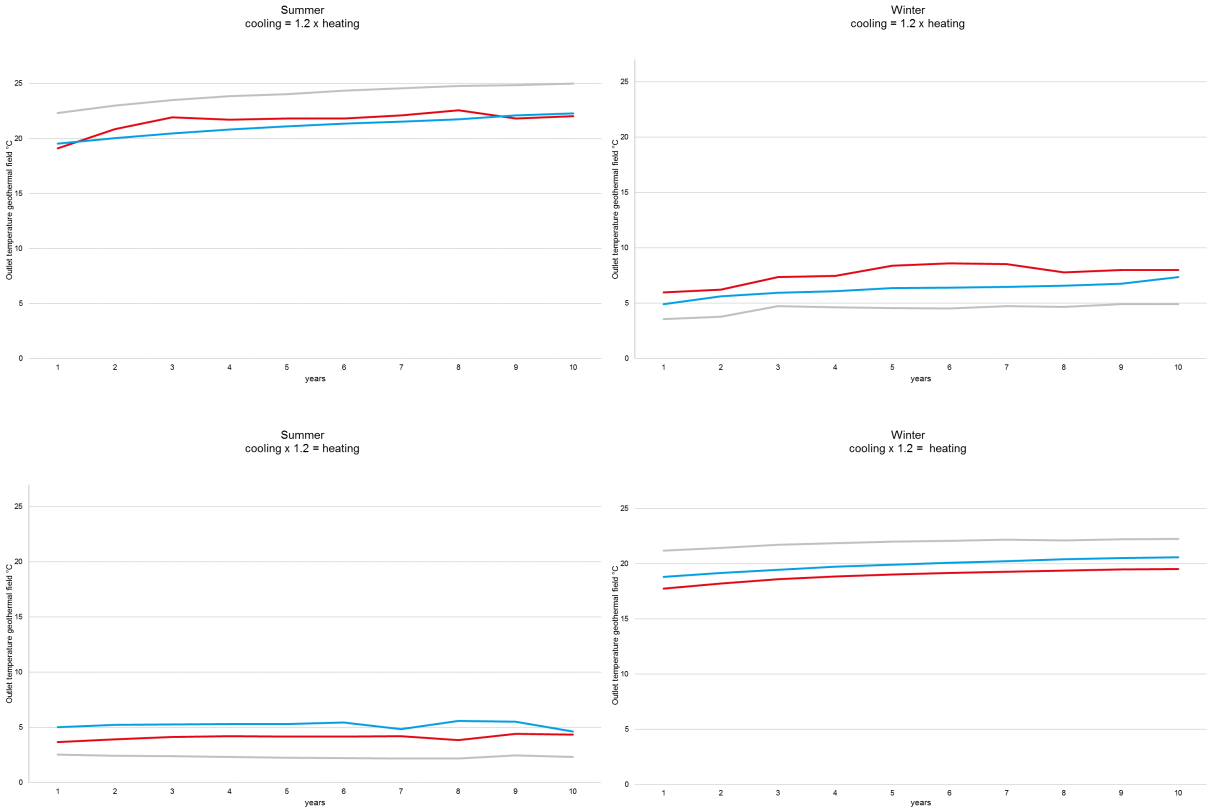

Figure 31 Comparison of the pipe models in summer & winter for imbalanced loads

Both variants running an imbalanced load show that the 24-pipe system matches the original configuration of the International Airport Calgary more accurately. Especially on summer days, the 9-pipe system is not as precise as the 24-pipe model. The computation time for one year varies enormously for the different pipe systems. The 128-pipe model simulation requires 94 minutes to compute one year. The 24-pipe model and the 9-pipe model need 3.5 and 1.8 minutes respectively for simulating a year. This results in the fact that the 24-pipe system provides a good combination of a short calculation time and sufficient accuracy representing the original situation of the International Airport in Calgary.

5.4 Principles of the variant analyses

To create a better understanding of how the analyses are going to be compared, this section describes the method of the evaluation. To rate the quality of the variants, this thesis uses the required non-renewable primary energy demand per year as well as the value of the number of system changes per year, simulated in a 15-minute time step. The total number of time steps thus is 35.040.

The number of system changes gives feedback on the longevity of the building system's components. Therefore, the manufacturers of heat-pumps, fluid pumps, and valves give a warranty for their devices according to the total number of switch-on processes.

Furthermore, the usage of non-renewable primary energy represents the quality of a variant in regards to energy efficiency. The less non-renewable primary energy an optimization variant employs, the less total energy or the more renewable energy this system variant uses. This is an indicator of an energy-efficient building system. The non-renewable primary energy required by geothermal-heat-pump system is defined by the auxiliary heater/cooler, the electrical energy for the fluid pumps and the electrical energy of the heat-pump. The individual principles of the auxiliary heater/cooler are explained in Appendix C, where all components of the plant simulation are expounded upon in detail. To keep the calculation simple, in combination with the fact that the electrical energy demand of the auxiliary heater/cooler is minor in comparison to the other sources for non-renewable energy, the COP of the auxiliary heater/cooler for both temperature levels is set to 1. The primary energy factor for electricity with 1.6 is chosen in accordance with the new German code DIN 18599-10 of 2017. [3]

The following figure shows the evaluation diagram of this master thesis. The x-axis defines the number of system changes per year, while the y-axis represents the total amount of non-renewable primary energy. The diagram is subdivided into four parts. The two upper parts display a bad performance in accordance with the non-renewable primary energy. The two areas to the right do not perform well in the sense of longevity. A building system is most efficient, when it is in the lower left part of the diagram in figure 32.

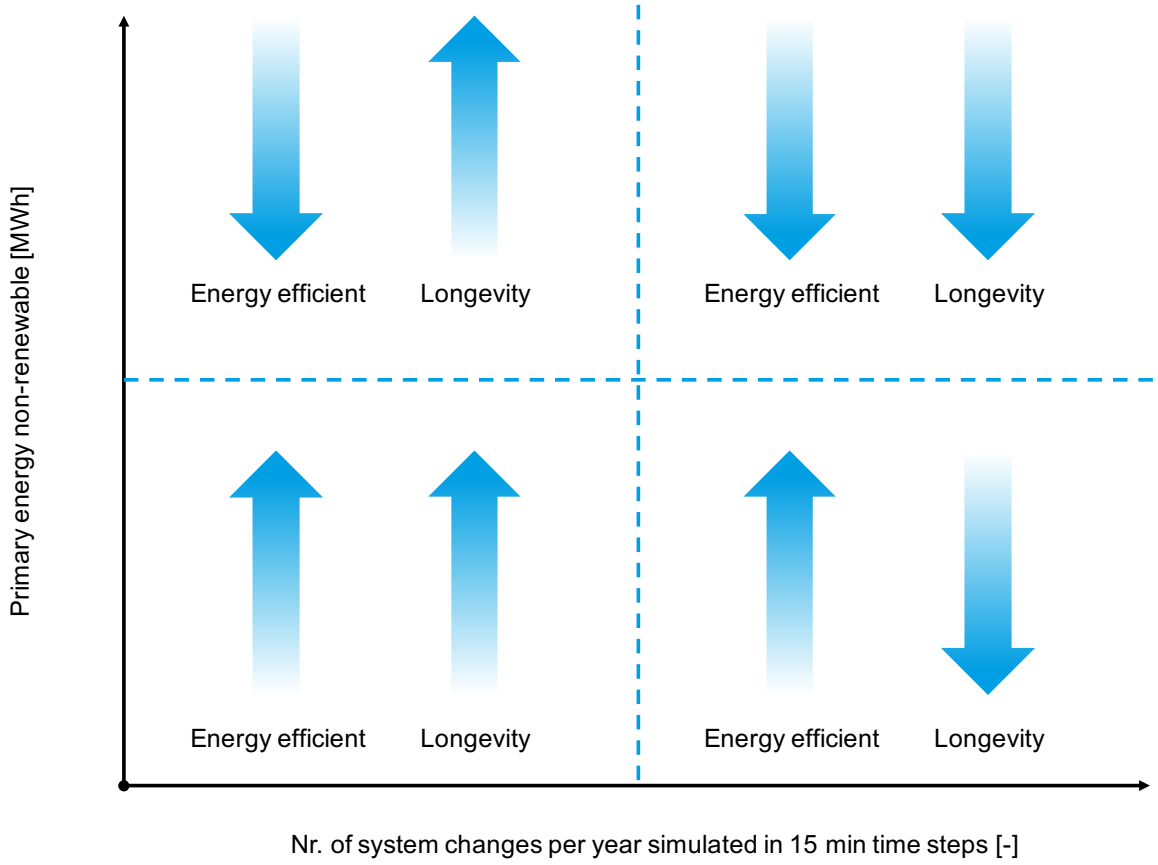

Figure 32 Evaluating diagram for building system variants

5.5 Evaluation of the fixed parameters of the geothermal field

This section examines characteristic values of a geothermal field. The dimensioning of the geothermal field must be done at the beginning of the design process of the building system. This optimization category represents factors which cannot be adjusted over the life time of the building system. The values of the optimization variants are compared with the base case model described in the previous section 5.2. An overview of the analyzed values is depicted in the ensuing figure 33. By changing and comparing the values to the initial status, the impact of the individual values can be distinguished. In the attached section, five categories of characteristic values are parsed. This thesis scrutinizes the thermal conductivity of the ground, the undisturbed ground temperature, the fluid used in the geothermal loop, different variants of the architecture of the geothermal borehole pipes and a variation of different building loads. In section 5.6 the operational variations of adjustable components of the building system is performed.

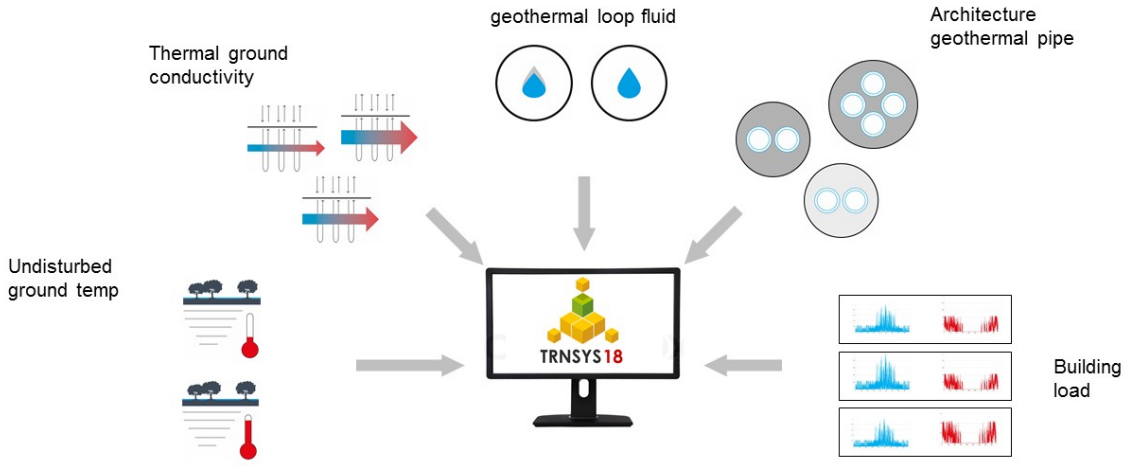

Figure 33 Overview of the fixed parameters of the geothermal field

5.5.1 Thermal conductivity of the ground

The first value that is of a significant influential nature to the performance of a geothermal heat-pump system, is the thermal conductivity of the ground. For the International Airport of Calgary project, the mean thermal conductivity of the mixture of clay and silicate layers in the ground is measured at 2.85 W/(m K). The thermal conductivity describes the energy flow in form of heat through a body, in this case the ground. The thermal conductivity is thus a material specific property which characterizes the thermal behavior of a material. The thermal conductivity depends on the density, the thermal diffusivity and the specific heat capacity of a ground. It can be calculated according to the following equation.

$$\lambda_{th} = \rho_{th} \times c_p \times a_{th} \qquad \text{Equ. 3} \qquad [21]$$

λ_{th}	Thermal conductivity of the ground	[W/(m K)]
ρ_{th}	Density of the ground	[kg/m^3]
c_p	Specific heat capacity	[J/K]
a_{th}	Thermal diffusivity	[m^2]

To evaluate the influence of the thermal conductivity of the ground, two further variants of the geothermal heat-pump system have been calculated for 10 years. In the following diagram, the number of system changes per year is contrasted with the non-renewable primary energy consumption per year. The three variants just differ in the thermal conductivity of the ground. The base case model is pictured in grey, while the variants with different ground conductivities are illustrated in blue. The thermal ground conductivity is set to vary between 1.8 and 3.8 W/(m K).

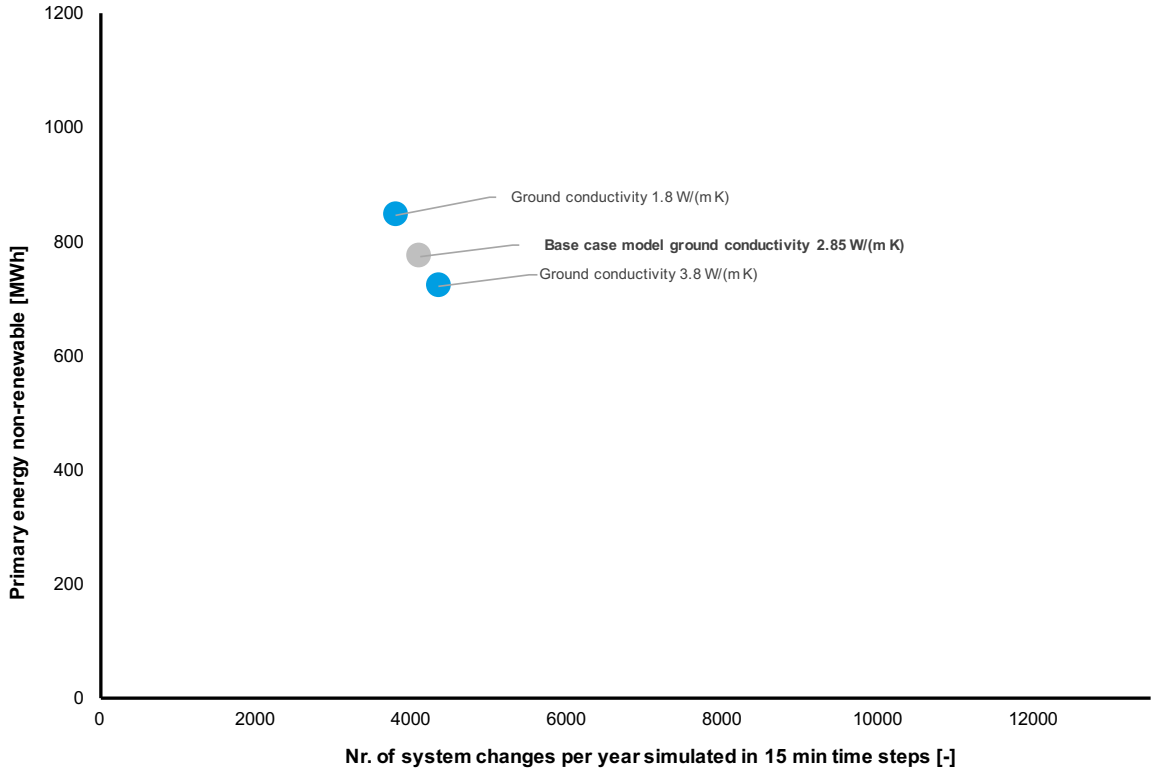

Figure 34 System variations according to the thermal conductivity of the ground

As shown in the diagram (Figure 34), the thermal conductivity of the ground does not influence the system change rate significantly. But the demand of non-renewable primary energy is affected strongly. The thermal conductivity influences the thermal heat transfer to the ground and therefore the performance of the geothermal field varies. If the thermal conductivity rises, more energy can be transferred. This leads to the fact that more renewable primary energy is utilized and the amount of non-renewable primary energy decreases. This shows a linear relationship between the thermal conductivity and the usage of renewable primary energy. This is not the case with the number of system changes.

5.5.2 Undisturbed ground temperature

A very characteristic value of a geothermal field is the undisturbed, initial ground temperature. In general, the initial ground temperature represents the mean outdoor temperature of the location below a depth of more than ten meters for all periods of the year. [21] The temperature profile in figure 35 displays a location in the temperate zone. The temperature behavior of the ground is fairly similar for all latitudes. The initial ground temperature in Calgary is 7.44 °C. [32] To investigate the influence of the initial ground temperature, an optimization variant with an initial ground temperature of 12.44°C has been calculated.

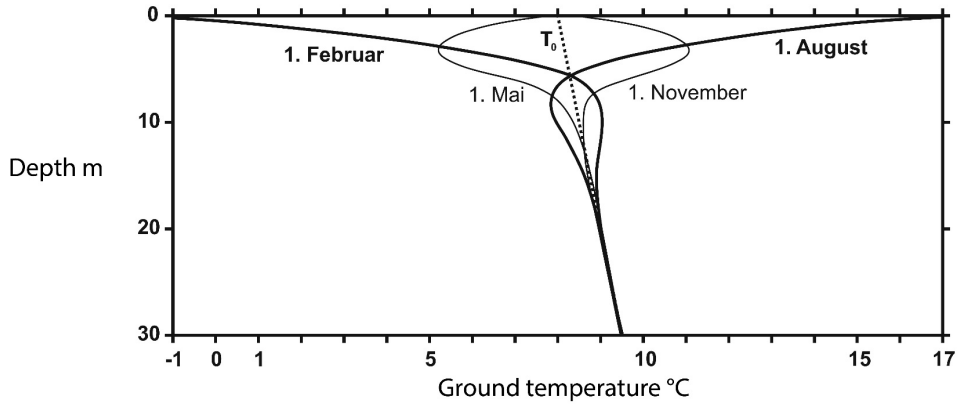

Figure 35 Schematic temperature profile of the ground in the temperate latitudes [21]

The comparison of the two variants in the following figure proves that there is only a slight difference between the two initial ground temperatures in regards to the number of system changes. The initial temperature of the ground primarily influences the amount of non-renewable primary energy. As the heat transfer rate of the geothermal field depends on the temperature difference between the ground and the fluid of the geothermal loop, a geothermal system with a higher ground temperature performs worse than a geothermal field with a lower temperature in the case of a cooling demand. Consequently, the amount of non-renewable primary energy rises.

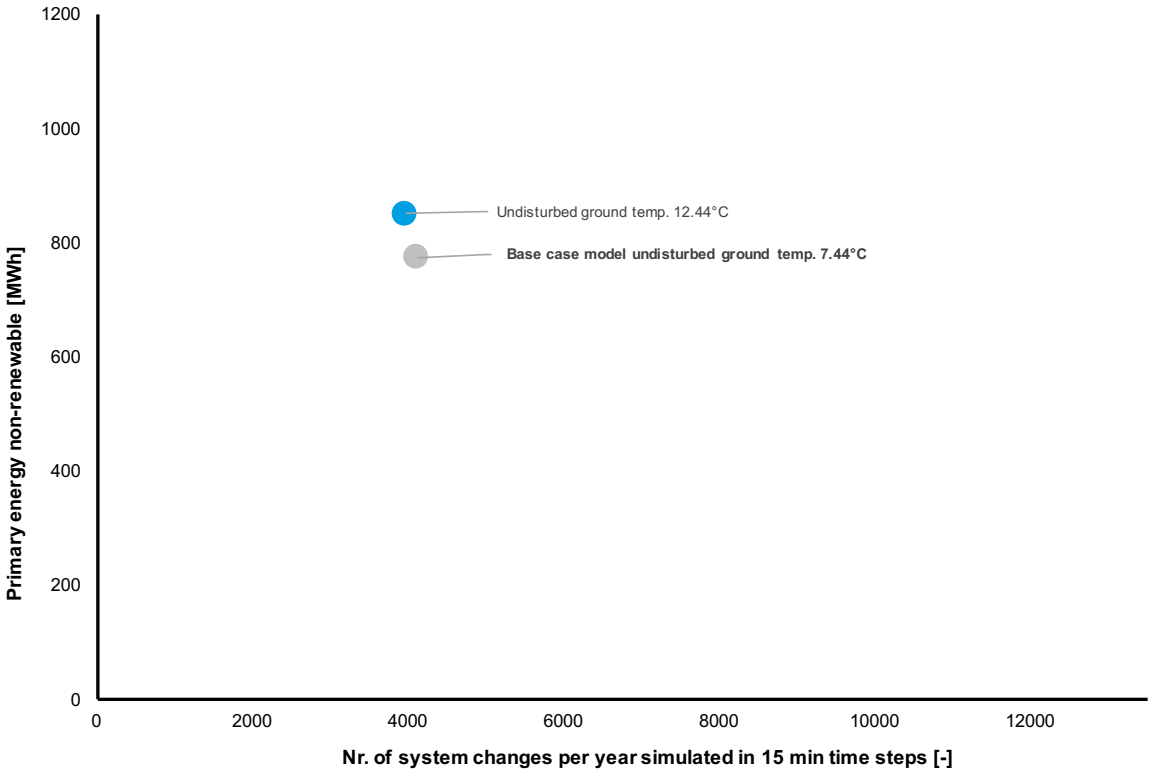

Figure 36 System variations according to the undisturbed ground temperature

5.5.3 Architecture of the geothermal borehole pile

Another parameter which has a significant effect on the thermal behavior of the geothermal field is the architecture of the pipe. The geothermal borehole pipe is defined by its diameter, the implemented piping system and the thermal grout conductivity. In general, one distinguishes between coaxial-, single-, double- or triple-u pipes. The advantage of more pipes in one borehole is that more flow is generated, but also the single pipes influence the heat transfer rate of each other. If more pipes are implemented in a single borehole, the surface area between the pipes and the ground decreases, while the surface area to another heat transferring pipe rises. [21]

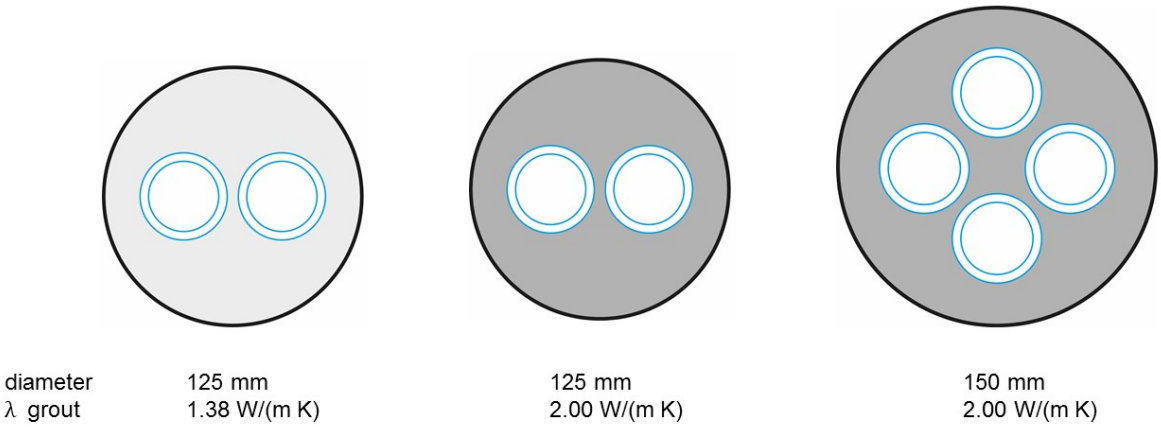

Figure 37 Variation of different borehole pipes

The architecture of the geothermal borehole pipe varies according to the previous figure. The first pipe represents the geothermal borehole implemented at the airport in Calgary. It has a diameter of 125 mm while a single-u pipe is integrated and the thermal grout conductivity is 1.38 W/(m K). In the first variation, the dimension of the pipe stays the same, but the thermal grout conductivity rises to 2.0 W/(m K). The second variant has a geothermal piping system with two double-u pipes. To implement a double-u pipe, the pipe diameter of the borehole must be enlarged from 125 mm to 150 mm The thermal grout conductivity for this variant is also 2.0 W/(m K).

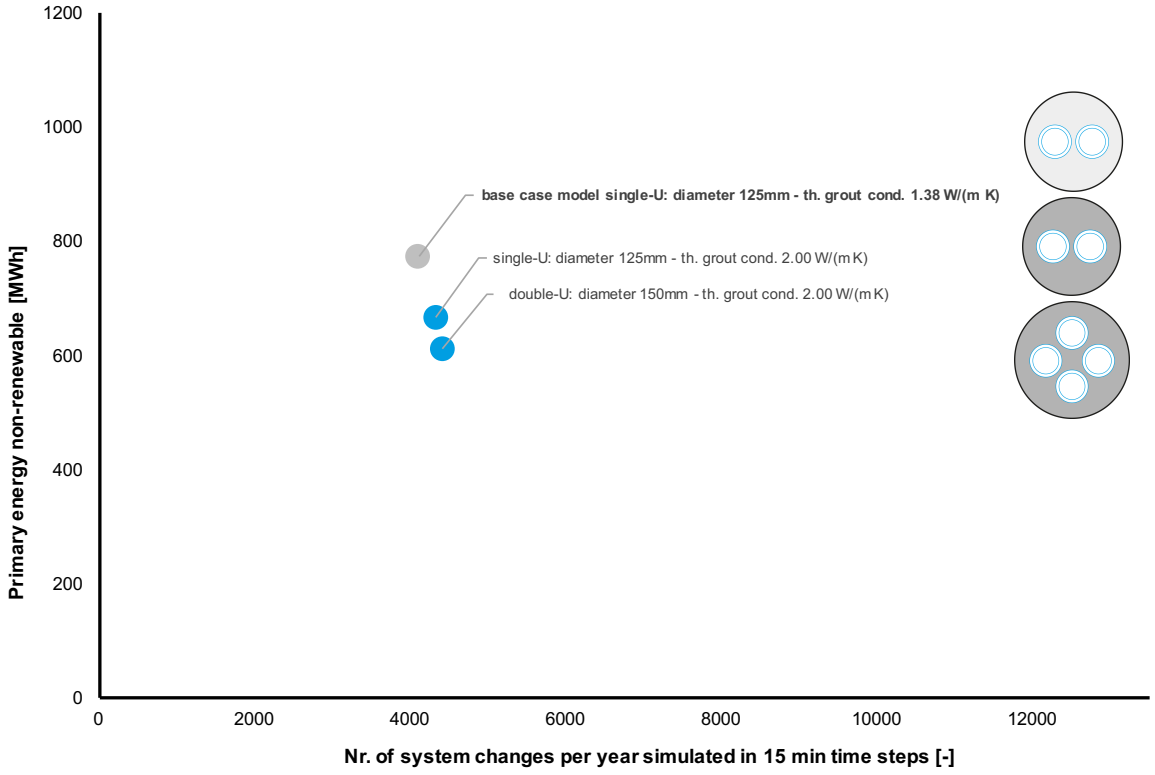

Figure 38 System variations according to different borehole pipes

The variations of the different geothermal boreholes show relatively similar numbers of system states. If the grout conductivity of a geothermal borehole rises, the non-renewable primary energy decreases compared with a lower grout conductivity. The same coherence can be observed in relation to the number of pipes in a borehole, but the improvement between the two different piping systems is not as big as the improvement when changing the grout material. If the thermal grout conductivity, as well as the number of pipes in a borehole rises, the energy transfer to the building system can be performed at a higher level by using more renewable primary energy.

5.5.4 Fluid of the geothermal loop

A further impact on the performance of a geothermal loop is created by the fluid used in the piping system. A very important aspect of the used medium is that in winter times the temperatures in the loop can fall below 0°C. This causes water to freeze, which means that a medium with a lower freezing point must be implemented. The crucial fact about a fluid that has a lower freezing point is the increase of viscosity. By increasing the kinematic viscosity of a liquid, the pump power in the geothermal field rises significantly. The properties of different fluids are provided in Appendix A. In the examined case, however, those effects cannot be observed since the values for both types of fluids are equal.

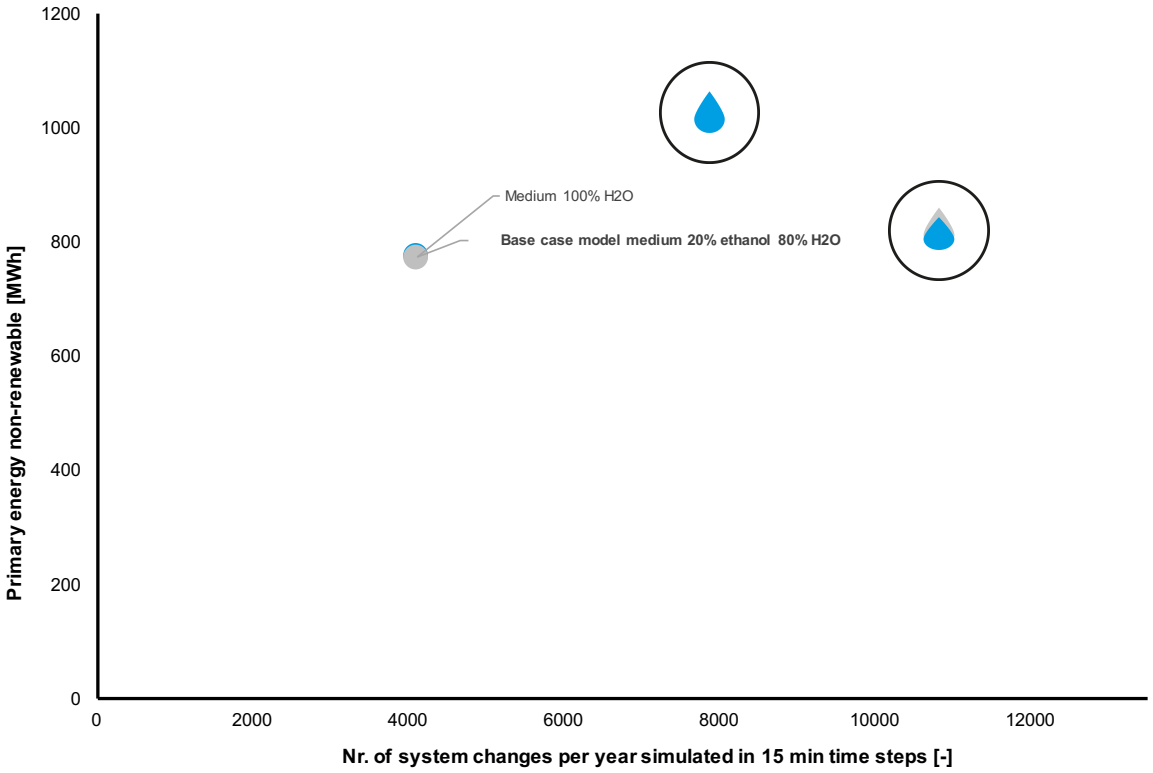

Figure 39 System variations according to the fluid in the geothermal loop

5.5.5 Variation of the building load

A major impact on the geothermal field is created by the building load. In this section, the effects of three different building loads are analyzed. As described in section 5.3, the balance of the building load has a major impact on the performance of the geothermal field. To determine for the influence of the building load, several ratios of imbalance of the building loads are evaluated first. To have a constant foundation for the analysis, the aim of this evaluation is to generate an imbalanced load that is in a dynamic equilibrium after an appropriate computation time. The building load of the base case model is balanced. In the following diagram the outlet temperature of the geothermal field on a summer day is represented for three different building loads. The base case building load is illustrated in grey. Furthermore, imbalanced loads with a 20 % and 40 % higher cooling load than heating load are implemented.

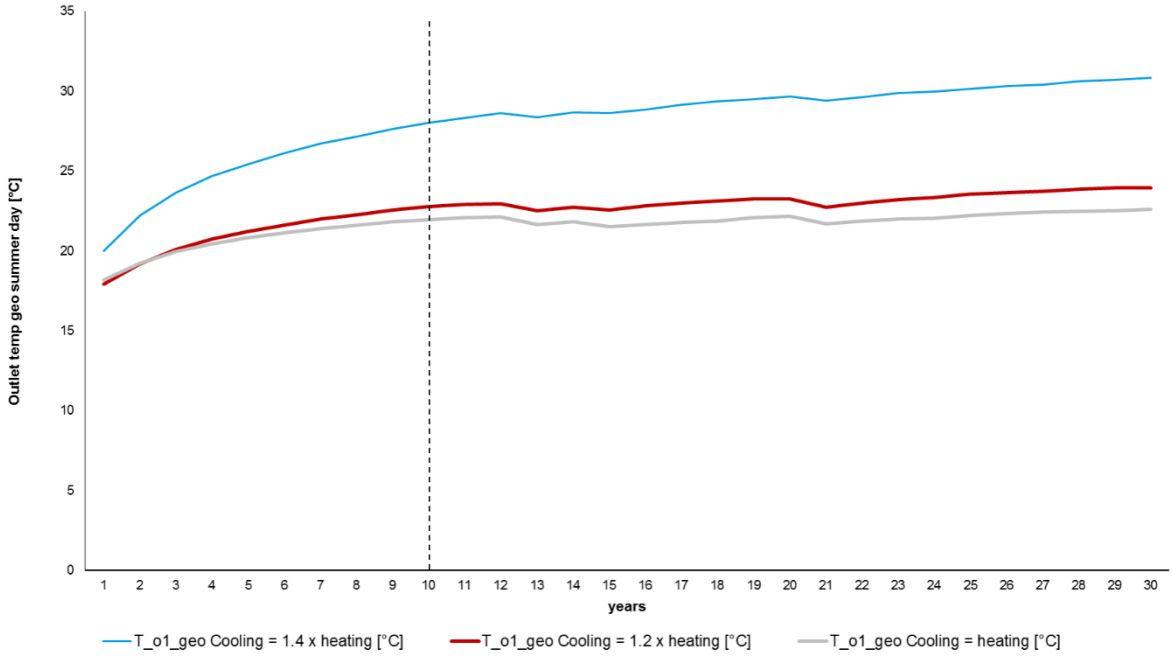

Figure 40 Outlet temperatures of the geothermal field for different loads [summer day]

The diagram of the three different imbalanced loads in figure 40 shows a variation in the outlet temperatures of the geothermal field on a typical summer day. For bigger imbalances of the load, higher outlet temperatures of the geothermal field are obtained. Conclusions can be drawn by looking at the slope of the individual graphs. The outlet temperature of the imbalanced load with a 40 % higher cooling demand constantly rises. In comparison, the slopes of the balanced and 20 % imbalanced loads decrease consistently and after a calculation time of 10 years nearly both outlet temperatures do not rise anymore. This results in the fact that these two variants are in a dynamic equilibrium at this point.

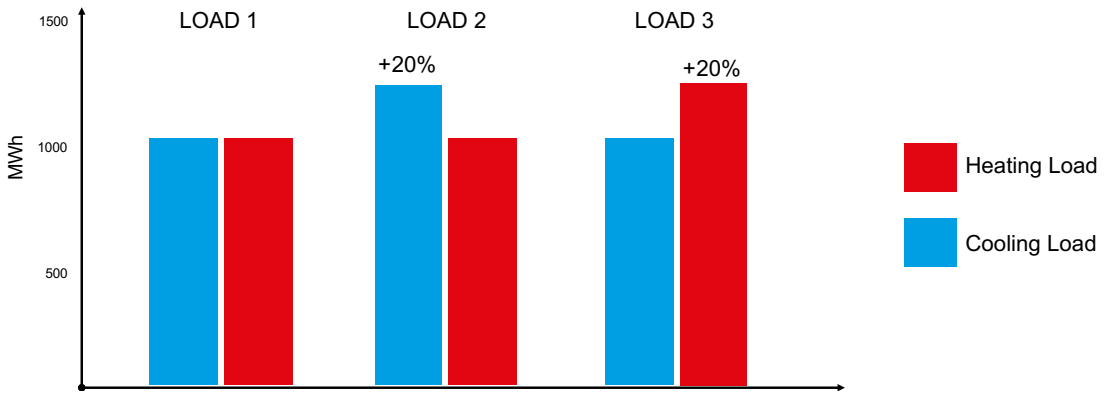

Figure 41 Variation of the thermal building load

Two additional loads have been examined. Load 2 increases the cooling load by 20 %, while Load 3 raises the heating load by 20 %. In relation to the three different building loads, all variants according to the performance of the system are calculated and illustrated in figure 42. This figure displays three different locations of the variants. The imbalanced load with the greater cooling demand requires the highest amount of non-renewable primary energy. The imbalanced load with the higher heating demand also performs in that range. The main reason for the vertical movement of the optimization variants is the fact that the total heating/cooling demand is increased by 20 % and not because of the different performance of the building system.

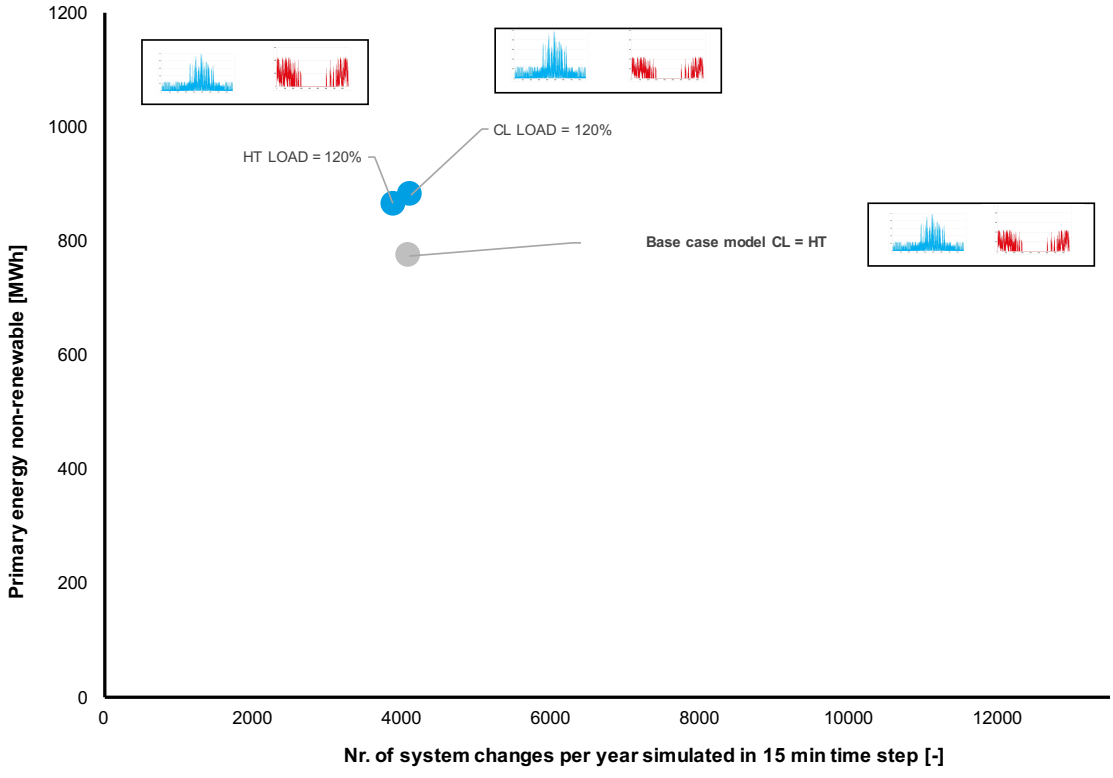

Figure 42 System variations according to the building load

5.6 Evaluation of the adjustable factors of the building system

The second major part of the evaluation, examines the adjustable components of the building system. In this section, the effects of four different components of the building services are scrutinized by changing key factors of the control strategy. The four components consist of the two heat exchangers, the heat-pump/chiller, the hydraulic separators and the fluid pumps. The single components and the variations of the control strategies are demonstrated in the following sections. As in the previous chapter, the variations of the components are compared to the base case model, which represents the specific, idealized situation of the International Airport in Calgary. Each component is varied with two further values of the characteristic control strategy.

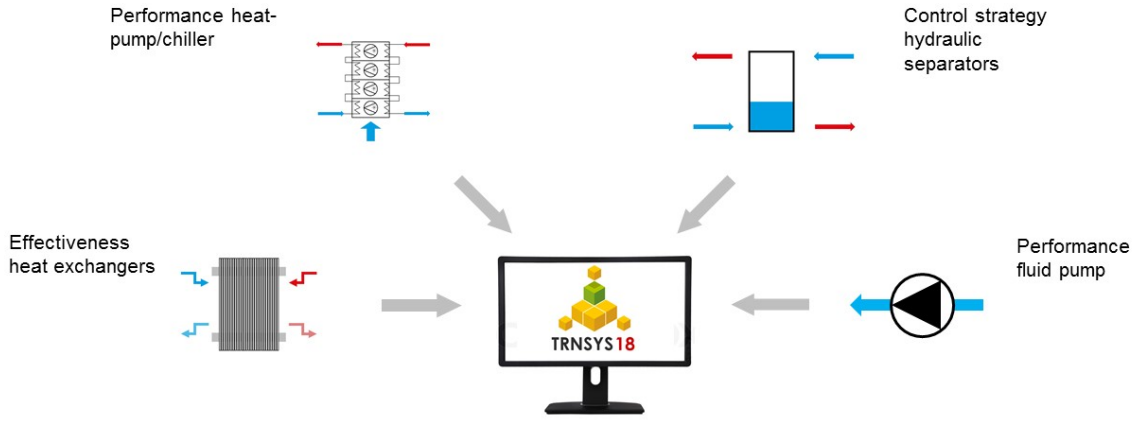

Figure 43 Overview of the adjustable factors of the building system

5.6.1 Variation of the performance of the heat-pump/chiller

The first evaluated component of the building system is the heat-pump/chiller. As mentioned in Appendix B, the component acts as a chiller in the cooling mode, and as a heat-pump when heating energy is required. The key property of the heat-pump/chiller system is the heating/cooling capacity of the device. In the base case model of the International Airport, a device with stages of 244 kW of cooling/heating capacity is implemented. While using the components as a chiller to supply the building with cooling energy, the waste heat can be utilized to fill up the hydraulic hot water separator, or can be dumped into the geothermal field. The same process is implemented in reverse when the heating mode is activated. By varying the heating/cooling capacity of the system, the performance of the whole building simulation changes. The capacity of the base case model is designed in such a way that it fills up the hydraulic separators within one hour. The heating/cooling capacity of the optimization variants are set to 157 kW and 477 kW. The heat-pump/chiller components of the variations are also sized according to two further compact screw compressors from the Bitzer Group. The data sheets of the two systems are provided in Appendix A.

To gain a better understanding of the step-wise operation of the heat-pump/chiller device, the following figure 44 illustrates the dynamic process of the stages activation according to a dynamic heating demand. The diagram illustrates a dynamic output of the simulation tool TRNSYS. The x-axis shows an hourly time step for a typical winter day. The left y-axis represents the power in the simulation, while the right y-axis represents the signals for the control of the components. As displayed at hour 10, the heating demand, illustrated in dark red, exceeds 244 kW. The number of activated stages rises to 1, represented by the light green line. With a further stage, the heating capacity of the heat-pump increases, as pictured in orange. The dark green line shows the controller of the heat-pump. This is regulated according to the status of the hydraulic separator. The same process can be seen at hour 22, where the heat demand rises above 488 kW and a third stage of the heat-pump device is activated. The same principle is operated in reverse for the cooling demand and the chiller. This principle of the heat-pump/chiller system is implemented in every variant of the optimization.

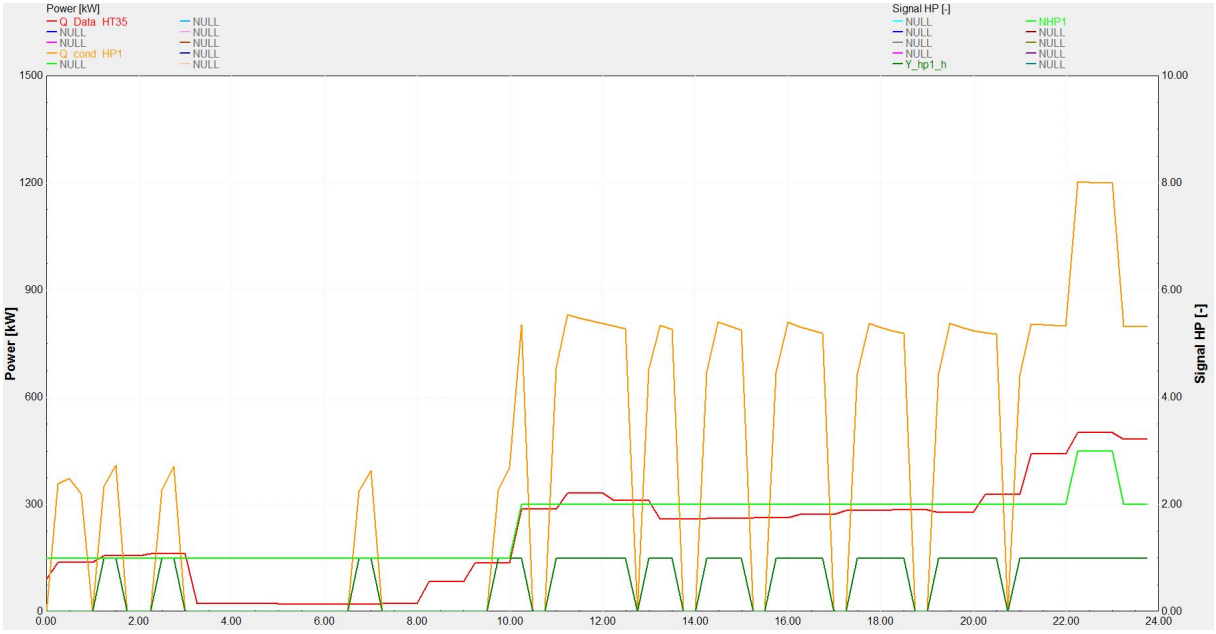

Figure 44 Dynamic behavior of the heat-pump/chiller system in the heating mode

The calculation in Appendix B to size the heat-pump/chiller system forms the basis of the variation of the system states. The higher the heating/cooling capacity of the device, the shorter the refilling-time of the hydraulic separators. This leads to the result that a heat-pump/chiller with a higher performance is less frequently in the system state when the hydraulic separator is filled up. If the performance of the heat-pump is low, the component needs more time to fill up the hydraulic separators.

The analysis of the different heat-pump system in the subsequent figure 45 shows a wide range of the number of system changes per year. The heat-pump/chiller component has only a small influence on the primary energy consumption. The evaluation of the different capacities shows that a linear relation between the heat-pump/chiller device and the system performance exists. The more power the heat-pump/chiller has, the more often the system changes its state since it needs less time to fill up the storage.

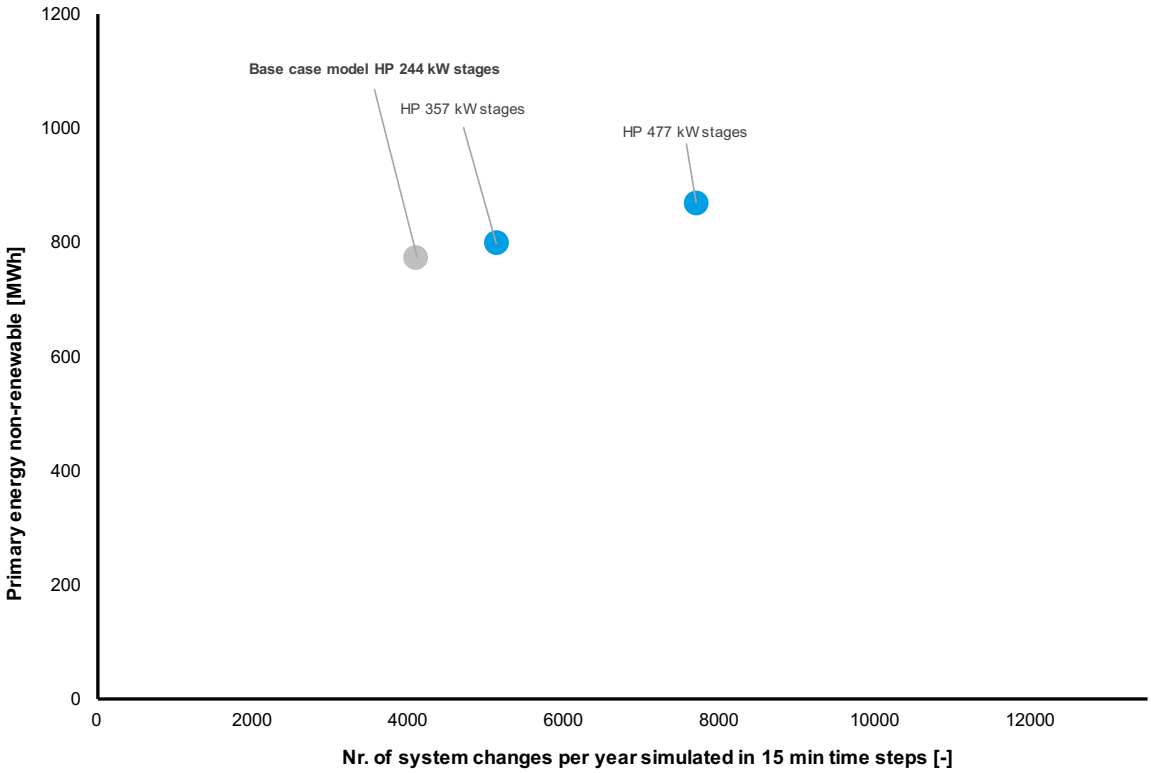

Figure 45 System variations according to the power of the heat-pump

The variation of the heating/cooling capacity of the geothermal system mainly affects the number of system changes. The higher the heating/cooling capacity of the device, the more non-renewable primary energy is needed. This is caused by the oversized devices which need more electrical energy and this results in a small amount of additional primary energy. Moreover, the number of system changes is influenced significantly by the heat-pump/chiller performance. As introduced in a previous chapter, the load duration curve of the thermal heating and cooling load demonstrates that the thermal energy demand of the building is extraordinarily high only for a few hours a year. For the main part of the year, the thermal load is constantly around 250-300 kW. This shows that a heat-pump/chiller device with a higher capacity is oversized for the system, which leads to the high number of system changes.

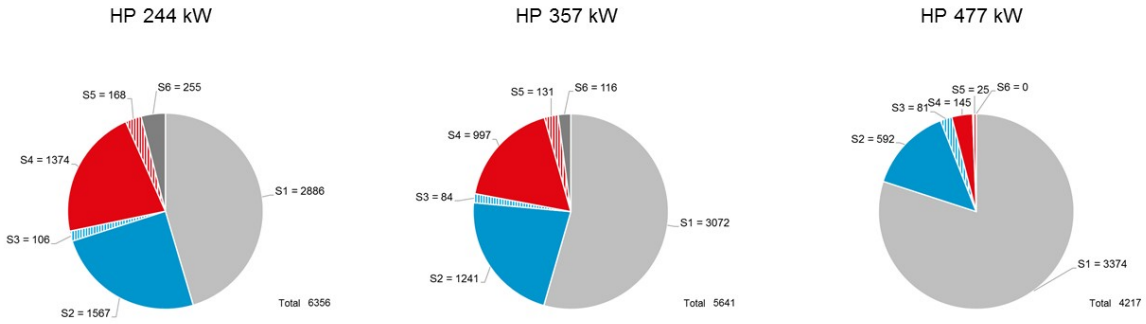

Figure 46 Occurrence of system states according to different capacity levels [hours/year]

The trend of the oversized heat-pump/chiller is shown when looking at the occurrence and total number of system states. The higher the capacity of the heat-pump/chiller device, the shorter the refilling time of the hydraulic separators. This trend also explains, why the share of system state 1 increases with a higher capacity of the device. This shows that a system with a high capacity changes its state very often.

The heat-pump/chiller with a power of 477 kW has a heating and cooling COP of 3-4, whereas the COP of the base case model is 5.0 for cooling and for 3.9 for heating. A further observation of this analysis is that with a lower capacity of the stages of the device, the ratio between the heating and cooling COP increases and becomes more balanced.

5.6.2 Variation of the control strategy of the hydraulic separators

An additional factor of interest in the operation of the building system is the set point temperature of the hydraulic separator. In case of the heating mode, the building demands a temperature of 35°C. The higher the temperature of the hydraulic separator is above this value, the longer the hydraulic separator can provide energy for the building system. In the base case model, the temperature difference was set to 5 K. In the following analysis, the temperature difference is varied to 2.5 K and 0 K. The same temperature difference was chosen for the cold water hydraulic separator at a supply temperature level of 6°C. This simulation assumes that the water is freezing at a temperature of 0°C, which makes temperature differences greater than 5°C unreasonable.

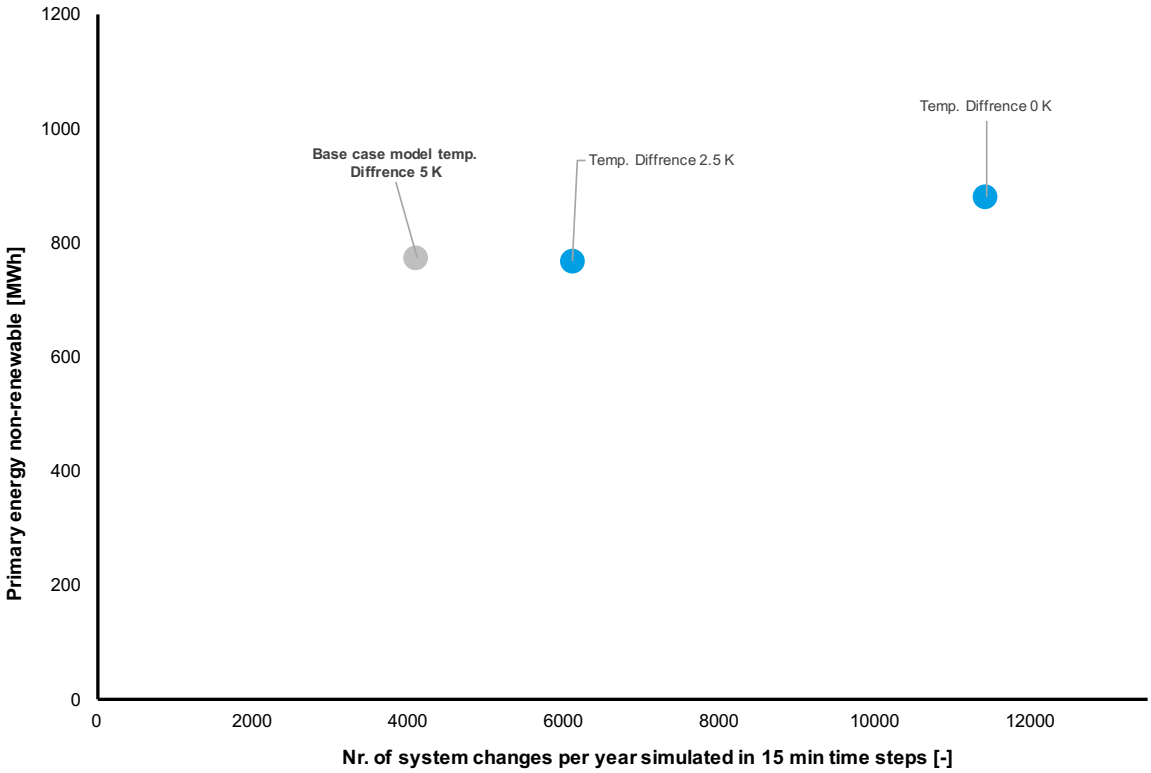

Figure 47 System variation according to the control strategy of the hydraulic separators

The evaluation of the hydraulic separators features, as well as the previous operational analysis, a wide variation in the number of system changes, but a small influence on the primary energy consumption. A variation in the required non-renewable primary energy is just seen when the temperature difference is 0 K. In this case, the supply temperature is not matched in every single time step and the auxiliary heater/cooler must compensate the missing thermal energy. This leads to the result that the non-renewable primary energy demand increases. By increasing the temperature difference of the hydraulic separator, the number of system changes rises. This leads back to the fact that the hydraulic separators in this case are able to supply the building with heating and cooling energy longer. Both variations outline a higher number of system changes, which ends up in a linear relationship between the temperature difference and the amount of system changes.

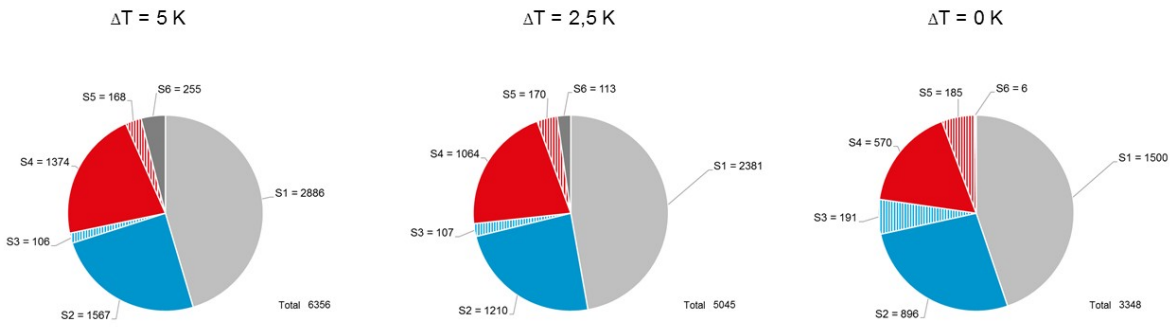

Figure 48 Occurrence of system states for different control strategies HW [hours/year]

Looking closer at the occurrences and the total numbers of system states, further results can be noted. By increasing the temperature difference by means of the of the control strategy of the hydraulic separators compared to the supply temperatures, the share of the system state 6 rises. Furthermore, the total number of system states increases, as the temperature difference grows. The bigger the temperature difference of the hydraulic separators compared to the supply temperature, the better the building system performs in terms of acting in one system state constantly and not having a high number of on and off signals for the components. An advantage of having a low temperature difference is that the free heating and cooling mode is utilized more often.

5.6.3 Variation of the performance of the heat exchangers

Another part of the system worth evaluating are the plate heat exchangers. As analyzed in the initial system of the airport in Calgary, the performance of a heat exchanger is mainly defined as the effectiveness at transferring energy from one loop to another. This generally depends on the two fluids, the material, as well as on the distances and the surface of the plates of the heat exchanger. This is defined by the number and size of the single plates utilized for the heat exchanger. The effectiveness of heat exchangers is calculated according to the following equation.

$$\varepsilon_{HX} = \frac{T_{load,out,set} \times T_{load,in}}{T_{source,in} \times T_{load,in}} \qquad \text{Equ. 4} \qquad [26]$$

ε_{HX}	Efficiency plate heat exchanger	[-]
T_{load}	Temperature load side of the plate heat exchanger	[°C]
T_{source}	Temperature source side of the plate heat exchanger	[°C]

For the next set of variants, the performance of the heat exchangers is studied. Therefore, the heat exchanger performances is varied by changing the transfer rate. The effectiveness in the base case model with 0.57 is not ideal because the heat exchangers, as outlined in a previous chapter, are not running at their optimum at the International Airport. To evaluate the effect of the plate heat exchanger, the effectiveness is varied from 0.2 to 0.8. The different variants are illustrated in the subsequent figure 49.

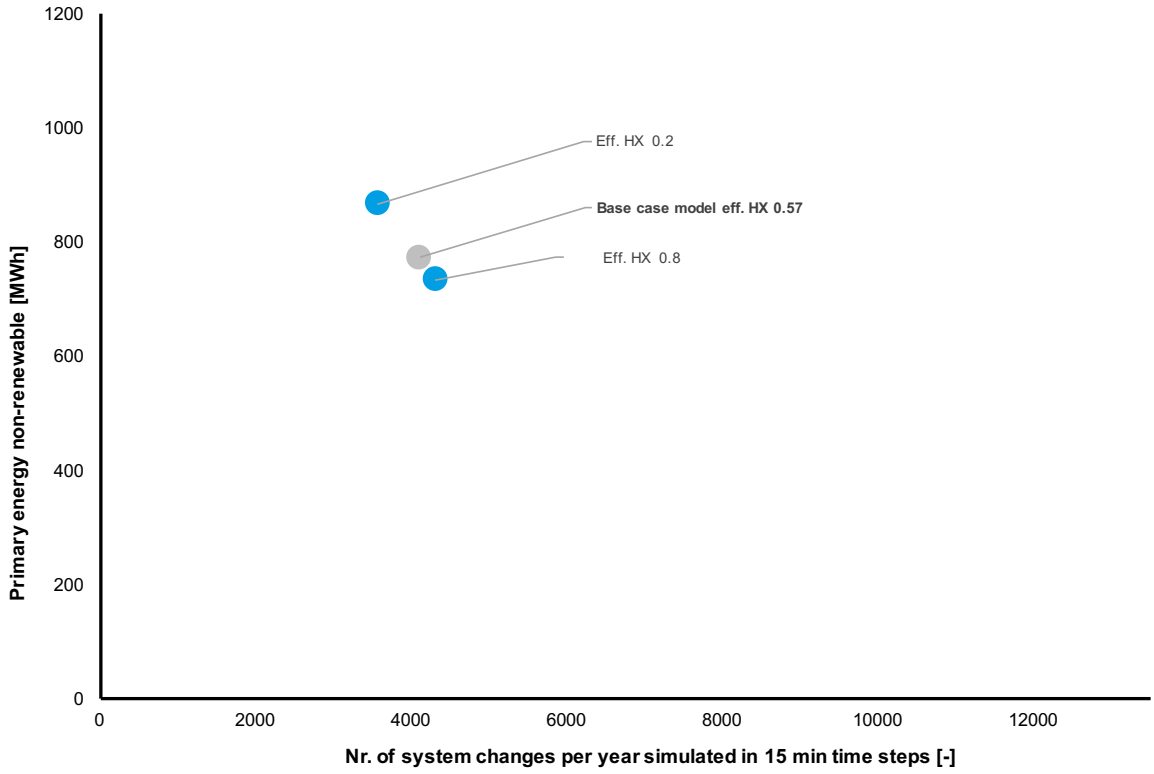

Figure 49 System variations according to the effectiveness of the heat exchangers

The performance of the heat exchangers has a minor effect on the number of system states and a moderate effect on the demand of non-renewable primary energy. In the case of the low performance with 0.2 effectiveness, the number of the system changes decreases. This leads to the fact that the system is acting more often in a single system state. It points out that the system needs more time to transfer energy to the supply loop. A system with bad performance of the plate heat exchangers is not able to supply the building well enough with renewable primary energy. If the effectiveness of the heat exchanger is high, the increase of system changes is hardly notable, but the amount of non-renewable primary energy decreases.

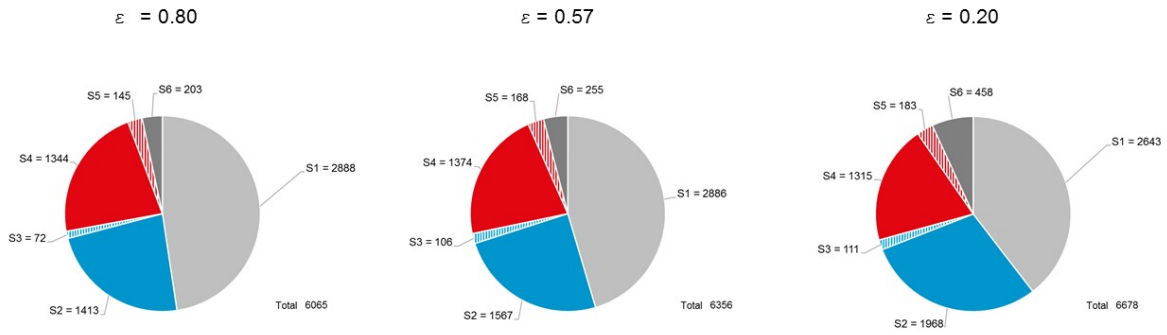

Figure 50 Occurrence of system states for varying the effectiveness of the HX [hours/year]

The different occurrences of the system states related to the variants with different effectiveness levels of the heat exchangers are illustrated above in figure 50. The total number of system states stays nearly consistent, but the percentage of the single states varies. By increasing the effectiveness of the heat exchangers, the prevalence of the system state 1 decreases. With better efficiency of the heat exchangers, the amount of hours in active heating and cooling mode decreases as well. This has the effect that the efficiency of the heat exchangers influences the extent of integrating the geothermal field into the building system. If the efficiency increases the geothermal field performs better and less non-renewable primary energy is needed.

5.6.4 Variation of mass flow

Finally, an investigation of the influence of the mass flow of the system is done. By reducing the mass flow to 75 % and 50 % of the initial design of the base case model, one tries to figure out the effect of the mass flow on the total building system. In general, the mass flow of the system is designed according to the geothermal piping system.

The reduction of the flow shows that the mass flow has an influence on the number of system changes and on the non-renewable primary energy consumption. The smaller the mass flow, the higher the amount of non-renewable primary energy and the lower the number of system changes. The overall effects are not as significant as the effects caused by the other components of the building system, but the mass flow influences both indicators of the analysis. The increase of the primary energy demand can be elucidated by the lower mass flow rates resulting in less thermal energy extracted from the ground. When less thermal energy from the ground is transported, the requirement for more non-renewable primary energy increases and the system must stay longer in a single system state to fill up the hydraulic separators.

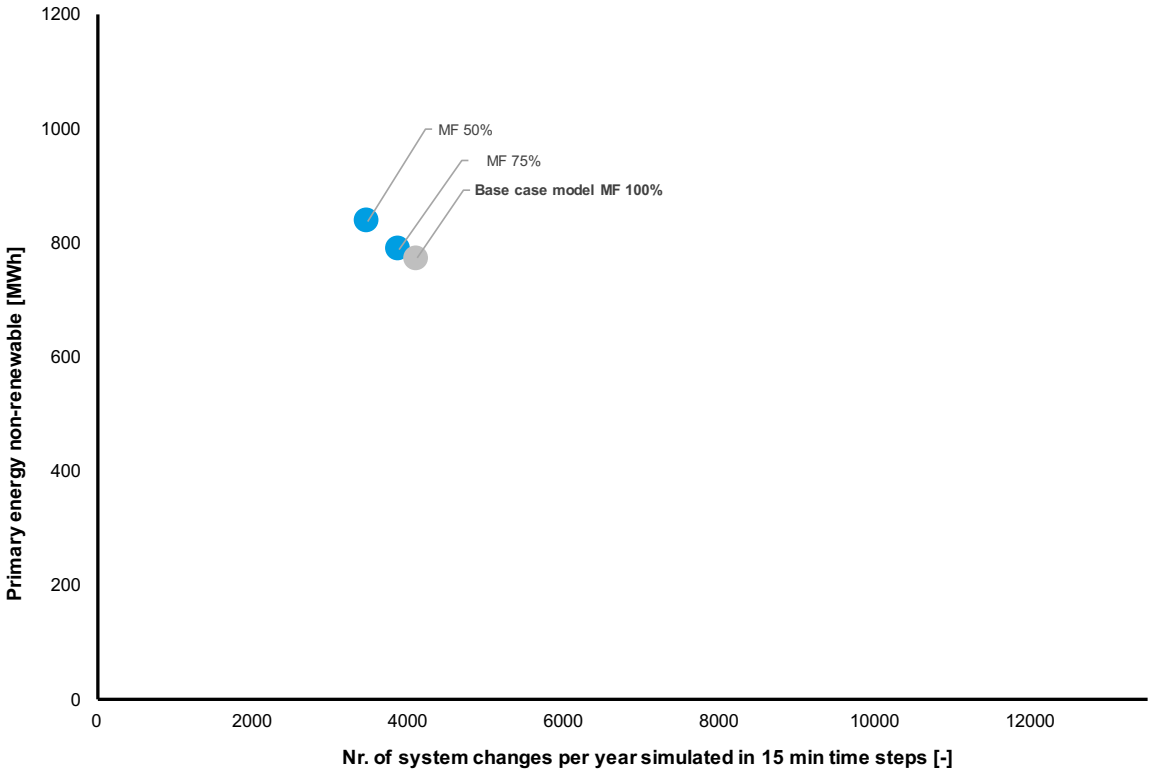

Figure 51 System variations according to reduction of the mass flow of the system

6. Comparison of the optimization variants

7. Discussion

8. Outlook

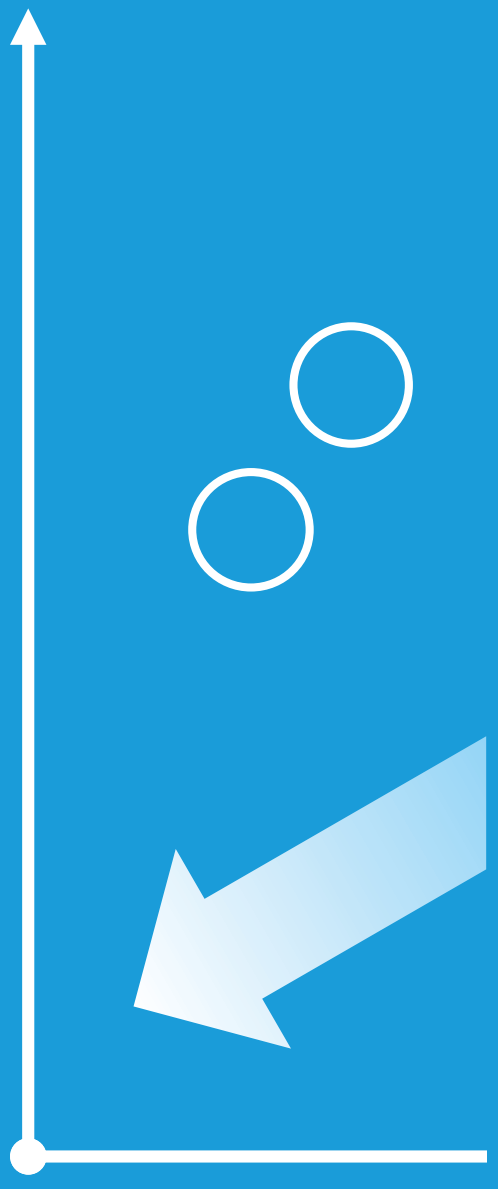

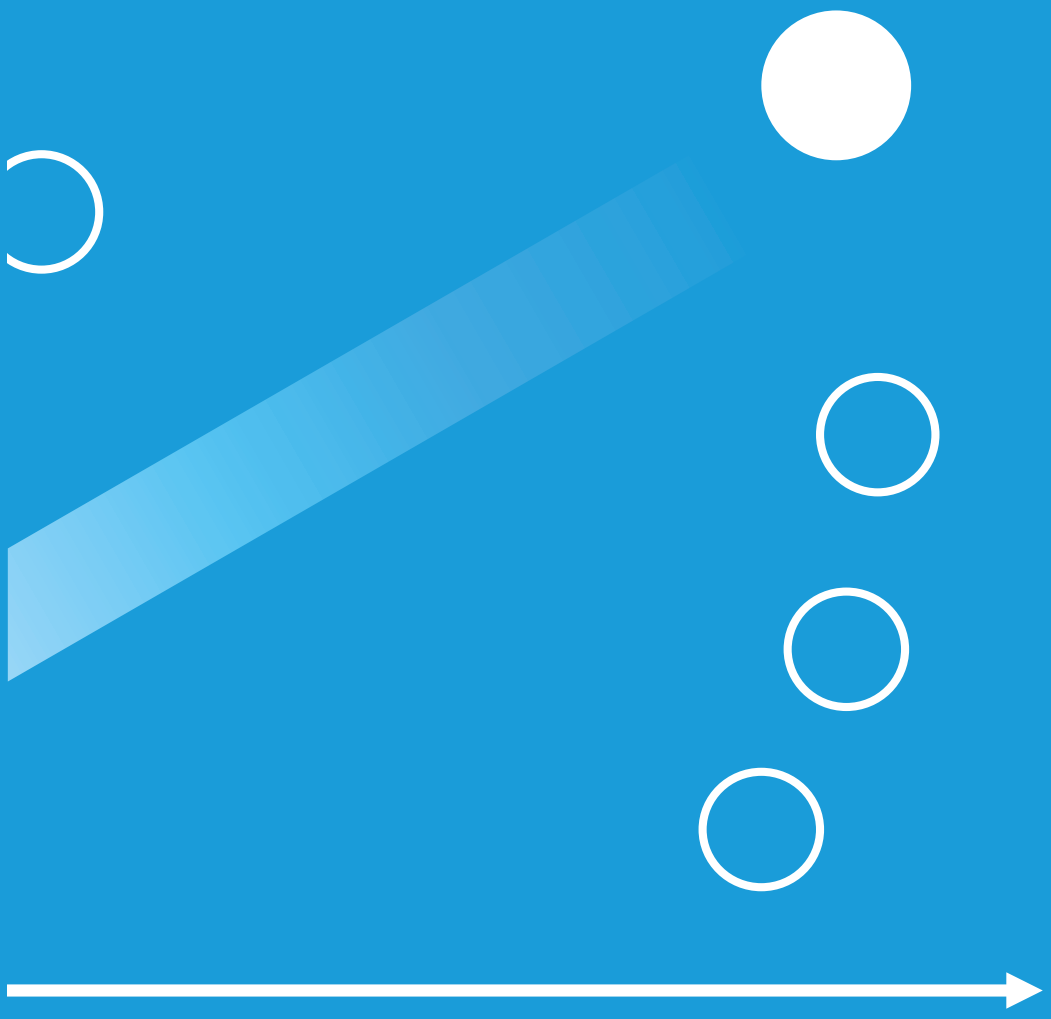

6. Comparison of the optimization variants

This chapter is concerned with the comparison of the two categories of optimization variants. As pointed out in the previous chapter, the different key indicators have various influences on the non-renewable primary energy consumption and on the number of system changes per year. To evaluate the single system variations, the terms of energy efficiency and longevity are coming up. If a variant lowers the amount of non-renewable primary energy consumption, this is an indicator of a more energy-efficient building system. This leads to a linear relation between a vertical movement in figure 52 and an energy-efficient system. A horizontal movement in the diagram represents a change in the longevity of the system, because the number of on and off switches is lower when the number of system changes decreases. In this thesis, the longevity is also an indicator of the ability of a system to stay in the same system state while the circumstances of the simulation are changing. This leads to more robustness of the system against changes in operation circumstances. When a system is more robust, it has better overall long term performance.

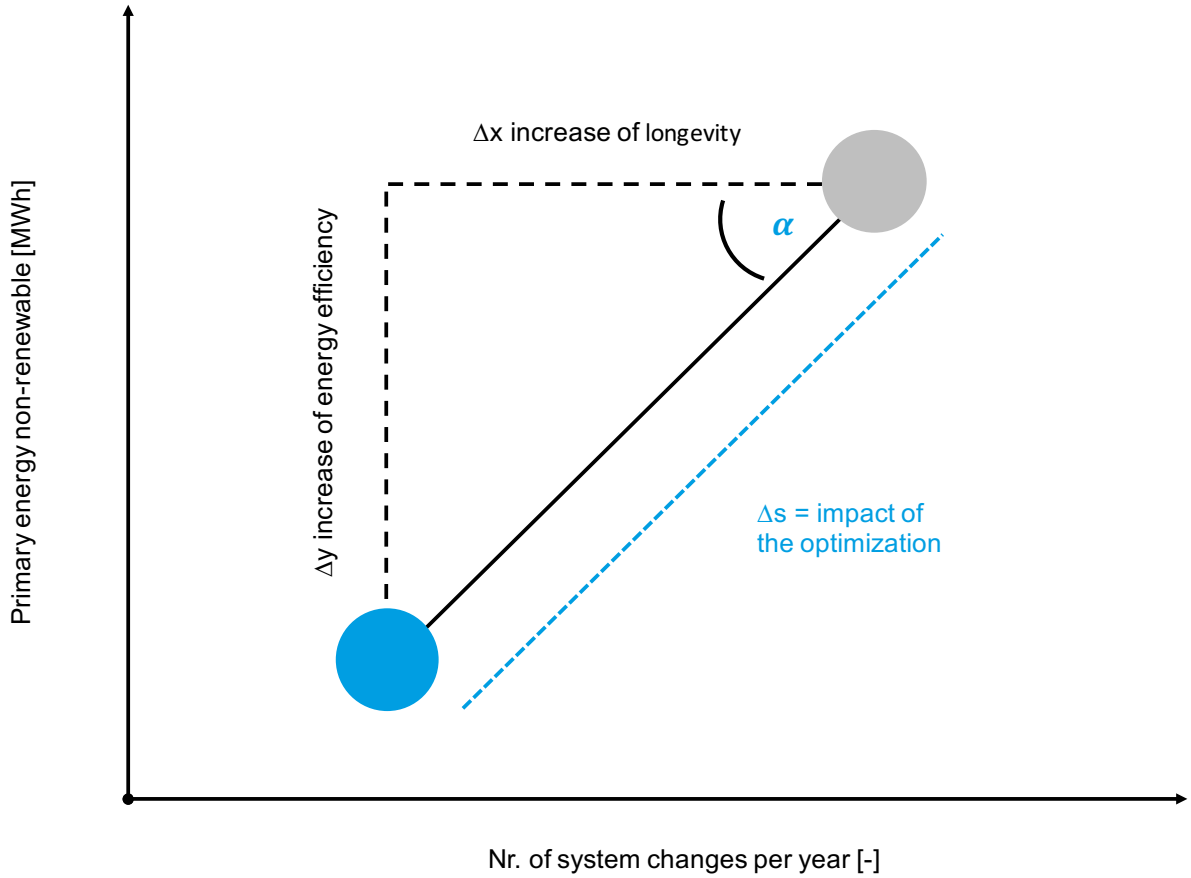

Figure 52 Influence of the position of an optimization variant

According to the horizontal and vertical movement, the influence of an optimization variant can be constituted through the length s and the angle α of the overall movement. An angle of 0° between the base case model and optimization variant in the diagram just has an influence on the longevity of the system while an angle of 90° represents an improvement in the energy efficiency of the building system. With an angle of 45° the optimization variant has a positive effect on energy efficiency, as well as on the longevity. When the angle shows values below 0° or above 90°, at least one criterion of the analysis is negative.

In the following table the different fixed and variable components over the life time are outlined. The upper part of the table lists the variants with the fixed parameters of the geothermal field. The lower part describes the adjustable values of the building system. Table 3 lists the individual horizontal and vertical changes, the length of the total movement and the angle of the system variants.

Table 3 Comparison of the effects of the different system variants

Variant	Paramter	Number of system changes per year [-]	Primary energy non-renewable [MWh]	delta x [cm]	delta y [cm]	delta s [cm]	alpha [°]
Base case model	-	4105	772	-	-	-	-
Base case model medium 20% ethanol 80% H2O	Medium 100% H2O	4105	772	0.0	0.0	0	-
base case model single-U: diameter 125mm - th. grout cond. 1.38 W/(m K)	single-U: diameter 125mm - th. grout cond. 2.00 W/(m K)	4332	666	-0.3	1.0	1	106
base case model single-U: diameter 125mm - th. grout cond. 1.38 W/(m K)	double-U: diameter 150mm - th. grout cond. 2.00 W/(m K)	4410	612	-0.4	1.5	2	104
Base case model ground conductivity 2.85 W/(m K)	Ground conductivity 1.8 W/(m K)	3804	847	0.4	-0.7	1	298
Base case model ground conductivity 2.85 W/(m K)	Ground conductivity 3.8 W/(m K)	4351	723	-0.3	0.5	1	123
Base case model undisturbed ground temp. 7.44°C	Undisturbed ground temp. 12.44°C	3955	850	0.2	-0.7	1	284
Base case model temp. Diffrence 5 K	Temp. Diffrence 0 K	11430	881	-8.9	-1.0	9	186
Base case model temp. Diffrence 5 K	Temp. Diffrence 2.5 K	6108	767	-2.4	0.0	2	179
Base case model eff. HX 0.57	Eff. HX 0.8	4309	734	-0.2	0.3	0	125
Base case model eff. HX 0.57	Eff. HX 0.2	3566	867	0.7	-0.9	1	307
Base case model MF 100%	MF 75%	3870	788	0.3	-0.1	0	333
Base case model MF 100%	MF 50%	3475	837	0.8	-0.6	1	322
Base case model HP 244 kW stages	HP 357 kW stages	5134	797	-1.2	-0.2	1	190
Base case model HP 244 kW stages	HP 477 kW stages	7698	868	-4.4	-0.9	4	191

The evaluation of the different optimization variants shows a wide array of effects. Generally, it is to state that the optimizations of the fixed values have a major effect on the non-renewable primary energy demand and only have a minor influence on the number of system changes of the building system. For the operational optimization of the adjustable values of the building system, the results nearly are reverse. In general, the building system components strongly influence the number of system changes, but the non-renewable primary energy is not significantly affected. Still, the effects of the building system components are bigger than the effect of the geothermal field.

The analysis of the angles of the improvement variants shows that no single factor is able to generate an angle between 0° and 90°. This substantiates that an improvement in both analyzing factors is not possible by changing only one fixed or adjustable value of the system.

The first part of table 3 outlines that the fixed parameters of the geothermal field with the greatest impact on the number of system changes are the thermal ground conductivity and the implemented borehole pipes. The ability to use the geothermal field as a renewable energy source and, consequently, use less non-renewable primary energy is also affected the most by the thermal conductivity of the ground and the geothermal borehole pipe. The variation of the fluid of the geothermal loop and the undisturbed ground temperature of the geothermal field have a smaller effect on the performance of the system.

Apparently, the heat-pump and the reduction of the control strategy of the hydraulic separator have an enormous effect on the number of system changes and thus on the longevity of the building system. These components also affect the energy efficiency slightly. The biggest potential of the adjustable factors of the building system of a geothermal heat-pump system is in the transfer rate of the heat exchangers. Further, the mass flow has a moderate influence on the required non-renewable primary energy, as well as on the number of system changes. If the mass flow is too small, the demand of non-renewable primary energy rises, but the number of system changes decreases.

7. Discussion

Firstly, this chapter answers the initial scientific questions. It points out which influence the single analysis categories have on the performance and the energy efficiency of the building system and further evaluates which category has more saving potential. In a second step, through an analysis of the best and worst cases of the evaluated categories, this chapter gives feedback on the performance and the potential of the International Airport's building system.

The comparison of the fixed and adjustable factors of the variants of the building system shows different kinds of results. To answer the two initial scientific questions, this chapter analyzes the impact of the two variation categories. Firstly, the fixed parameters of the geothermal field have nearly no influence on the state of the building system and are mainly responsible for the performance of the geothermal field. Secondly, the adjustable components of the building system do not influence the energy efficiency of a building system as much as they do the number of changes of the system state. In general, the impact of the adjustable components is bigger and does influence both analyzing criteria. Overall, the adjustable factors have an influence on the longevity and the energy efficiency while the fixed parameters of the geothermal field just affect the energy efficiency of the system.

This confirms the overall hypothesis of this master thesis that the impact of the operation of the building system, represented through the adjustable components of the system, has a bigger effect on the energy efficiency and longevity of a geothermal heat-pump system in comparison with the fixed design parameters of the geothermal field.

This phenomenon is also shown in the following figure. The potential of energy savings and the number of variations in the system changes is outlined for the two categories. By combining all considered variations of the optimization categories with each other, the overall potential of the analyzed categories is shown. The diagrams show that the array of the influence for the adjustable factors has a much wider range in case of the number of system changes and does affect the non-renewable primary energy demand. The set parameters of the geothermal field almost exclusively influence the potential of saving non-renewable primary energy.

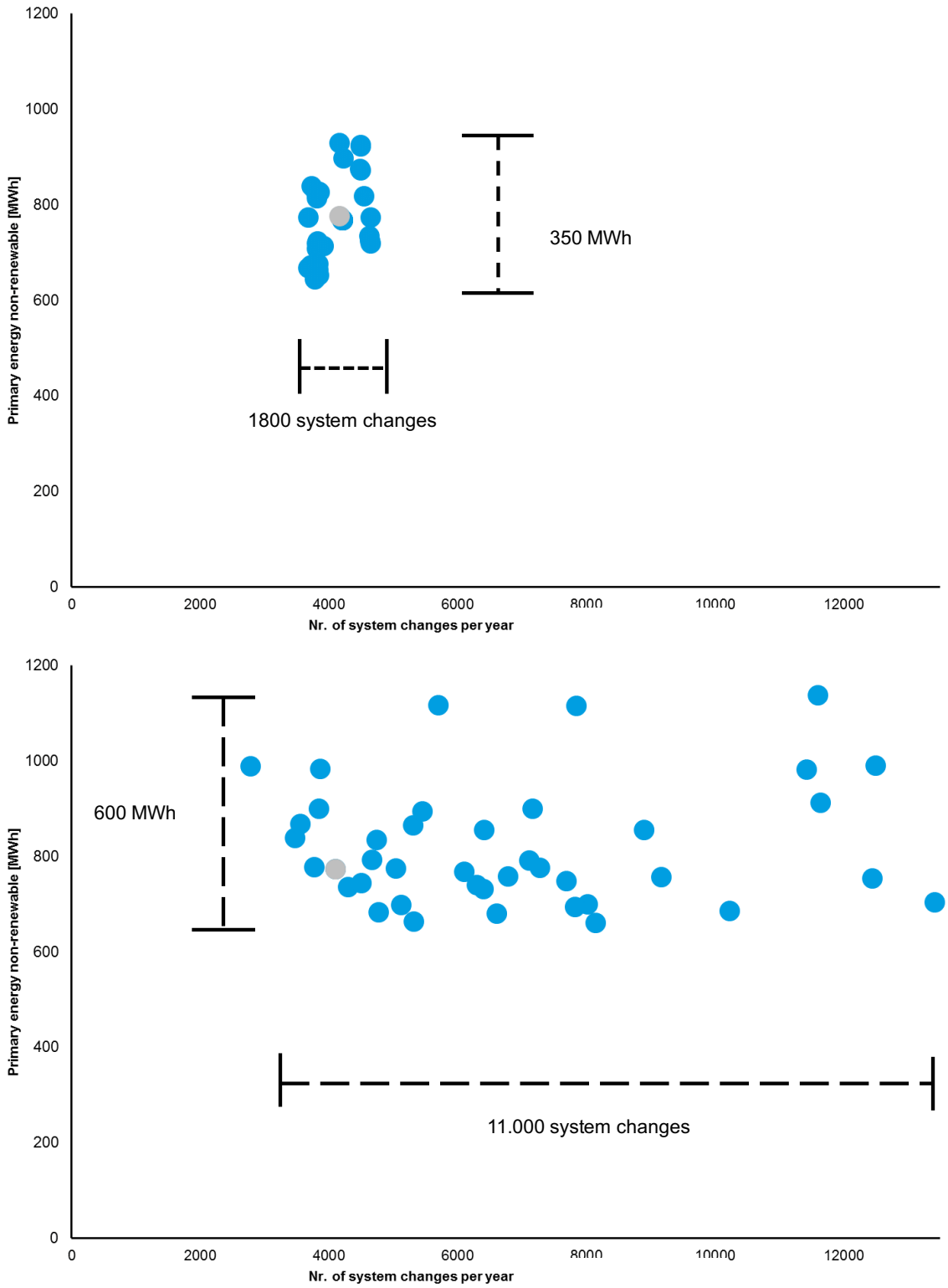

Figure 53 Potential of the adjustable components (below diagram) and fixed parameters (top diagram) of the building system

Furthermore, the best and worst cases of the building system in accordance with the analyzed parameters of the two categories are shown to create feedback for the implemented building system of the International Airport in Calgary. Firstly, the best and worst cases for the variation of the fixed parameters of the geothermal loop are outlined in the subsequent table 4.

Table 4 Best/ worst case scenario of the fixed parameters of the geothermal field

	Thermal ground conductivity	**Borehole pipe**	**Undisturbed ground temp.**	**Medium**
Base case model	2.85 W/(m K)	Diameter 125 Single-U Grout conductivity 1.38 W/(m K)	7.44°C	Brine
Worst case model	1.8 W/(m K)	Diameter 125 mm Single-U Grout conductivity 1.38 W/(m K)	12.44	H20
Best case model	3.8 W/(m K)	Diameter 150 mm Double-U Grout conductivity 2.00 W/(m K)	7.44°C	Brine

As pointed out in the comparison of the individual analyzed components and parameters of the geothermal field, the International Airport Calgary still has potential to improve its performance regarding energy efficiency and longevity of the building system. The best case of the analysis of the fixed parameters of the geothermal field just makes sense theoretically, because the geothermal loop is fixed underneath the building of the airport. In general, one must distinguish between parameters which are set by the location of the building and parameters which can be defined by the design team. The thermal conductivity and the initial temperature of the ground perform according to the location of the building. In this case, the design of the geothermal heat-pump system cannot be adjusted. In theory, with a better thermal ground conductivity the system would perform better in the sense of using less non-renewable primary energy. Furthermore, the fluid implemented in the geothermal field does not affect the performance of the building system significantly.

A real improvement in the design phase of the geothermal system would have been to use a different kind of geothermal borehole pipe with a better grout conductivity. The grout conductivity especially limits the performance of the geothermal heat-pump system, because the thermal grout conductivity of the base case model with 2.85 W/(m K) is high and has potential for using more thermal energy of the ground. In addition, a double-u pipe also would have created an improvement in energy efficiency and would have saved a lot of non-renewable primary energy. The following table 5 shows the best and worst case of the evaluation of the variable components of the building system.

Table 5 Best/ worst case scenario of the variable components of the building system

	Stage capacity heat-pump/chiller	**Temperature difference of the hydraulic separators**	**Effectiveness heat exchang-ers**	**Mass flow**
Base case model	244 kW	∆T 5 °C	0.57	100 %
Worst case model	477 kW	∆T 0 °C	0.2	50 %
Best case model	244 kW	∆T 5 °C	0.8	100 %

It should be noted that some of these components can be adjusted by changing the control strategy of the component and some can be adjusted by replacing the whole device. These components are still able to be adjusted, however. Consequently, the performance of the heat exchangers and the heat-pump can only be improved by replacing the devices.

The temperature difference and the mass flow of the geothermal loop work effectively in the building system of the International Airport in Calgary. Only the performance of the heat exchangers is not optimal. If the heat exchangers worked with an effectiveness of 0.8, energy savings would increase and a lower number of system changes could be reached.

8. Outlook

Building energy simulation allows engineers and architects to gain very deep insight into the energy flows of the building and its HVAC system. The quality and significance of the conclusions are strongly conditional on the scope and level of the complexity of the model, as well as on the calculation detail. Safety factors, assumptions and a lack of communication deteriorate the quality of the design of a building and its building services. Today, in the rapid design process of buildings, a detailed and high-quality design service is rarely put into practice. [33] This results in lower quality of the design and realization of a building and a performance gap between the intended and the built edifice.

As shown in this master thesis, an energy optimization of a building system is almost always possible. Reducing the thermal load of a building is one way to optimize its energetic behavior. Reducing the required energy to supply the building is another method to generate energy savings, which is often not considered. The key factor of this optimization strategy is the correct insurance to size the HVAC system according to the local circumstances and the building system itself. The sizing has a decisive influence of generating a long-lasting and energy-efficient building system. A right-sized system in this sense is not defined by powerful, oversized components, which have a high number of on and off switches of the devices. High-performing systems consider the thermal load of the building in detail and look very accurately into the functionality of the building system's components. Furthermore, correct sizing the building system is not enough. The control strategies and the adjustment in consultation with the other components of the system have an even bigger potential to save energy and creating longevity for the devices, as shown in this master thesis.

Sizing an appropriate building system requires detailed information about the part and peak loads of the building. Determining the ratio of the part and peak loads is crucial to size the building system. Modular system devices can improve the efficiency of a building system significantly, as they adapt to changes in circumstances, e.g. a change in the building usage. Furthermore, the concept of multiple boilers for buildings with widely varying building loads can increase the efficiency. Beyond that, a high effective maintenance and a constant adaption to the local situation of the building system is necessary to operate efficient building services.

This master thesis gives feedback on the modern building design industry that the potential of saving energy is not treated with a myriad of national and international codes and standards to control the process of a building. Energy-efficient, climate responsive constructions require a whole building perspective that integrates architectural and engineering concerns early in the design process. This master thesis advises to change the whole building process and return to a building process determined by detailed quality in the design and the built construction.

Climate responsive building with right-sized building services and high-quality constructed structures generate much greater energy savings than rapidly built edifices, with no adaption to the user behavior and the location, resulting in oversized HVAC systems. With the ongoing digitalization, all kinds of measured data are available. Hence, the possibility to implement intelligent control strategies and automatically adapting HVAC system are feasible and are mandatory for an energy-efficient building system. The key for a promising, high-quality standard in the future building industry are holistically planned buildings to generate efficiency in the built environment.

Appendix A

Appendix B

Appendix C

Bibliography

List if Figures

List of Tables

Declaration of Autonomy

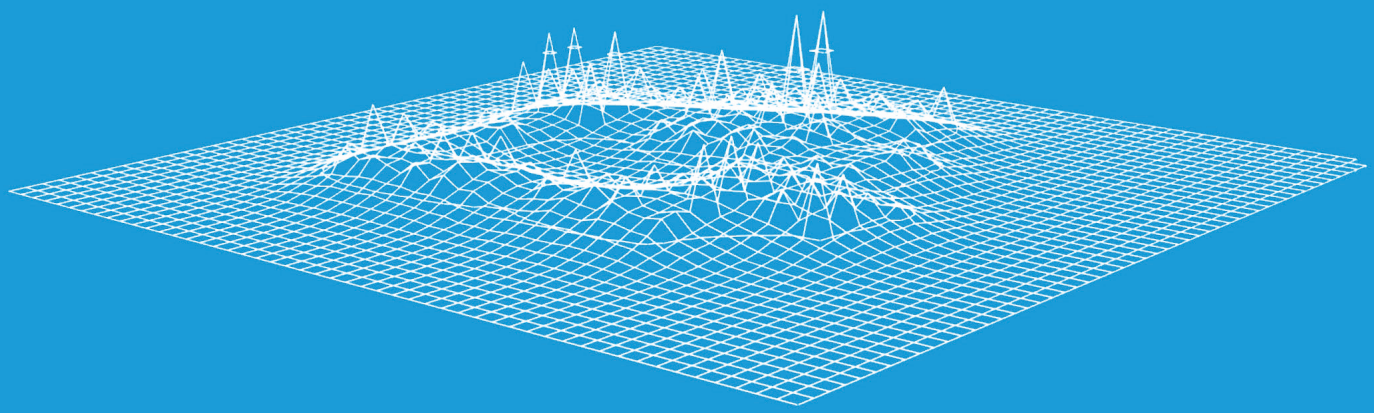

Appendix A – Project specific information

** This data is calculated and provided by the Transsolar Energietechnik GmbH in their former project with the International Airport Calgary*

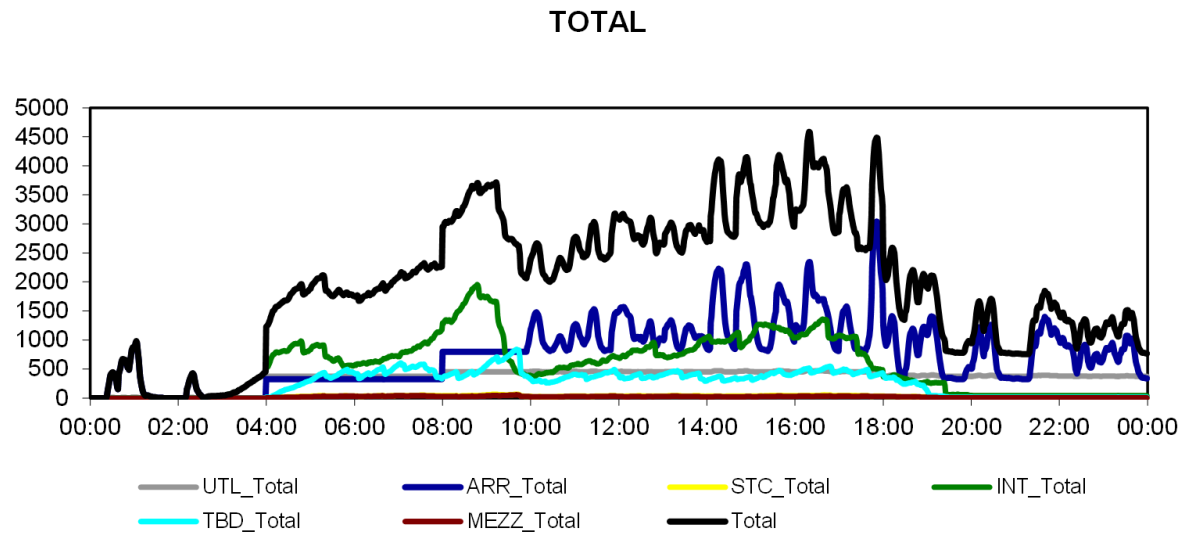

Figure 54 Distribution of the occupancy rates in the International Airport Calgary *

Wärmeträger-flüssigkeit	dynam. Viskosität μ (kg/(m s) od. (Pa s)	spez. Wärme-kapazität c (J/(kg K)	Dichte ρ (kg/m^3)	Wärmeleitfähigkeit λ (J/(s m K)
Wasser	0,0018	4217	1000	0,562
Ethylenglycol 25%	0,0052	3795	1052	0,480
Ethanol 25%	0,0046	4250	960	0,440
Propylenglycol 30%	0,0108	3735	1038	0,450
Calciumchlorid 20%	0,0037	3050	1195	0,530
Methanol 25%	0,0040	4000	960	0,450

Figure 55 Material properties of different fluids for a geothermal loop [21]

	connection power	power during operation	stand-by power	operation	energy demand
	[kW]	[kW]	[kW]	[h/day]	[MWh/year]
Total [kW]	**8'543**	**5'755**	**1'114**		**32'410**
Lighting	705	**705**	0	16	**4'117**
Emergency lighting	-	-	-	-	-
Outside + routing lighting	-	-	-	-	-
Permanent IT lighting	-	-	-	-	-
Baggage handling	1'004	**816**	-	-	**2'634**
CTX scanners	13	**13**	0.2	9	**45**
Retail spaces	308	**308**	62	14	**1'800**
Food & beverage space	362	**362**	145	14	**2'375**
Mechancial / electrical rooms	2'116	**1'481**	444	14	**9'161**
Waiting/screenin related equipment	123	**123**	25	13	**682**
Tenant warehouse	57	**57**		24	**495**
Elevators	636	**210**	8	10	**827**
Freight elevator	410	**135**	3	10	**523**
Moving walkway	39	**13**	2	10	**56**
Escalator	291	**96**	7	10	**393**
Material lift	4	**1**	0.3	10	**6**
BMS base loads	85	**85**	85	24	**747**
IT power	1'400	**560**	140	24	**4'906**
Ice melting 250kW	250	**250**		12	**1'095**
Drain heating	150	**150**		12	**657**
Display of flights	3	**3**	3	20	**29**
Advertising	50	**50**	50	24	**438**
Fids (Flight Information Display System)	78	**78**	78	24	**683**
Charging station for aircrafts at fixed links APF					
Fixed links mover	73	**73**	7	1	**88**
Elevators for luggage between check-in and baggage handling	-	-	-	-	-
Vehicles between airport & aircraft (GSE)	299	**99**	0	1.0	**36.0**
UPS	-	-	-	-	-
Recharging at Janitor rooms	-	-	-	-	-
Charging passengers	30	**30**	0	10	**113**
Material/waste electrical loads	2	**2**	0	20	**14**
Drainage pumps	56	**56**	56	24	**490**
Rain water collection/reuse	-	-	-	-	-
Water feature	-	-	-	-	-
pre-conditioning air system for aircrafts	-	-	-	-	-

Figure 56 Overview of the electrical power demand of internal devices *

usage	level	person density [m²/person]
arrivals hall	arrivals level	5.9
baggage claim	arrivals level	26.1
baggage handling	utilities, arrivals, international level	100.0
check-in	international departures level	7.0
circulation	utilities level	100.0
	arrivals level	50.0
	sterile corridor level	100.0
	international departures level	50.0
	transborder departures level	50.0
	mezzanine	50.0
holdroom	international departures level	18.9
	transborder departures level	10.9
jetbridges	sterile corridor & international level	100.0
	transborder level	100.0
lounge	utilities level	12.0
	arrivals level	12.0
	transborder & mezzanine level	12.0
mechanical loads	utilities, arrivals, sterile corridor, international, transborder & mezzanine	100.0
high load electrical/ mechanical/IT rooms	utilities, arrivals, sterile corridor, international, transborder & mezzanine	100.0
office	utilities, arrivals, international, transborder	12.0
food & beverage	arrivals level	15.0
	international departures level	15.0
	transborder level	15.0
retail	arrivals level	15.0
	international departures level	15.0
	transborder level	15.0
sanitary	utilities level	50.0
	arrivals level	50.0
	international departures level	50.0
	transborder level	50.0
storage	utilities, arrivals, sterile corridor, international, transborder & mezzanine	100.0
utilities	utilities level	200.0
tenant warehouse	utilities level	100.0
waiting / screening	utilities & arrivals level	3.6
	international departures level	17.7

Figure 57 Overview of the 17 implemented zones in the thermal simulation *

Auslegung: Kompakt-Schraubenverdichter CS

Vorgabewerte

Verdichtertyp	CSH8573-110Y
Kältemittel	R134a
Bezugstemperatur	Taupunkt
Verdampfung	5,00 °C
Verflüssigung	50,0 °C
Flüss.unterk. (im Verfl.)	0 K
Sauggasüberhitzung	10,00 K
Nutzbare Überhitzung	100%
Betriebsart	Standard
Netzversorgung	400V-3-50Hz
Leistungsregler	100%
Zusatzkühlung	Automatisch
Maximale Druckgastemp.	110,0 °C

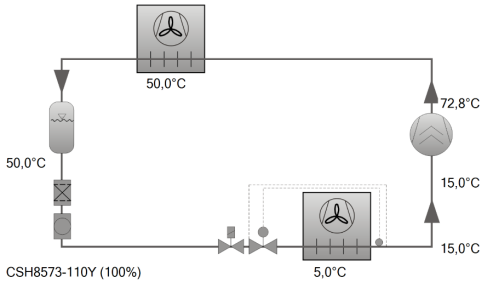

Ergebnis

Verdichter	**CSH8573-110Y-40P**
Leistungsstufen	100%
Kälteleistung	240 kW
Kälteleistung *	240 kW
Verdampferleist.	240 kW
Leistungsaufnahme	69,9 kW
Strom (400V)	118,5 A
Spannungsbereich	380-415V
Verflüssigerleistung	309 kW
Leistungszahl	3,43
Leistungszahl *	3,43
Massenstrom ND	6238 kg/h
Massenstrom HD	6238 kg/h
Betriebsart	Standard
Flüss.temp.	50,0 °C
Ölvolumenstrom	0,88 m³/h
Kühlungsmethode	--
Druckgastemp. Ungekühlt	72,8 °C

*nach EN12900 (10K Sauggasüberhitzung, 0K Flüssigkeitsunterkühlung, siehe T.Daten/ Hinweise)

Einsatzgrenzen Standard

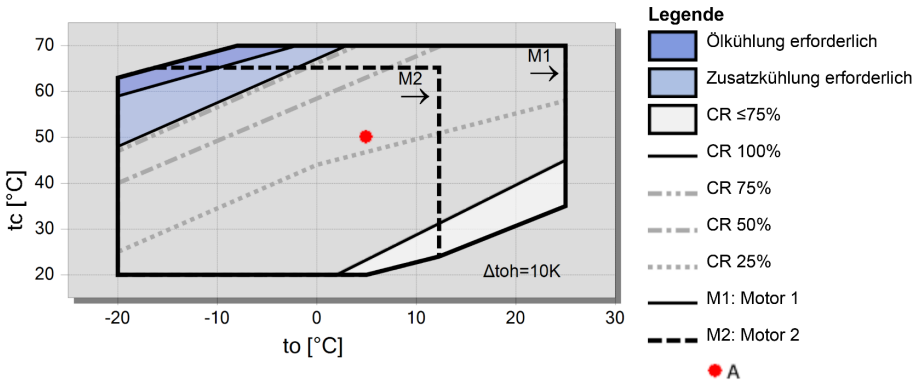

Figure 58 Data sheet compact screw compressor CSH8573-110Y by Bitzer [30]

BITZER Software v6.7.0 rev1849 | 14.03.2018 / Alle Angaben ohne Gewähr. | 4 / 8

Auslegung: Kompakt-Schraubenverdichter CS

Vorgabewerte

Verdichtertyp	CSH9563-160Y
Kältemittel	R134a
Bezugstemperatur	Taupunkt
Verdampfung	5.00 °C
Verflüssigung	50.0 °C
Flüss.unterk. (im Verfl.)	0 K
Sauggasüberhitzung	10.00 K
Nutzbare Überhitzung	100%
Betriebsart	Standard
Netzversorgung	400V-3-50Hz
Leistungsregler	100%
Zusatzkühlung	Automatisch
Maximale Druckgastemp.	110.0 °C

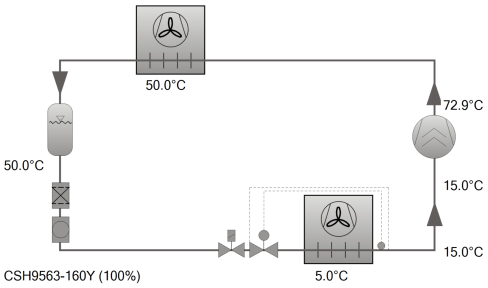

Ergebnis

Verdichter	**CSH9563-160Y-40D**
Leistungsstufen	100%
Kälteleistung	357 kW
Kälteleistung *	357 kW
Verdampferleist.	357 kW
Leistungsaufnahme	104.4 kW
Strom (400V)	172.2 A
Spannungsbereich	380-415V
Verflüssigerleistung	461 kW
Leistungszahl	3.42
Leistungszahl *	3.42
Massenstrom ND	9295 kg/h
Massenstrom HD	9295 kg/h
Betriebsart	Standard
Flüss.temp.	50.0 °C
Ölvolumenstrom	1.43 m³/h
Kühlungsmethode	--
Druckgastemp. Ungekühlt	72.9 °C

*nach EN12900 (10K Sauggasüberhitzung, 0K Flüssigkeitsunterkühlung, siehe T.Daten/ Hinweise)

Einsatzgrenzen Standard

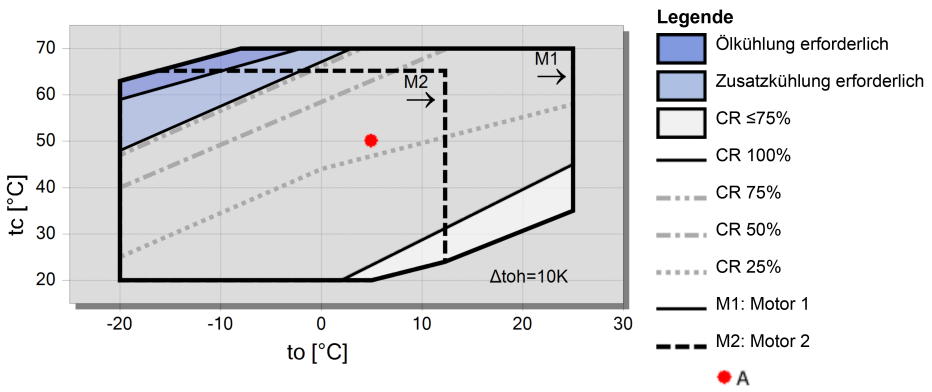

Figure 59 Data sheet compact screw compressor CSH9563-160Y by Bitzer [30]

Selection: Compact Screw Compressors CS

Input Values

Compressor model	CSH9583-280Y
Refrigerant	R134a
Reference temperature	Dew point temp.
Evaporating SST	5,00 °C
Condensing SDT	50,0 °C
Liq. subc. (in condenser)	0 K
Suct. gas superheat	10,00 K
Useful superheat	100%
Operating mode	Standard
Power supply	400V-3-50Hz
Capacity Control	100%
Additional cooling	Automatic
Max. discharge gas temp.	110,0 °C

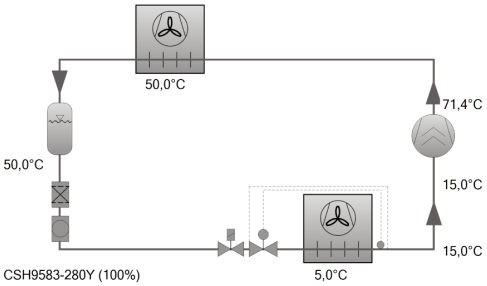

Result

Compressor	**CSH9583-280Y-40D**
Capacity steps	100%
Cooling capacity	472 kW
Cooling capacity *	472 kW
Evaporator capacity	472 kW
Power input	132,5 kW
Current (400V)	227 A
Voltage range	380-415V
Condenser Capacity	604 kW
COP/EER	3,56
COP/EER *	3,56
Mass flow LP	12288 kg/h
Mass flow HP	12288 kg/h
Operating mode	Standard
Liquid temp.	50,0 °C
Oil volume flow	1,43 m³/h
Cooling method	--
Discharge gas temp. w/o cooling	71,4 °C

*According to EN12900 (10K suction gas superheat, 0K liquid subcooling, see T.Data/ Notes)

Application Limits Standard

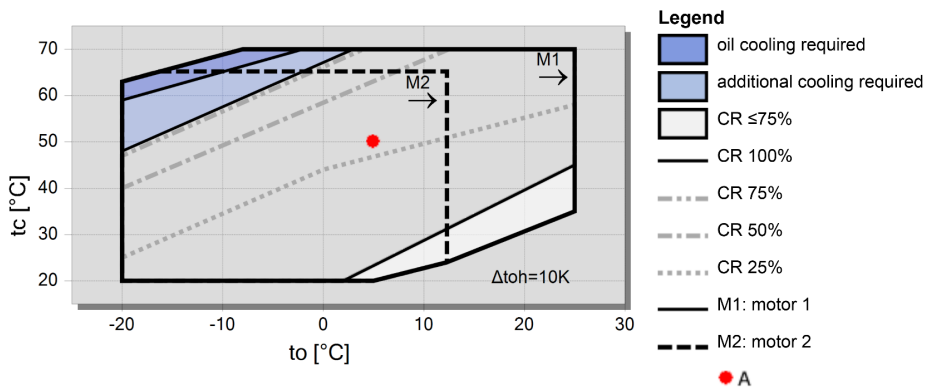

Figure 60 Data sheet compact screw compressor CSH9583-280Y-40D by Bitzer [30]

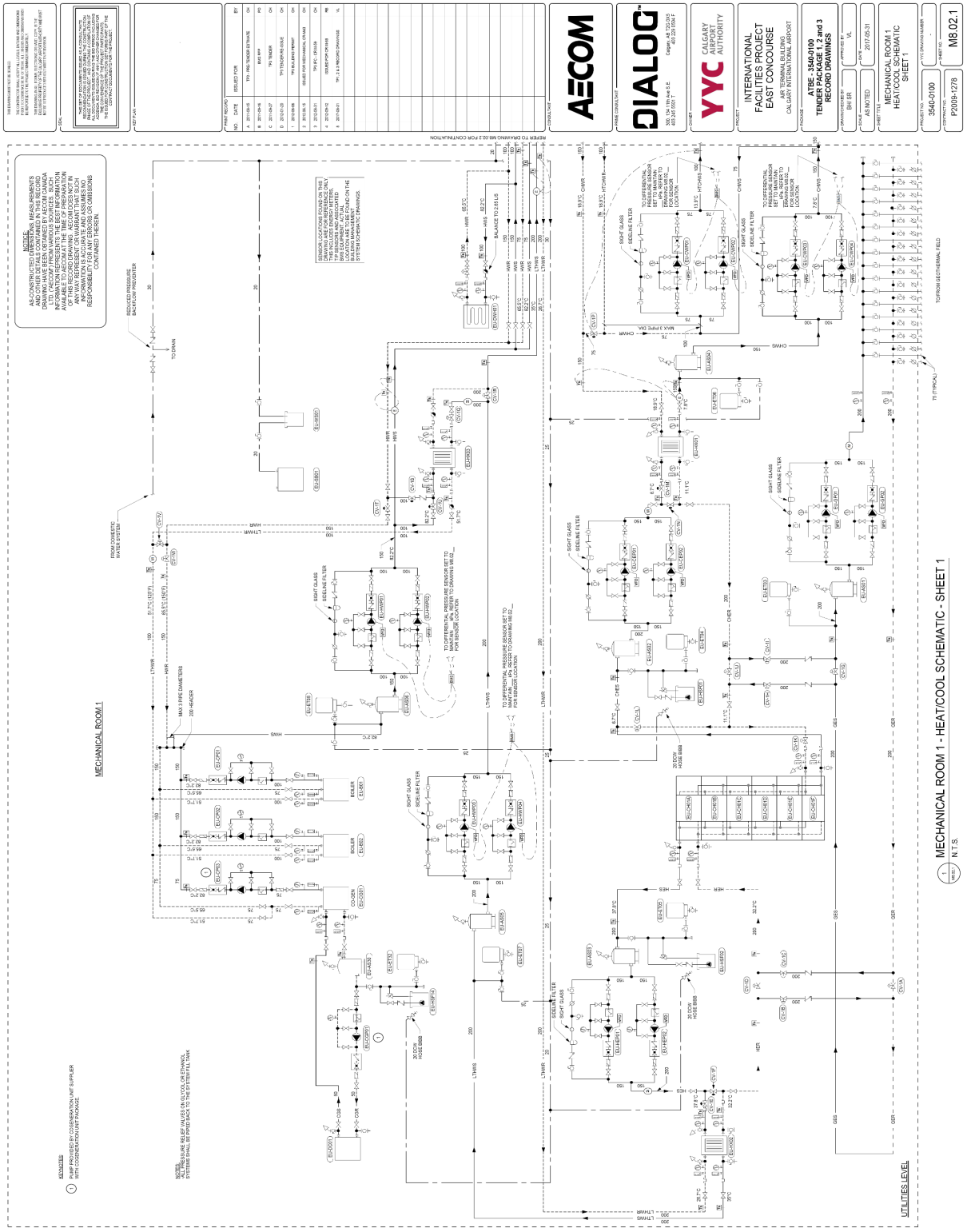

Figure 61 Schematic drawing MR01*

Appendix B – Subsystems of the plant simulation

The following paragraphs describe the subsystems of the plant simulation in detail. As mentioned in 5.1 the detailed analyses of the single components of the plant simulation are moved to the Appendix B to keep the focus of the thesis on the quality of the results of the optimizations. The following paragraphs describe the single subsystems, how they are implemented in the plant simulation, why physical and mathematical assumptions had to be made and how the project specific data of the International Airport Calgary is implemented.

Geothermal field

The component of the geothermal field describes the first subsystem of the building simulation. It is represented by the TRNSYS type 501 for the ground layers and by type 31 for the piping system. The geothermal loop is based on the superposition borehole model.

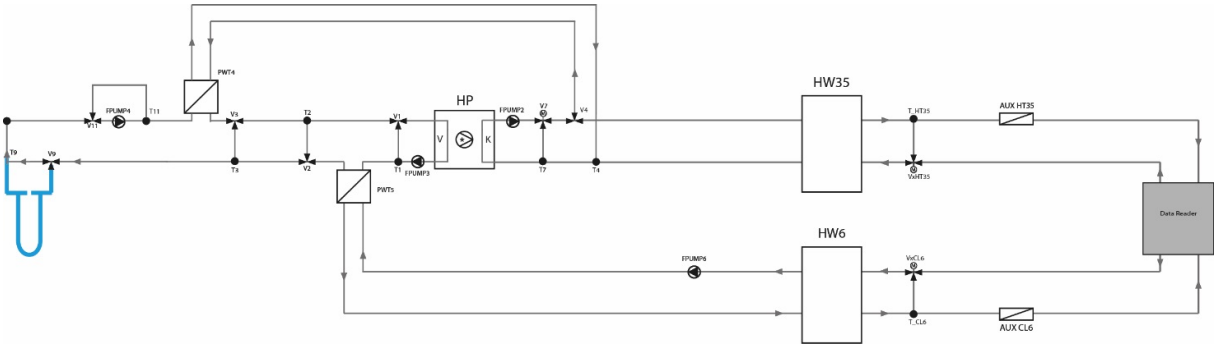

Figure 62 Location of the subsystem geothermal field in the plant simulation

The superposition borehole model describes the behavior of a multi-borehole system and calculates the thermal exchange between the borehole pipes and the ground. It also calculates the interaction between the boreholes with themselves. The superposition borehole model has been developed by Dr. D. Pahud. By an assign statement, the superposition borehole model reads in the data of a geothermal field in form of a "*.geo"*-file and a "*.bor"*-file. In the "*.geo"*-file, the location of the single boreholes, the depth, the different ground layers and their properties, the quality of the calculating mesh and coordinates for a horizontal and vertical cuts through the geothermal field are implemented. In the "*.bor"*-file the type and the properties of the outer and inner borehole pipes, as well as the grout characteristics are defined. [34]

By using the thermal properties of the ground and the borehole pipes the interaction between the ground and the pipes, as well as between the piping system itself can be calculated. The geothermal pipe system is separated into different hydraulic groups. The hydraulic groups are connected in series and manage the mass flow in the geothermal loop. If the geothermal field simulation is not divided into hydraulic groups, all geothermal borehole pipes are supplied in parallel at the same time. [34]

Depending on the different seasons, the geothermal field utilizes the ground temperature in different manners. In the summer period, heat is injected in the ground. During winter time, heat is extracted. Depending on the temperature of the inlet and outlet of the geothermal field, the thermal energy can be determined according to the following equation.

$$P_{Geo} = \dot{m}_{Geo} \times c_{Geo} \times (T_{Inlet,\ Geo} - T_{Outlet,\ Geo}) \qquad \text{Equ. 5} \qquad [21]$$

$\dot{m}_{Geo}$	Mass flow of the geothermal loop	[kg/h]
c_{Geo}	Specific heat capacity of the geothermal medium	[J/(kg K)]
T	Temperature of the geothermal medium	[°C]

Hydraulic separator

In the building simulation of the geothermal heat-pump system hydraulic separators are implemented. The key indicator of the performance of a hydraulic separator is the control strategy and the tank volume. The hydraulic separators are connected to the thermal loads of the building and form the connection between the load and source side. By using a water tank, it is possible to generate a thermal capacity that can supply the building with energy over a certain amount of time. Depending on the volume and the size of the heat-pump/chiller, it is possible to manage the buffer time of the hydraulically separator.

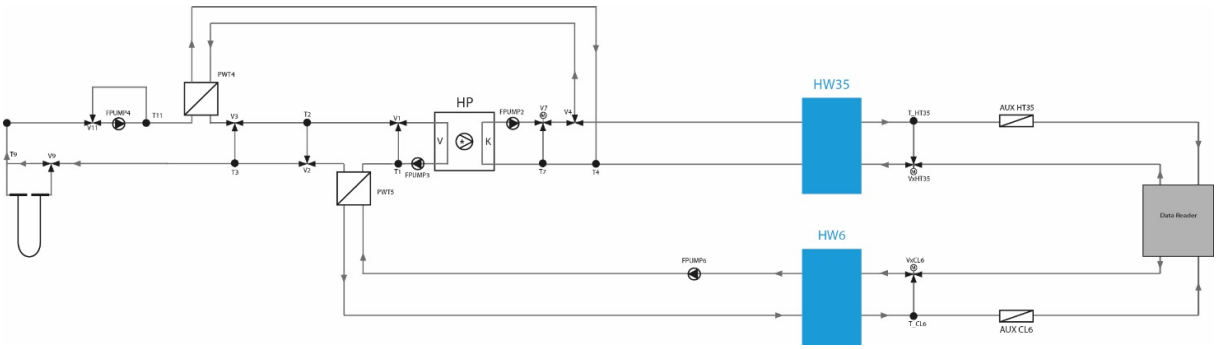

Figure 63 Location of the subsystem hydraulic separator in the plant simulation

In the TRNSYS type 4, the control function of the hydraulic separator is managed by the temperature levels at different heights in the water storage. The controller of a hot water storage gives the order to heat the storage, when the second lower node falls below a certain temperature level. It stops heating up the storage, when the upper second node exceeds the set point temperature. This is called an on/off controller. In comparison to a normal controller, the on/off-

controller depends on two different values to achieve that the amount of turning on and off the system is reduced. For the hot-water side, the set temperature is 40°C, including a temperature difference of 5°C correlated to the supply temperature of 35°C. For the cold-water storage, the controller operates in reverse and operators at a set temperature of 1°C, also including the same temperature difference in accordance to the supply temperature level of 6°C. The principles of the controller are illustrated in the following equation and figure.

$$Y_{heating,on} = T_{node\ n-1} < T_{set\ ,heating} \quad \text{Equ. 6}$$

$$Y_{heating,off} = T_{node\ 2} > T_{set\ ,heating} \quad \text{Equ. 7}$$

$$Y_{cooling,on} = T_{node\ 2} > T_{set\ ,cooling} \quad \text{Equ. 8}$$

$$Y_{cooling,off} = T_{node\ n-1} < T_{set\ ,cooling} \quad \text{Equ. 9}$$

$Y_{on/off}$	On/off-controller of mode	[-]
T_{node}	Temperature at certain height in the hydraulic separator	[°C]
T_{set}	Specific defined set temperature of mode	[°C]

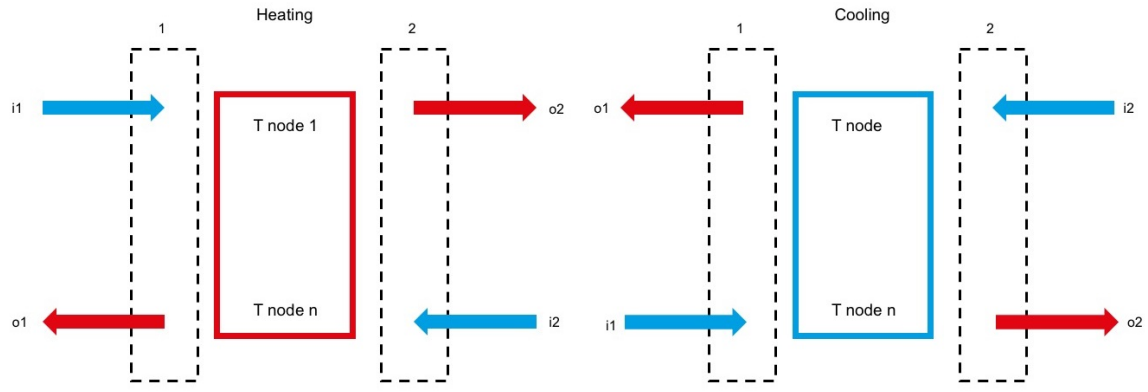

Figure 64 Schematic of the control strategy of the hydraulic separators

Heat-pump/chiller

A further main component of the building simulation is the heat-pump. It is represented by the TRNSYS type 401. The component acts as a heat-pump during the heating mode and as a chiller in the cooling period. As mentioned in chapter 2.5, a heat-pump is utilized to generate a higher temperature level. In case of a simultaneously heating and cooling demand, the chiller generates cooling energy, while the waste heat of this process is used to supply the hot water side.

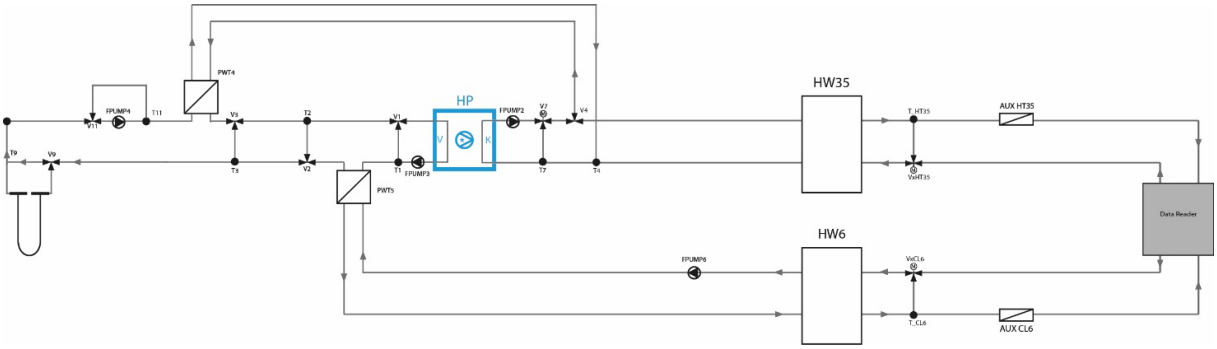

Figure 65 Location of the subsystem heat-pump/chiller in the plant simulation

The implemented compact screw compressor is sized according to the compact screw compressor CSH8573-110Y by Bitzer, illustrated in Appendix A. The cooling power of the chiller is 244 kW. Its condenser works in a temperature range of a minimum of 20°C and a maximum of 70°C. The evaporator temperature range of the chiller is between -20°C to 25°C. [30]

The COP in the cooling mode at the design point is 3.4, while the COP in the heating mode is 4.4. The sizing of the heat-pump correlates strongly with the heating and cooling demand of an edifice. In combination with the fact that the heating and cooling demand is varying from 100 kWh to more than 1000 kWh a stepwise activation of single 244 kW chiller stages is implemented. This also represents the reality. Chillers in building systems normally are divided into single sub-elements to generate a more accurate adaption to the building load. The chiller mode of the implemented component is illustrated in the following figure 66. In the heating mode, the control strategy of the heat-pump runs vice versa.

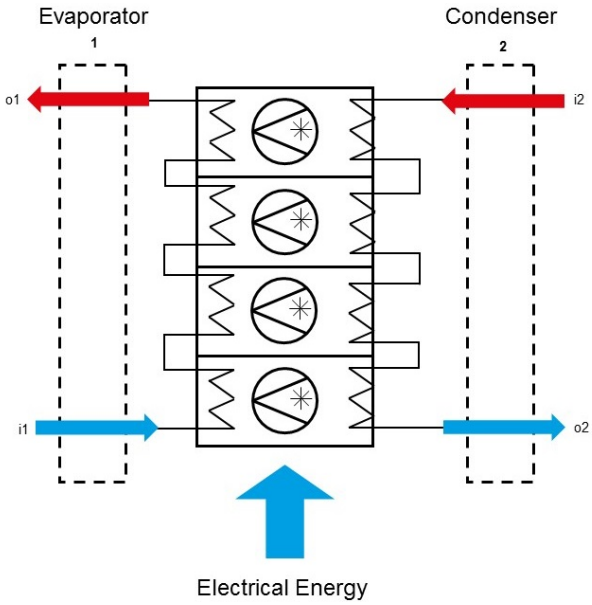

Figure 66 Schematic chiller mode

Data reader

The thermal energy demand in the uncoupled system simulation is implemented through a data reader, based on the TRNSYS type 109. This type serves the main purpose of reading data in the format of an hourly time step. TYPE 109 reads free-formatted files. The data reader connects the hourly heating and cooling demand of the building with the building system. To calculate the energy flows in the building system, one needs to implement the mass flow, as well as the supply and return temperatures of the building. Based on this information, the building system can calculate the thermal energy to provide the heating and cooling energy for the edifice. The implemented heating and cooling demand is analyzed in detail in 4.2.

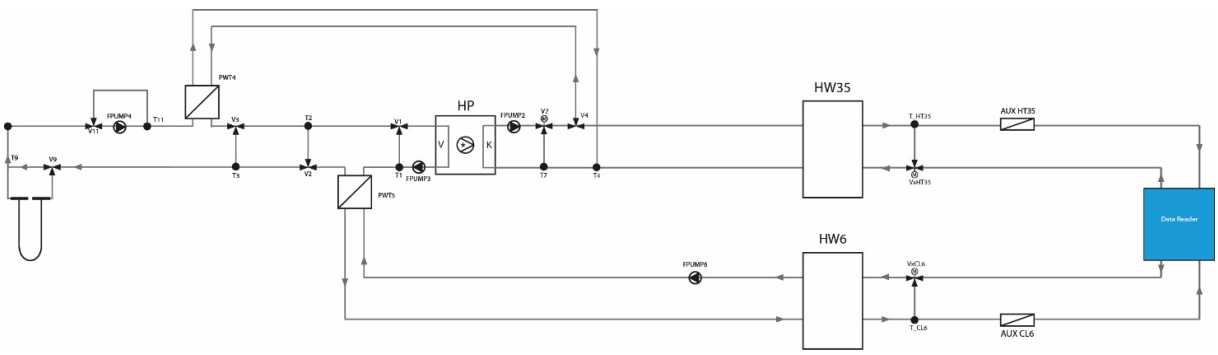

Figure 67 Location of the subsystem data reader in the plant simulation

Plate heat exchangers

On the one hand, the plate heat exchangers connect the geothermal loop with the hydraulic separators, when the heat-pump is not activated (state 3 & 5). On the other hand, the heat exchangers link the geothermal field with the heat-pump/chiller device in the active heating and cooling mode of the building system (State 2 & 4).

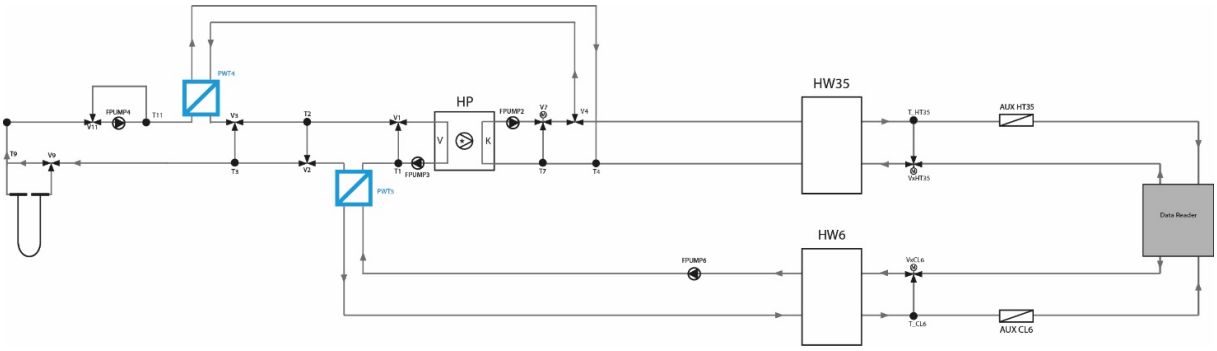

Figure 68 Location of the subsystem plate heat exchanger in the plant simulation

The plate heat exchangers are represented by the type 91 in TRNSYS. This heat exchanger operates with a constant effectiveness, which is independent of the system configuration. The maximum possible heat transfer rate is calculated related to the properties of the implemented fluids, as well as on the maximum and minimum temperature differences of the fluids on both sides of the heat exchanger. The thermal transfer rate is determined by the effectiveness of the heat exchanger, which depends on the plate area and the thermal properties of the two fluids. The specific effectiveness of the plate heat exchanger is calculated according to the following equation.

$$\varepsilon_{HX} = \frac{(T_{set,out} - T_{load,in})}{(T_{set,in} - T_{load,out})} \qquad \text{Equ. 10} \qquad [26]$$

ε_{HX}	Effectiveness of heat exchanger at design point	[-]
$T_{set,in/out}$	Set inlet/outlet temperature	[°C]
$T_{laod,in/out}$	Load temperature at the design point	[°C]

T-Valve

In the plant simulation six t-valves are implemented. The t-valves have different functions depending on the components that must be controlled. One function of a t-valve is to handle the mixture of the supply and return flow of a component. This is called fraction bypass. Using a fraction bypass, energy can be saved. This control function is used by t-valve 20 and t-valve 22, shown in figure 69. Furthermore, t-valves control the direction of the flow. Through opening and closing of the valve, depending on the individual controller, the mass flow can adapt to a specific system states. This principle is used by the t-valves 1, 2, 3 and 7 in the plant simulation. These t-valves are managing the direction of the flow in the single system states.

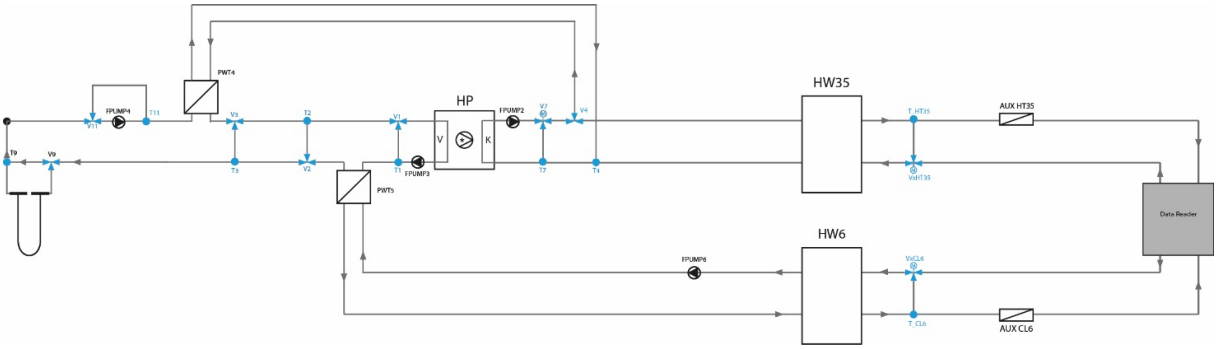

Figure 69 Location of the subsystem t-valve in the plant simulation

The t-valve component in TRNSYS consists of two types. Type 953 describes the tempering valve controller of the component. In type 11 the tee-piece is managed. This structure is represented in figure 70. In case of t-valve 20, the tee-piece mixes two inlet streams of the same fluid at different temperature levels to generate a higher temperature level for the supply system. This results in the fact that the return flow temperature of the building is mixed with the generated hot water to the supply temperature level. The principle of the t-valves is displayed in the following figure 70.

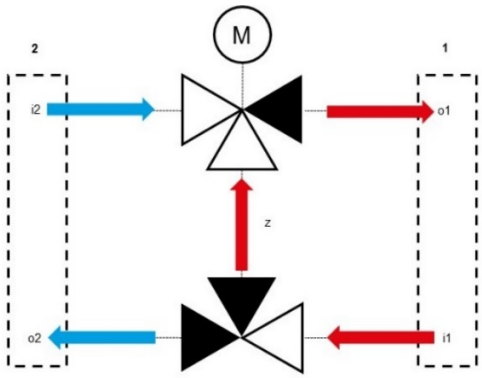

Figure 70 Schematic control strategy t-valve

Fluid Pumps

Every fluid loop needs an individual fluid pump to manage the mass flow. The key issue of the effectiveness of a fluid pump is the pressure drop caused by the fluid. The pressure drop depends on the mass flow and the dynamic viscosity of the transported media. Based on the pressure drop, one can calculate the induced electrical energy demand of the pipes. A part of the generated heat is transferred into the atmosphere, while the other part of the energy is heating up the fluid. In this plant simulation, the total induced energy is transmitted into the fluid. This assumption has been done to fulfill the overall energy balance.

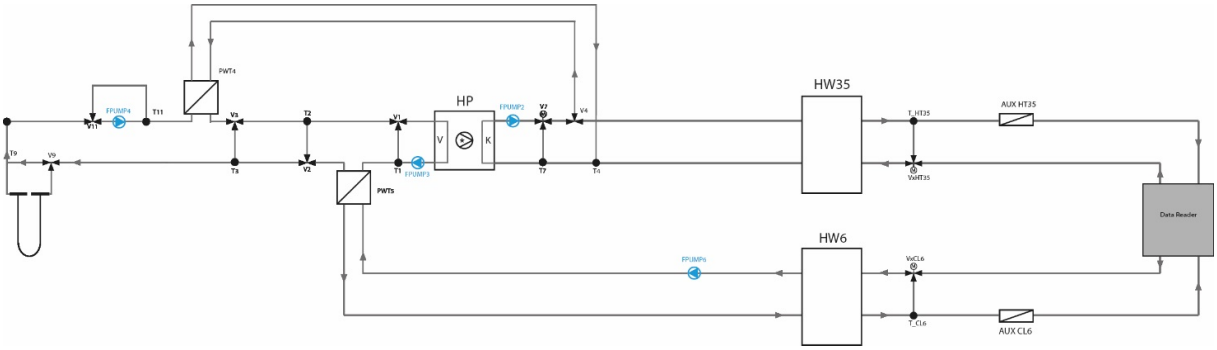

Figure 71 Location of the subsystem fluid pump in the plant simulation

In the system simulation of the International Airport Calgary, four fluid pumps are implemented. The mechanical efficiency is set to 50 %. By using the mass flow through the fluid pump, the pressure drops, the density of the fluid and the mechanical efficiency of the pump, the TRNSYS type 3 can calculate the electrical energy demand, depicted in the following equation.

$$P_{el} = \frac{\dot{m}_{fpump} \times \Delta p}{\rho \times n_{fpump,mec}} \qquad \text{Equ. 11} \qquad [35]$$

P_{el}	Electrical energy demand of the fluid pump	[Wh]
$\dot{m}_{fpump}$	Mass flow of the fluid pump	[kg/h]
ρ	Density of the medium of the fluid pump	[J/(kg K)]
$n_{fpump,mec}$	Mechanical efficiency factor of the fluid pump	[-]
Δp	Pressure drop of the fluid pump	[Pa]

Fluid pump 4 of the plant simulation has a special task. This fluid pump must cover the pressure drop of the geothermal field. This results in a separate calculation of the mass flow to generate a realistic representation of the electrical energy demand of the operation of the geothermal system. To stay in the range of a laminar flow, the Reynolds number is set to 2300. The length of the implemented piles is 132 m as mentioned in section 4.3. The electrical energy demand of the fluid pump of the geothermal field is calculated as follows.

$$\Delta p_{fpump,4} = \frac{L \times \rho \times \nu^2 \times \lambda}{d_i \times 2} \quad \text{with} \quad \lambda = \frac{c}{RE} \qquad \text{Equ. 12} \qquad [35]$$

Δp	Pressure drop of the pile system	[Pa]
L	Length of the geothermal piles	[m]
ρ	Density of the medium of the pump	[kg/m^3]
ν	Velocity of the medium of the pump	[m/s]
d_i	Inner diameter of the geothermal piles	[m]
λ	Friction coefficient	[-]
c	Factor for the tubes	[-]
RE	Reynolds number	[-]

Auxiliary heater/cooler

The last component of the building system of the plant simulation of the International Airport of Calgary is the auxiliary heater/cooler. This component is artificially implemented in the uncoupled plant simulation and does not exist in the real building services of the airport in Calgary. The integration of an artificial heater/cooler is a common way to run an uncoupled plant simulation, because the supply temperatures for the heating and cooling load must be reached in every time step of the simulation. This condition must be fulfilled, because the building load does not adapt to the building system. Another reason, why it is good to integrate an auxiliary heater/cooler is that the device can be used as an indicator for the performance of a building system. Since an auxiliary heater/cooler normally is not implemented, a high demand of an auxiliary heater/cooler gives you feedback on the functionality of the whole building system. If the plant simulation must add a lot of auxiliary energy, the simulation does not work accurate enough. In the optimization variants, this indicator is used to analyze the single variants of the system.

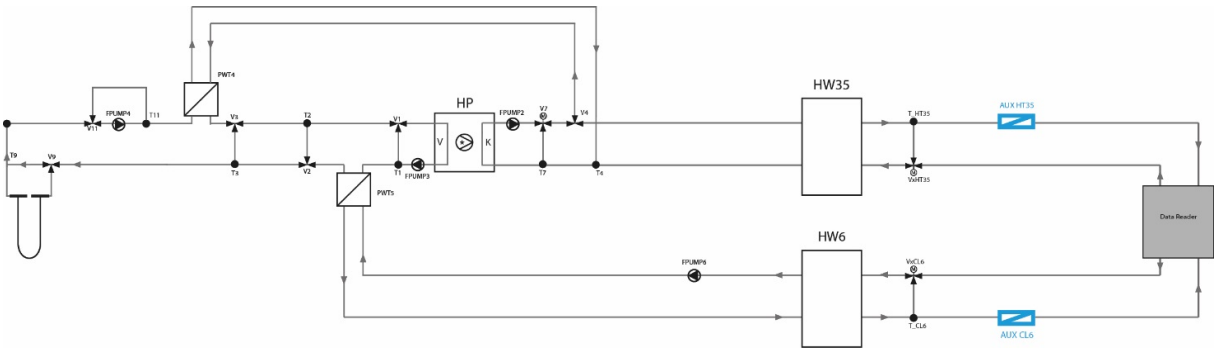

Figure 72 Location of the subsystem auxiliary heater/cooler in the plant simulation

In the TRNSYS simulation, the auxiliary heater/cooler component is implemented in the form of three single equations and is not summed up in a specific simulation type. If the outlet temperature of the hydraulic separator does not reach the set point temperature of the supply system, the controller of the auxiliary heater/cooler turns to 1 and gives the order to calculate the missing energy. In the system states of the free heating/cooling mode, as well as in the system states, where the hydraulic separators feed the building without an energy generation, the auxiliary heater/cooler is deactivated to avoid an artificial supply of the building. The following equations display the control strategy of an auxiliary cooler. The operation of an auxiliary heater is controlled reverse.

$$T_{out,cooling} = T_{in,cooling} + \frac{Q_{aux,cooling} \times 3600}{\dot{m}_{aux} \times c_{p,medium}} \quad \text{Equ. 13}$$

$$Q_{aux,cooling} = \dot{m} \times c_{p,medium} \times \left(T_{set,cooling} - T_{in,cooling}\right) \times Y_{aux,cooling} \quad \text{Equ. 14}$$

$$Y_{aux,cooling} = IF\ (T_{in,cooling} > T_{set,cooling}) \quad \text{Equ. 15}$$

$Q_{aux,cooling}$	Thermal energy of the auxiliary cooler	[kW]
$\dot{m}_{aux}$	Mass flow of auxiliary cooler	[kg/h]
$c_{p,medium}$	Specific heat capacity of the medium	[J/(kg K)]
$Y_{aux,cooling}$	Switch of auxiliary cooler	[-]
$T_{in/out}$	Inlet/outlet temperature of the auxiliary cooler	[°C]
T_{set}	Set temperature of the auxiliary cooler	[°C]

Appendix C – System states of the plant simulation

State 1: No heating – no cooling energy generation

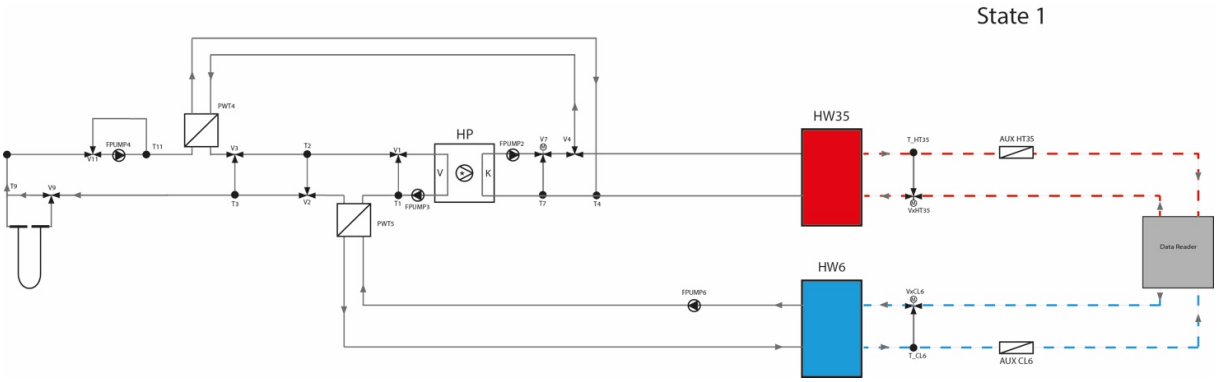

Figure 73 System state 1

State 2: No heating – just cooling energy generation; thermal source chiller + geo

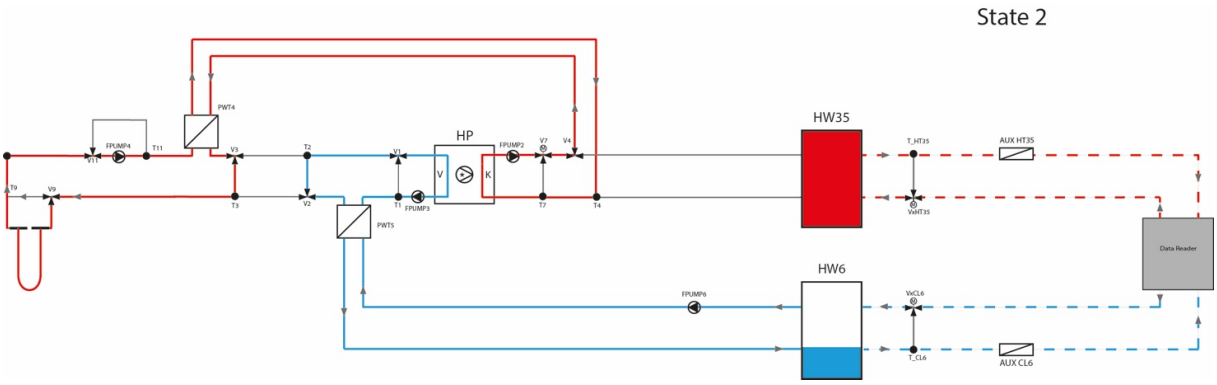

Figure 74 System state 2

State 3: No heating – just cooling energy generation; free cooling mode; just geo

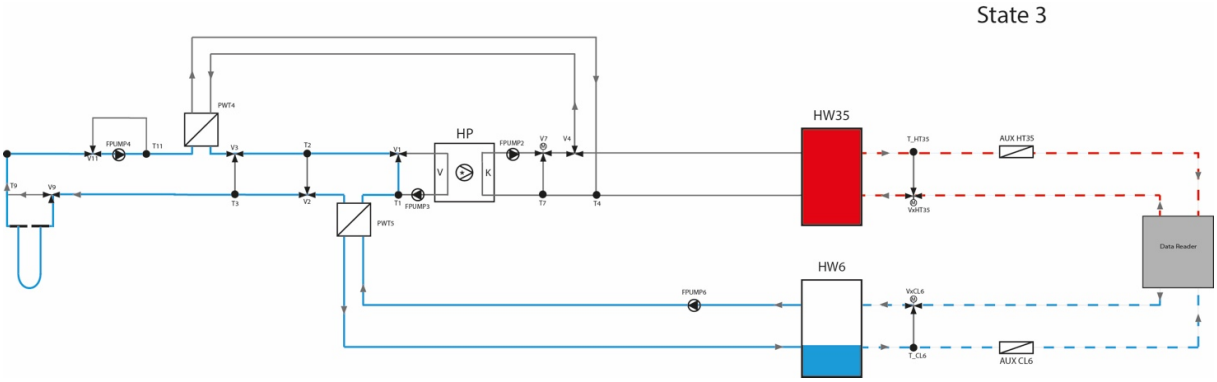

Figure 75 System state 3

State 4: Just heating – no cooling energy generation; thermal source heat-pump + geo

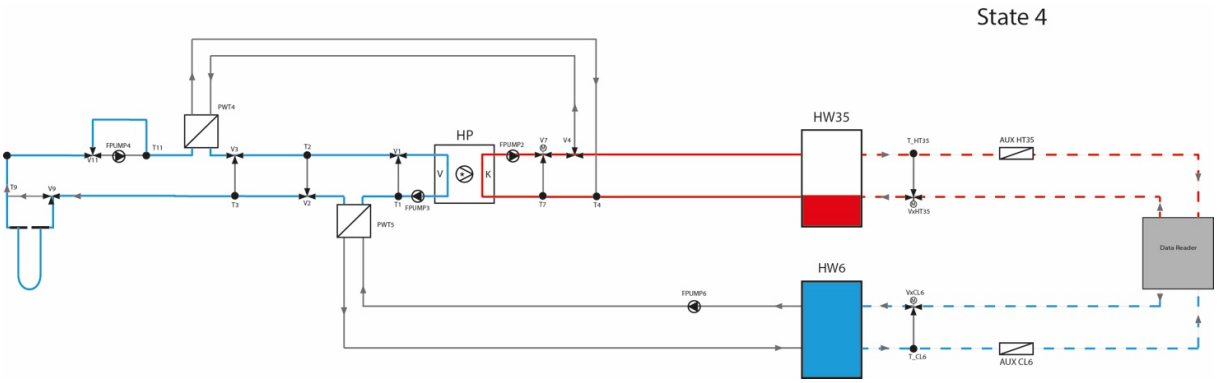

Figure 76 System state 4

State 5: Just heating – no cooling energy generation; free heating mode; just geo

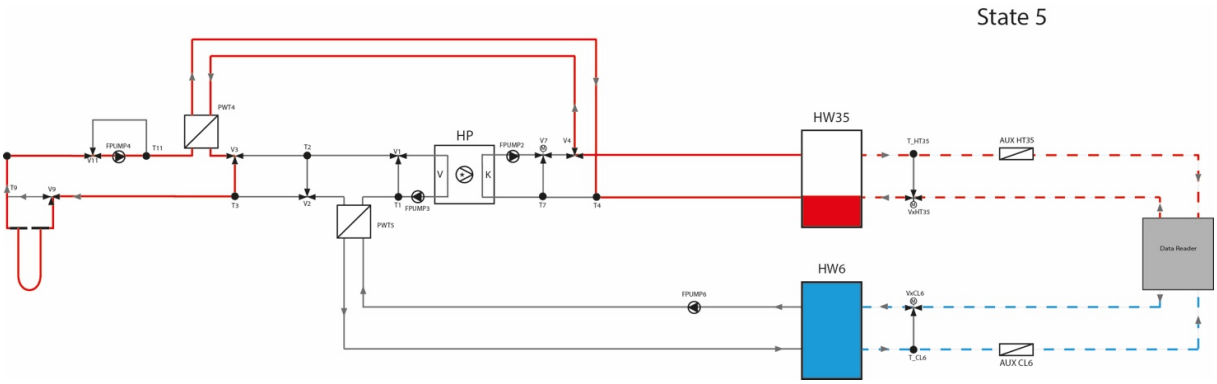

Figure 77 System state 5

State 6: Heating & cooling energy generation; thermal source heat-pump/chiller

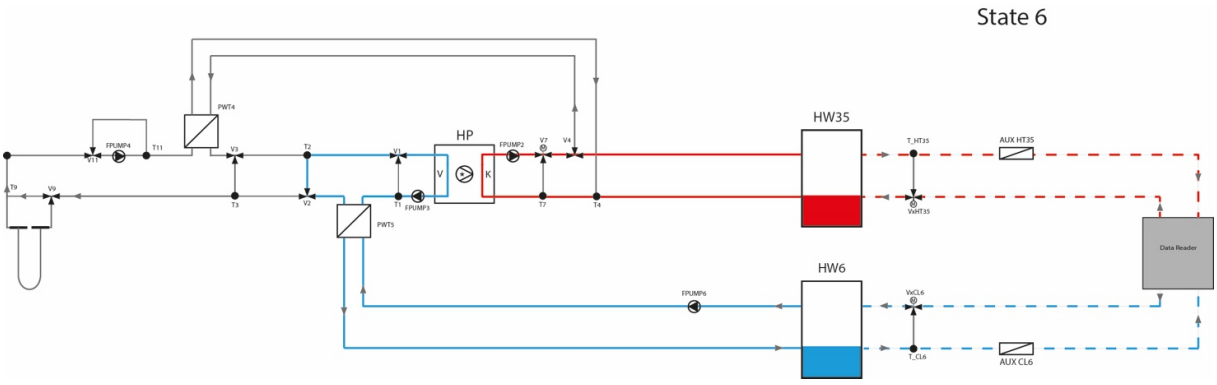

Figure 78 System state 6

Bibliography

[1] H. L. -. Z. f. i. Gebäudetechnik, performance gap in der Schweiz - Brisanz. Ursachen und Einflüsse auf die Differenz von geplantem Energiebedarf und gemessenem Verbrauch in Gebäuden.

[2] E. u. T. Bayerisches Staatsministerium für Wirtschaft und Medien, "www.energieatlas.bayern.de," 02 2018. [Online]. Available: https://www.energieatlas.bayern.de/unternehmen/gebaeude.html.

[3] D. D. I. f. N. e.V., DIN V 18599 - 10, Berlin: Beuth Verlag GmbH, 2017.

[4] D. L. M. J. R. Donella H. Meadows, The Limits to Growth: The 30-Year Update, Chelsea Green Publishing, 2004.

[5] B. M. -. R. c. H. S. Stiftung, "www.relaio.de," [Online]. Available: (http://www.relaio.de/topics/artikeluebersicht/suffizienz-konsistenz-effizienz.html). [Accessed 01 Feb 2018].

[6] D. Fuhrhop, Verbietet das Bauen - Eine Streitschrift, München: oekom Verlag, 2015.

[7] Umweltbundesamt, "www.umweltbundesamt.de," [Online]. Available: https://www.umweltbundesamt.de/themen/wirtschaft-konsum/konsum-umwelt-zentrale-handlungsfelder#textpart-1. [Accessed 29 Jan 2018].

[8] I. P. o. C. Change, Chlimate Change - The Physical Science Basis, Cambridge: Cambridge University Press, 2013.

[9] Arup, Event Report The Building Perdormance Gap - closing it through better measurement, London, 2012.

[10] V. Doda, Occupants Mind the performance gap, München, 2017.

[11] U. G. B. Council, Building Zero Carbon - the case for action, London, 2014.

[12] C. E. P. Group, "https://www.cibse.org/," 27 Nov 2017. [Online]. Available: https://www.cibse.org/getmedia/55cf31bd-d9eb-4ffa-b2e2-e567327ee45f/cb11.pdf.aspx.

[13] G. R. D. Carolyn Kipsang - Kenya Electricity Generation Company Limited, Cost model for geothermal wells, Australia, 2015.

[14] P. V. Marian Keeler, Fundamentals of Integrated Design for Sustainable Building, New Jersey, 2009.

[15] S. L. S. Hausladen, Clima Design, München, 2004.

[16] U. D. o. Energy, "https://energy.gov/," 27 Nov 2017. [Online]. Available: https://energy.gov/eere/buildings/building-technologies-office.

[17] M. F. V. B. Stanford University - Tobias Maile, Building Energy Performance Simulation Tools - a Life-Cycle and Interoperable Perspective, Stanford, 2007.

[18] M. J. D. -. U. o. Wisconsin, "http://sel.me.wisc.edu/trnsys/index.html," The Board of Regents of the University of Wisconsin System, [Online]. Available: http://sel.me.wisc.edu/trnsys/features/features.html. [Accessed 12 Dez 2017].

[19] U. o. W.-M. Solar Energy Laboratory and T. E. GmbH, TRNSYS 18 - A TRaNsient SYstem Simulation program.

[20] O. o. E. E. &. R. E. -. U. D. o. Energy, "www.energy.gov," [Online]. Available: https://www.energy.gov/energysaver/heat-and-cool/heat-pump-systems/geothermal-heat-pumps. [Accessed 18 Dez 2017].

[21] P. D. I. Stober and P. D. K. Bucher, Geothermie, Heidelberg Springer-Verlag GmbH, 2014.

[22] N. R. Canada, 13 Nov 2017. [Online].Available:http://www.nrcan.gc.ca/energy/publications/efficiency

[23] B. G. e.V., "www.geothermie.de," 24 Nov 2017.
[Online]. Available: http://www.geothermie.de/wissenswelt/geothermie/einstieg-in-die-geothermie/oekologische-aspekte.html.

[24] Umweltbundesamt, "www.umweltbundesamt.de," 24 Nov 2017.
[Online]. Available:
https://www.umweltbundesamt.de/themen/oberflaechennahe-geothermie-welche-auswirkungen-hat .

[25] D.-I. H. D. Baehr, Thermodynamik, Berlin: Springer Verlag , 2012.

[26] P. D.-I. W. Pistohl, Handbuch der Gebäudetechnik, Düsseldorf: Werner Verlag, 1998.

[27] E. a. C. C. C. National Inquiry Response Team Meteorological Service of Canada "https://calgary.weatherstats.ca/," 07 Nov 2017.
[Online]. Available: https://calgary.weatherstats.ca/.

[28] E. a. C. C. C. National Inquiry Response Team Meteorological Service of Canada "http://climate.weather.gc.ca," 25 Oct 2014.
[Online]. Available: http://climate.weather.gc.ca. [Accessed 04 11 2017].

[29] m. AG, "https://www.meteoblue.com,"
[Online]. Available
https://www.meteoblue.com/en/weather/forecast/modelclimate/calgary_canada_5913490. [Accessed 10 Jan 2018].

[30] B. K. GmbH, "https://www.bitzer.de,"
[Online]. Available: https://www.bitzer.de. [Accessed 12 Feb 2018].

[31] M. Kammerlander and P. D.-I. T. Auer, Master's Thesis
Impact of selected controlling parameters on energy and comfort analyzed by coupled dynamic simulation of building and energy supply system, München , 2016.

[32] C. E. -. A. N. Corp., "Geo-exchange Thermal Conductivity Report," Calgary, 2011.

[33] D. W. Kessing, Interviewee, *The FuturArc Interview.* [Interview]. http://www.futurarc.com/index.cfm/editorial/futurarc-interview/2017-may-jun-interview-wolfgang-kessling/ May 2017.

[34] D. D. Pahud, "http://www.repository.supsi.ch," 05 Feb 2018. [Online]. Available: http://repository.supsi.ch/3042/1/29-Pahud-1996-SBM.pdf.

[35] P. D.-I. E.-R. Schramek, Taschenbuch für Heizung + Klimatechnik, München Oldenburg Industrieverlag, 2009.

List of Figures

FIGURE 1 DIMENSIONS OF SUSTAINABILITY (OWN REPRESENTATION BASED ON [5]) 1
FIGURE 2 THERMAL COMFORT (OWN REPRESENTATION BASED ON [15]) 9
FIGURE 3 COMPONENTS OF A BUILDING ENERGY SIMULATION 10
FIGURE 4 INTERACTION BETWEEN THERMAL AND BUILDING SYSTEM SIMULATION 11
FIGURE 5 SIMULATION SITUATION FOR THE INTERNATIONAL AIRPORT CALGARY 12
FIGURE 6 GEOTHERMAL HEAT-PUMP SCHEMATIC (OWN REPRESENTATION BASED ON [21]) 14
FIGURE 7 GEOTHERMAL UTILIZATION IN SUMMER & WINTER 15
FIGURE 8 COMPARISON OF THE MEASURED & SIMULATED COOLING DEMAND 19
FIGURE 9 SCHEMATIC DRAWING OF A HEAT EXCHANGER (OWN REPRESENTATION BASED ON [26]) 20
FIGURE 10 PERFORMANCE OF THE HEAT EXCHANGERS IN THE CHW LOOP 21
FIGURE 11 PERFORMANCE OF THE HEAT EXCHANGERS IN THE LTHW LOOP 22
FIGURE 12 GLOBAL RADIATION CALGARY (OWN REPRESENTATION BASED ON [27] & [28]) 24
FIGURE 13 AMBIENT TEMPERATURE CALGARY (OWN REPRESENTATION BASED ON [27] & [28]) 25
FIGURE 14 HUMIDITY CONDITIONS CALGARY (OWN REPRESENTATION BASED ON [27] & [28]) 26
FIGURE 15 WIND DIRECTION/VELOCITY CALGARY (OWN REPRESENTATION BASED ON [27] & [28]) 27
FIGURE 16 SYSTEM BOUNDARY ENERGY BALANCE FOR MR01 28
FIGURE 17 TOTAL ENERGY BALANCE FOR MR01 29
FIGURE 18 LOCATION OF THE ROOMS SUPPLIED BY MR01 33
FIGURE 19 ANNUAL HEATING & COOLING DEMAND 34
FIGURE 20 LOAD DURATION CURVE FOR THE HEATING & COOLING DEMAND 35
FIGURE 21 DIMENSIONS OF THE IMPLEMENTED SINGLE-U-PIPE [MM] 36
FIGURE 22 LOCATION OF THE GEOTHERMAL BOREHOLES OF MR01 37
FIGURE 23 STRUCTURE PLANT SIMULATION 43
FIGURE 24 PERFORMANCE OF THE COMPONENTS IN THE BASE CASE MODEL 44
FIGURE 25 OCCURRENCE OF THE SYSTEM STATES OF THE BASE CASE MODEL [HOURS/YEAR] 44
FIGURE 26 ENERGY BALANCE OF THE BASE CASE MODEL 45
FIGURE 27 ENERGY BALANCE ERRORS PER SYSTEM STATE FOR THE BASE CASE MODEL 46
FIGURE 28 DEVELOPMENT OF THE TEMPERATURE LEVEL OF THE GEOTHERMAL FIELD OVER 10 YEARS 47
FIGURE 29 OVERVIEW OF THE PIPE MODELS 48
FIGURE 30 COMPARISON OF THE PIPE MODELS IN SUMMER & WINTER FOR A BALANCED LOAD 48
FIGURE 31 COMPARISON OF THE PIPE MODELS IN SUMMER & WINTER FOR IMBALANCED LOADS 49
FIGURE 32 EVALUATING DIAGRAM FOR BUILDING SYSTEM VARIANTS 50
FIGURE 33 OVERVIEW OF THE FIXED PARAMETERS OF THE GEOTHERMAL FIELD 51
FIGURE 34 SYSTEM VARIATIONS ACCORDING TO THE THERMAL CONDUCTIVITY OF THE GROUND 52
FIGURE 35 SCHEMATIC TEMPERATURE PROFILE OF THE GROUND IN THE TEMPERATE LATITUDES [21] 53
FIGURE 36 SYSTEM VARIATIONS ACCORDING TO THE UNDISTURBED GROUND TEMPERATURE 54
FIGURE 37 VARIATION OF DIFFERENT BOREHOLE PIPES 55
FIGURE 38 SYSTEM VARIATIONS ACCORDING TO DIFFERENT BOREHOLE PIPES 55
FIGURE 39 SYSTEM VARIATIONS ACCORDING TO THE FLUID IN THE GEOTHERMAL LOOP 56
FIGURE 40 OUTLET TEMPERATURES OF THE GEOTHERMAL FIELD FOR DIFFERENT LOADS [SUMMER DAY] 57
FIGURE 41 VARIATION OF THE THERMAL BUILDING LOAD 58
FIGURE 42 SYSTEM VARIATIONS ACCORDING TO THE BUILDING LOAD 58
FIGURE 43 OVERVIEW OF THE ADJUSTABLE FACTORS OF THE BUILDING SYSTEM 59
FIGURE 44 DYNAMIC BEHAVIOR OF THE HEAT-PUMP/CHILLER SYSTEM IN THE HEATING MODE 60
FIGURE 45 SYSTEM VARIATIONS ACCORDING TO THE POWER OF THE HEAT-PUMP 61

FIGURE 46 OCCURRENCE OF SYSTEM STATES ACCORDING TO DIFFERENT CAPACITY LEVELS [HOURS/YEAR] 62
FIGURE 47 SYSTEM VARIATION ACCORDING TO THE CONTROL STRATEGY OF THE HYDRAULIC SEPARATORS 63
FIGURE 48 OCCURRENCE OF SYSTEM STATES FOR DIFFERENT CONTROL STRATEGIES HW [HOURS/YEAR] 64
FIGURE 49 SYSTEM VARIATIONS ACCORDING TO THE EFFECTIVENESS OF THE HEAT EXCHANGERS 65
FIGURE 50 OCCURRENCE OF SYSTEM STATES FOR VARYING THE EFFECTIVENESS OF THE HX [HOURS/YEAR] 66
FIGURE 51 SYSTEM VARIATIONS ACCORDING TO REDUCTION OF THE MASS FLOW OF THE SYSTEM 67
FIGURE 52 INFLUENCE OF THE POSITION OF AN OPTIMIZATION VARIANT 70
FIGURE 53 POTENTIAL OF THE ADJUSTABLE COMPONENTS (TOP DIAGRAM) AND FIXED PARAMETERS (BELOW DIAGRAM) OF THE BUILDING SYSTEM 74
FIGURE 54 DISTRIBUTION OF THE OCCUPANCY RATES IN THE INTERNATIONAL AIRPORT CALGARY * 82
FIGURE 55 MATERIAL PROPERTIES OF DIFFERENT FLUIDS FOR A GEOTHERMAL LOOP [21] 82
FIGURE 56 OVERVIEW OF THE ELECTRICAL POWER DEMAND OF INTERNAL DEVICES * 83
FIGURE 57 OVERVIEW OF THE 17 IMPLEMENTED ZONES IN THE THERMAL SIMULATION * 84
FIGURE 58 DATA SHEET COMPACT SCREW COMPRESSOR CSH8573-110Y BY BITZER [30] 85
FIGURE 59 DATA SHEET COMPACT SCREW COMPRESSOR CSH9563-160Y BY BITZER [30] 86
FIGURE 60 DATA SHEET COMPACT SCREW COMPRESSOR CSH9583-280Y-40D BY BITZER [30] 87
FIGURE 61 SCHEMATIC DRAWING MR01* 88
FIGURE 62 LOCATION OF THE SUBSYSTEM GEOTHERMAL FIELD IN THE PLANT SIMULATION 89
FIGURE 63 LOCATION OF THE SUBSYSTEM HYDRAULIC SEPARATOR IN THE PLANT SIMULATION 90
FIGURE 64 SCHEMATIC OF THE CONTROL STRATEGY OF THE HYDRAULIC SEPARATORS 91
FIGURE 65 LOCATION OF THE SUBSYSTEM HEAT-PUMP/CHILLER IN THE PLANT SIMULATION 92
FIGURE 66 SCHEMATIC CHILLER MODE 93
FIGURE 67 LOCATION OF THE SUBSYSTEM DATA READER IN THE PLANT SIMULATION 93
FIGURE 68 LOCATION OF THE SUBSYSTEM PLATE HEAT EXCHANGER IN THE PLANT SIMULATION 94
FIGURE 69 LOCATION OF THE SUBSYSTEM T-VALVE IN THE PLANT SIMULATION 95
FIGURE 70 SCHEMATIC CONTROL STRATEGY T-VALVE 95
FIGURE 71 LOCATION OF THE SUBSYSTEM FLUID PUMP IN THE PLANT SIMULATION 96
FIGURE 72 LOCATION OF THE SUBSYSTEM AUXILIARY HEATER/COOLER IN THE PLANT SIMULATION 98
FIGURE 73 SYSTEM STATE 1 99
FIGURE 74 SYSTEM STATE 2 99
FIGURE 75 SYSTEM STATE 3 100
FIGURE 76 SYSTEM STATE 4 100
FIGURE 77 SYSTEM STATE 5 101
FIGURE 78 SYSTEM STATE 6 101

List of Tables

TABLE 1 GEOTHERMAL LAYERS OF THE GROUND IN CALGARY 36
TABLE 2 OVERVIEW SYSTEM STATES 38
TABLE 3 COMPARISON OF THE EFFECTS OF THE DIFFERENT SYSTEM VARIANTS 71
TABLE 4 BEST/WORST CASE SCENARIO OF THE FIXED PARAMETERS OF THE GEOTHERMAL FIELD 75
TABLE 5 BEST/WORST CASE SCENARIO OF THE VARIABLE COMPONENTS OF THE BUILDING SYSTEM 76

Declaration of Autonomy

I, Christian Hepf, declare that this thesis titled,

“Energy optimization of geothermal heat-pump system through dynamic system simulation”

and the work presented in it are my own. I confirm that:

- This work was done wholly or mainly while in candidature for a research degree at this University.
- Where any part of this thesis has previously been submitted for a degree or any other qualification at this University or any other institution, this has been clearly stated.
- Where I have consulted the published work of others, this is always clearly attributed.
- Where I have quoted from the work of others, the source is always given. With the exception of such quotations, this thesis is entirely my own work.
- I have acknowledged all main sources of help.
- Where the thesis is based on work done by myself jointly with others, I have made clear exactly what was done by others and what I have contributed myself.

City, Date

Signature